Hydrogen interactions with defects in crystalline solids

S. M. Myers

Sandia National Laboratories, Albuquerque, New Mexico 87185

M. I. Baskes

Sandia National Laboratories, Livermore, California 94550

H. K. Birnbaum

Materials Research Laboratory, University of Illinois, Urbana, Illinois 61801

J. W. Corbett

Department of Physics, State University of New York, Albany, New York 12222

G. G. DeLeo

Department of Physics, Lehigh University, Bethlehem, Pennsylvania 18015

S. K. Estreicher

Department of Physics, Texas Tech University, Lubbock, Texas 79409

E. E. Haller

Materials and Chemical Sciences Division, Lawrence Berkeley Laboratory, Berkeley, California 94720

P. Jena

Department of Physics, Virginia Commonwealth University, Richmond, Virginia 23284

N. M. Johnson

Xerox Palo Alto Research Center, Palo Alto, California 94304

R. Kirchheim

Max-Planck-Institut für Metallforschung, Institut für Werkstoffwissenschaften, D-7000 Stuttgart 1, Germany

S. J. Pearton

AT&T Bell Laboratories, Murray Hill, New Jersey 07974

M. J. Stavola

Department of Physics, Lehigh University, Bethelehem, Pennsylvania 18015

Hydrogen interactions with imperfections in crystalline metals and semiconductors are reviewed. Emphasis is given to mechanistic experiments and theoretical advances contributing to predictive understanding. Important directions for future research are discussed.

CONTENTS

I. Introduction 560
II. Defects in Metals 561
  A. Point defects 561
  B. Solutes and solute-defect complexes 563
  C. Dislocations 564
  D. Internal boundaries 566
  E. Isolated metal clusters 567
III. Theory of Metals 567
  A. Electronic theories 567
    1. Jellium model 568
    2. Effective-medium theory 569
    3. Band-structure methods 570
    4. Cluster models 571
    5. Proton quantum mechanics 572
  B. Simulations 572
    1. Computational methods 572
    2. Dislocations and plastic deformation 573
    3. Grain boundaries and intergranular fracture 574
    4. Future research 574
IV. Mechanical Response of Metals 575
  A. Phase changes 575
  B. Plastic deformation 576
  C. Cohesion 579
V. Silicon 581
  A. Hydrogen-dopant complexes 581
  B. Deep levels and native defects 582

 Copyright ©1992 The American Physical Society

C. Hydrogen-induced defects 585
D. Charge states of migrating hydrogen 585
E. Hydrogen dimerization 585
F. Hydrogen migration 586
G. Future research 587
VI. Germanium 587
A. Ultrapure germanium 588
B. Shallow-level complexes containing hydrogen 589
C. Deep-level centers and dislocations 591
D. Future research 591
VII. Compound Semiconductors 592
A. Shallow donors in gallium arsenide 592
B. Shallow acceptors in gallium arsenide 594
C. Dopants in other compound semiconductors 594
1. AlGaAs 594
2. GaP 595
3. InP 595
D. Point and extended defects 595
E. Hydrogen migration and solution states 596
F. Future research 597
VIII. Theory of Semiconductors 597
A. Computational methods 598
B. Interstitial hydrogen 598
1. Experimental information 598
2. Isolated hydrogen in silicon 599
a. Neutral H 599
b. Charged states 600
c. Discussion 600
3. Hydrogen dimers 600
4. Hydrogen vibrations 601
5. Interstitial hydrogen in other hosts 601
a. Diamond 601
b. Germanium 602
c. Weakly ionic compound semiconductors 602
C. Interactions with impurities and defects 602
1. Hydrogen-vacancy complexes in silicon 603
2. Hydrogen complexes with group-III and group-V impurities in silicon 603
a. H-B pair 603
b. H-P pair 604
3. Hydrogen complexes with group-II and group-VI impurities in silicon 605
4. Hydrogen complexes in compound semiconductors 606
5. Interactions of hydrogen with interstitial oxygen 606
D. Future research 606
IX. Summary 607
Acknowledgments 609
References 609

I. INTRODUCTION

Hydrogen is a major reactant with solids as a result of its strong chemical activity, high lattice mobility, and wide occurrence as H_2 and a constituent of molecular gases and liquids. The consequences for materials science and technology are widespread and growing. In metallic systems, for example, the formation of hydride phases has been extensively investigated as a means to store H fuel (Kirchheim *et al.*, 1989). Furthermore, H embrittlement continues to be an important source of environmental degradation in structural alloys (Moody and Thompson, 1990).

In electronic materials H plays many roles, both beneficial and detrimental. It is incorporated into amorphous Si at elevated concentrations to passivate dangling bonds (Paesler *et al.*, 1989), and it is emerging as an important reactant with imperfections in single-crystal Si and the compound semiconductors (Pearton, Corbett, and Shi, 1987). It serves to passivate interfacial charge traps in SiO_2 on Si, but it also mediates the radiation sensitivity of these structures (Poindexter, 1989). Its presence in vitreous Si oxynitrides is essential to the memory properties of these materials (Stein, 1989). Chemisorbed H is now recognized to enhance the oxidation resistance of the Si surface, thereby facilitating processing (Higashi *et al.*, 1990). A variety of H-containing molecular species are used for layer growth on semiconductors, resulting in important H-solid interactions which are incompletely understood (Schuegraf, 1988). In a related area, H has proved to be a key stabilizing species in the growth of diamond films (Angus and Hayman, 1988; Bachmann and Messier, 1989).

The impact of H-materials interactions has been greatly increased by the recent proliferation of plasma environments. Metastable H-bearing ions and neutrals in these plasmas tend to react exothermically with exposed solids and thereby drive H into solution. Moreover, when particle kinetic energies exceed a few eV, the chemical reactions are augmented by athermal implantation. These effects can produce large H chemical potentials within the lattice, sufficient even to form defects and highly metastable phases. Such H interactions are now a critical issue for the walls of tokamak fusion reactors (Winter *et al.*, 1989). In the area of electronic materials, plasmas currently provide the principal means for H passivation of dopants in Si (Pearton, Corbett, and Shi, 1987), and they are increasingly being used for low-temperature layer growth (Rossnagel *et al.*, 1990).

The interactions of H with lattice imperfections are important and often dominant in determining the influence of this impurity on the properties of solids. Nevertheless, in general, these interactions are far less understood at a fundamental level than the behavior of H in perfect lattices. As well as reflecting the natural progression of research, this situation results from the variety and complexity of H-defect interactions and from the experimental and theoretical difficulties that have been encountered in their study. Within the past decade, however, research in the area has been stimulated on a broad front by both technological and scientific developments, as will be discussed herein. For example, the long-standing problem of H embrittlement has recently emerged in the new class of intermetallic superalloys intended for aerospace structural applications. Additionally, while decades of mechanical testing have not definitively established the dominant mechanisms of H embrittlement, the recent advent of more realistic interatomic potentials, and their growing use in computer simulations, raises the possibility that the associated lattice deformations can be illuminated from an atomistic perspective. In the area of electronic materials, the array of defects and dopants in crystalline semiconductors that are known to be electrically neutralized by H is growing

rapidly and extending to the compound semiconductors. Finally, in both metals and semiconductors, an array of atomistic experimental studies coupled with advanced theoretical methods has begun to yield striking progress in quantitatively understanding H-defect interactions.

The recent progress in understanding also raises the prospect that H will provide an increasingly useful probe of defects within materials. The low-temperature mobility and high reactivity of the H atom are conducive to controlled "decoration" of imperfections with minimal alteration of microstructure. Moreover, the three H isotopes and muon analog can be detected and configurationally and electronically characterized with high sensitivity using such tools as secondary ion mass spectrometry, nuclear-reaction profiling and channeling, nuclear decay, and infrared and Raman spectroscopy.

This review of H-defect interactions grew out of a panel meeting held by the authors in January 1990 and sponsored by the U.S. Department of Energy. Our objectives were to evaluate current fundamental understanding and to identify productive directions for experimental and theoretical research. In order to focus on the most basic and theoretically tractable aspects, we stressed the low-concentration regime where H-induced phase transitions are not prevalent and where H-H interactions do not dominate the system behavior. In addition, attention was given predominantly to two classes of hosts where substantial research has occurred and which are broadly representative of metallic and covalent materials. These hosts are the crystalline metals and the cubic crystalline semiconductors. In the case of semiconductors, the study of defect interactions is hampered by an incomplete understanding of the complicated H solution states; consequently, the solution condition in these materials was also addressed.

II. DEFECTS IN METALS

A. Point defects

The vacancy is arguably the simplest defect in metals, consisting of an empty lattice site with modest peripheral relaxation. Hydrogen is strongly bound to this imperfection in most metals, and the interaction has been investigated in depth using a combination of experimental and theoretical methods (Besenbacher, Myers, and Nørskov, 1985; Myers *et al.*, 1989; and references therein). These investigations provide a case study demonstrating general aspects of H behavior and illustrating several important experimental and theoretical methods.

The existence of an attractive interaction between interstitial solution H and the vacancy can be inferred from the open-volume character of the defect. In particular, whenever the surface chemisorption state of H is energetically favored over interstitial solution, as is usually the case (Nørskov and Besenbacher, 1987), the derivative of energy with respect to metal atomic density at the solution sites is positive. Under this condition the H is driven to enter the vacancy. Moreover, the local open volume associated with the vacancy is relatively large, being almost sufficient to appear to the H atom as a free surface. As a result the binding energy tends to be large and comparable to that for H in the chemisorbed state.

In considering trap binding energies it is important to specify the way in which they are expressed. Throughout this paper, binding energies are given in eV per H atom and are referenced to H in solution within the crystalline lattice. For reasons of consistency, the solution reference state is used even for H chemisorbed on surfaces, thereby departing from the usual practice of taking the isolated H atom in vacuum as the reference state for chemisorption. The energy difference between the two reference states is simply the energy change when a H atom is moved from solution to vacuum, and this difference can be obtained by combining the usually published heat of solution from H_2 gas with the known vacuum-dissociation energy of the H_2 molecule.

The occurrence of H trapping at vacancies has been demonstrated for a number of metals by positron annihilation, a probe specifically sensitive to the presence of vacancies. In the absence of H, vacancies produced by low-temperature irradiation are observed to disappear when the temperature is raised sufficiently for them to become mobile. This event is generally referred to as recovery stage III, since it follows the onset of interstitial mobility, stage I, and early microstructural evolution of defect clusters, stage II (Balluffi, 1978; Young, 1978). When H is present in the lattice, H-vacancy binding reduces the effective mobility of the vacancy and thereby delays recovery stage III, providing a signature of the trapping reaction.

Ion-beam experiments have quantified the strength of the H-vacancy interaction and have provided information on the local atomic configuration. Typically, H is ion implanted into the metal of interest, simultaneously creating vacancies to which the H is bound. During subsequent temperature ramping, nuclear-reaction profiling is used to monitor the release of H from the trapping region, and the binding energy is extracted by fitting to solutions of appropriate transport equations.

Table I summarizes the results of positron-annihilation and ion-beam experiments on H-vacancy interactions in metals. Binding energies from the positron experiments reflect less detailed analyses and may be less accurate. In several of the ion-beam studies, binding energies were also obtained for multiple occupancy of the vacancy, and the resulting values are smaller than those for single occupancy given in the table. In Al the lighter positive muon was also observed to be trapped by vacancy defects, as expected from its chemical similarity to H; the estimated binding energy is ≥ 0.4 eV (Brown *et al.*, 1979), comparable to that obtained for H.

Effective-medium theory (Nørskov and Besenbacher, 1987, and references therein), to be discussed in Sec. III.A, has been used to treat the H-vacancy interaction with considerable success. This theory is based on calcu-

TABLE I. Binding energies of H to vacancies in metals expressed relative to H in solution.

Host	Ion-beam experiments[a]	Positron experiments
Al	0.52 eV[b]	0.53 eV[c,d]
Fe	0.63[e]	
Ni	0.44[f]	0.57,[g] 0.44[h]
Cu	0.42[i]	≥0.4[j]
Zr	0.28[k]	
Nb		≤1.0[l]
Mo	1.03[m]	1.4[n]
Pd	0.23[o]	
Ta	0.42[p]	≤1.2[l]

[a]Reviewed by Myers *et al.* (1989).
[b]Myers, Besenbacher, and Nørskov (1985).
[c]Rajainmäki *et al.* (1987).
[d]Linderoth, Rajainmäki, and Nieminen (1987).
[e]Besenbacher *et al.* (1987).
[f]Myers *et al.* (1986).
[g]Rajainmäki *et al.* (1988).
[h]Szeles and Vértes (1987).
[i]Besenbacher, Nielsen, and Myers (1984).
[j]Lengeler *et al.* (1978).
[k]Lewis (1984).
[l]Hautojärvi *et al.* (1985).
[m]Myers and Besenbacher (1986).
[n]Linderoth, Rajainmäki, Nielsen, *et al.* (1987).
[o]Myers, Wampler, *et al.* (1985).
[p]Lee, Myers, and Spulak (1989).

lations of the energy required to embed a H atom within a homogeneous electron gas as a function of the unperturbed density of the gas. In treating true metals, the embedding energy is initially equated to that for a homogeneous electron gas with the same electron density as the site of interest, and corrections are then made using perturbation methods. This theory confirms the key qualitative insight that, in most metals, H is attracted to any defect that has an associated region of reduced electron density. Figure 1 compares the experimental H-vacancy binding energies of Table I with the predictions of effective-medium theory, as reviewed by Myers *et al.* (1989). The theoretical values were obtained by calculating the trapped and solution energies and taking the difference. Despite severe approximations made in the calculations, the consistency between theory and experiment is seen to be good.

Ion-channeling analysis has been used to determine the lattice location of H trapped at vacancies in numerous metals, including the bcc hosts V, Cr, Fe, Nb, Mo, Ta, and W and the fcc materials Al, Ni, Cu, Pd, Ag, and Pt (Picraux and Vook, 1974; Bugeat *et al.*, 1976; Picraux, 1976, 1981; Myers *et al.*, 1979; Ligeon *et al.*, 1980, 1986; Besenbacher, Bogh, *et al.*, 1984; Danielou *et al.*, 1984; Besenbacher, Myers, and Nørskov, 1985). In all of the cases investigated, the attached H occupies a position displaced from the vacancy center where optimum bonding is achieved. This behavior is in semiquantitative agreement with effective-medium theory (Bessenbacher, Myers, and Nørskov, 1985; Myers *et al.*, 1989). In Fe,

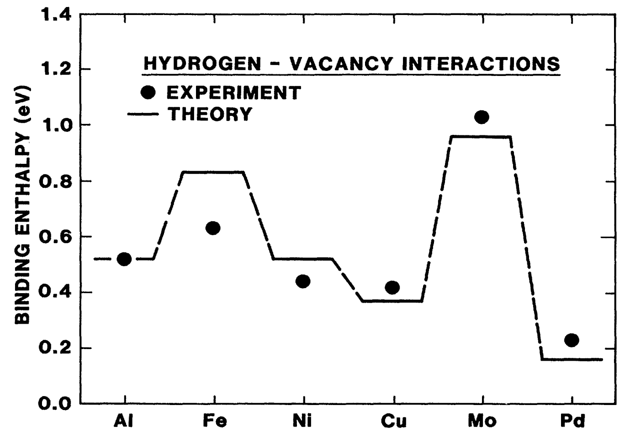

FIG. 1. Experimentally determined binding energies for H at vacancies in metals compared with the predictions of effective-medium theory.

for example, the position deduced from channeling analysis is on a line along the ⟨100⟩ direction between the vacancy center and a nearest-neighbor octahedral interstitial site, as depicted in Fig. 2, and is displaced from the octahedral site toward the vacancy by $\delta=0.04$ nm (Myers *et al.*, 1979; Picraux, 1981); by comparison, the theoretically predicted location is at $\delta=0.06$ nm (Besenbacher, Myers, and Nørskov, 1985). In the case of the Ni host, the quantum states of H in the vacancy have been calculated using the H potential from effective-medium theory (Besenbacher, Nørskov, *et al.*, 1985). Consideration of the thermal population of the excited states leads to the prediction of a temperature dependence in the H location below 50 K, and this effect has been observed in channeling experiments (Besenbacher, Nørskov, *et al.*, 1985).

The findings discussed above indicate a relatively advanced understanding of H in the metal monovacancy. Moreover, the success of effective-medium theory in accounting for the experimental observations suggests that this computational approach should have wide utility in semiquantitatively predicting H behavior. It is very desirable to apply other theoretical approaches discussed in Sec. III, such as cluster methods, band theory, and the

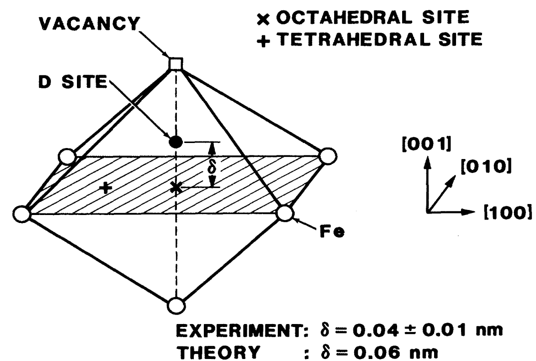

FIG. 2. Position of H bound to the monovacancy in Fe.

embedded-atom method, to the same interaction in order to assess the relative strengths and limitations of these techniques.

Metals with large vacancy concentrations occur in radiation environments where collisional atomic displacements are produced, as in fission and fusion reactors. Since the binding energy of H at the vacancy can be several times the activation energy for diffusion, the effects of such trapping on H transport can be large. This has important implications for fuel recycling and tritium inventory in the walls of tokamak fusion reactors, and it may also bear on radiation embrittlement in fission and fusion reactors. Smaller but still appreciable vacancy concentrations are caused by quenching from elevated temperatures and probably by cold working (Hull, 1975).

In contrast to the relatively well developed picture of H-vacancy binding, little is known of the interaction of H with self-interstitial atoms in metals. Since, from the preceding discussion, interstitial solution H is usually attracted to regions of reduced host-atom density and repelled where the density is increased, binding to the self-interstitial atom must depend on lattice distortions about that interstitial; consequently, the binding is expected to be weaker than at the vacancy. Rough theoretical estimates of the binding energy have been made for Ni, Cu, Fe, and Pd using the effective-medium approach; the resulting values are approximately 0.2 eV, with the minimum-energy positions being close to the four octahedral interstitial sites about the axis of the $\langle 100 \rangle$ interstitial dumbbell (Nørskov *et al.*, 1982). Further experimental and theoretical work is desirable in this area, since a unified, quantitative picture of H interactions at the monovacancy and self-interstitial defects would provide a valuable point of departure for the treatment of dislocations, boundaries, and solutes.

B. Solutes and solute-defect complexes

The interaction of H with solutes in metals is influenced both by the solute elastic distortion of the lattice structure and by electronic differences in H bonding between the host and impurity atoms. The resulting behavior is more complicated than in pure metals, and the degree of fundamental theoretical understanding is correspondingly less. Theoretical estimates of the two contributions to the binding have nevertheless been made in a semiempirical manner, making use of such measured properties as phonon frequencies and certain of the measured H-solute binding energies (Shirley and Hall, 1983, 1984; Shirley *et al.*, 1983). These calculations suggest that the binding is predominantly due to elastic distortion in the case of interstitial solutes such as N and O. For substitutional, transition-metal solutes there is a comparable contribution from the electronic effects, with the degree of attraction increasing with the size of the solute and its number of *d* electrons. The predicted H binding energies are usually modest for both the interstitial and substitutional solutes, being typically several tenths of an eV or less.

A substantial body of experimental information is available on the binding energies of solute-H pairs, and the data show illuminating trends that generally are consistent with the above theoretical ideas. The experimental results were obtained by a variety of methods, including internal friction, Mössbauer spectroscopy, perturbed angular correlation, inelastic neutron scattering, desorption, and ion-beam experiments. Selected findings are given in Table II. Here the entries are categorized by the structural configuration of the solute, which can be substitutional, or interstitial, or, in radiation environments, part of a solute-vacancy complex.

The strengths of the interactions in Table II are modest when the solute is not associated with vacancy defects, with the binding energy being less than 0.2 eV in all cases. These relatively weak attractive interactions are interpreted in terms of the combined effects of lattice deformation and differential chemical bonding, as discussed above. Since the open volumes produced by lattice strain about substitutional and interstitial impurities are much smaller than the volume of the vacancy, a correspondingly reduced effect on the binding energy relative to lattice solution is to be expected. Although the chemical binding of H atoms to metals is strong, with energies generally not less than about 2 eV as seen from heats of chemisorption and solution (Nørskov and Besenbacher, 1987), the *difference* in bonding that is responsible for the matrix trapping at metallic impurities tends to be much smaller. In the case of O and N impurities, which as isolated atoms would bond strongly to H, the trapping reaction is presumably diminished by metal-O and metal-N bonding.

Much stronger trapping was found at the solute-vacancy complexes associated with Co in Cu, In in Ni, Y in Fe, and Cs in Ni. These complexes were formed by ion irradiation of the alloys followed by vacancy trapping at the impurity atoms, as generally occurs at oversized species in radiation environments. It is believed that the relatively large H binding energies, which lie in the range 0.6–0.9 eV, reflect the combined effects of impurity reactivity and the open volumes associated with the attached vacancies, with the latter contribution being larger.

The interaction of H with solutes and solute-defect complexes is an important area for additional research. The lack of first-principles theoretical calculations is particularly noteworthy. Studies of this kind are needed not only to predict actual binding energies, but also to illuminate further the interplay of electronic effects and lattice distortions which underlies the observed trends in the energies. This improved understanding should then drive further experimentation with the ultimate goal of at least a semiquantitative prediction capability.

The study of H-solute interactions is exceptionally important from a technological perspective because concerns with H embrittlement and H storage usually arise in alloys rather than in metals, and because the use of alloying additions is one of the most accessible means of modifying H behavior. Conceivably, for example, the in-

TABLE II. Experimental H-solute binding energies in metals, expressed relative to H in solution.

	System	Binding energy (eV)	Reference
Substitutional	Ti in V	0.15	Tanaka and Kimura (1979)
		0.03–0.10	Pine and Cotts (1983)
	Ti in Fe	0.19	Pressouyre and Bernstein (1978)
	Ti in Ni	0.05–0.1	Thomas (1981)
	Fe in Ni	0.07–0.12	Thomas (1981)
	Co in Cu	0.12	Boolchand *et al.* (1983)
	Cr in Nb	0.105	Richter *et al.* (1983)
	Ti in Nb	>0.120	Richter *et al.* (1983)
	V in Nb	0.09	Matsumoto (1977)
Interstitial	C,N in V	0.13	Chang and Wert (1973)
	O in V	0.09	Chang and Wert (1973)
	C in Fe	0.03	Au and Birnbaum (1978a)
	N in Fe	>0.13	Au and Birnbaum (1978a)
	N in Nb	0.12	Pfeiffer and Wipf (1976)
		0.1	Richter *et al.* (1976)
	O in Nb	0.09	Baker and Birnbaum (1973)
	N in Ta	0.06	Rosan and Wipf (1976)
Sol.-vac. complex	Co in Cu	0.63	Boolchand *et al.* (1983)
	In in Ni	~0.6	Collins and Schuhmann (1986)
	Y in Fe	0.7–0.9	Myers *et al.* (1989)
	Cs in Ni	0.6–0.8	Myers *et al.* (1989)

troduction of appropriate alloying elements might inhibit detrimental interactions of H with dislocations and grain boundaries.

C. Dislocations

An understanding of the interactions between H and dislocations in metals is of considerable importance due to the influence of these effects on plastic flow and H mobility. In regions removed from the dislocation core, the energetics of the H have usually been treated within the framework of continuum mechanics. The formalism describes an elastic energy caused by the interaction between the stress field of the dislocation and the strain field around the interstitially dissolved H atom. Stresses around edge, screw, and mixed dislocations increase continuously with proximity to the core (Hirth and Lothe, 1968), implying a corresponding range of binding energies. The continuum model breaks down at the dislocation core, necessitating an atomistic treatment such as the embedded-atom and effective-medium methods described in Sec. III. While these continuum and discrete-atom descriptions have not reached the point of quantitatively predicting experimental observations, they account for the principle qualitative aspects of the behavior and provide an essential framework for the interpretation of data.

The strain around H atoms in fcc metals has cubic symmetry because the H atoms in solution occupy octahedral sites. The situation is in principle different for the bcc hosts, where the occupation of tetrahedral sites allows tetragonal distortions. In reality, however, from the absence of an internal friction peak and from measurements of Huang scattering (Peisl, 1978), it appears that the tetragonal distortion is absent or very small. Consequently, the interaction energy, being in general the product of a stress and a strain tensor, is simply expressed as (Kirchheim and Hirth, 1987)

$$E=(\sigma_{\rm I}+\sigma_{\rm II}+\sigma_{\rm III})V_{\rm H}/3\ , \tag{2.1}$$

where $V_{\rm H}$ is the partial molar volume of H and the σ are principal stresses. For an edge dislocation, one can derive the equation (Kirchheim, 1981)

$$E=-(A/r)\sin(\theta)\ , \tag{2.2}$$

where r is the distance from the dislocation core, θ is the angle between the glide plane and the position vector r, and A is a constant that contains the elastic constants of the material together with the Burgers vector of the dislocation and the partial molar volume of H. Thus the site energy for a H atom depends on the coordinates r and θ. In the case of the screw dislocation, the bracketed term in Eq. (2.1) is zero, and, as a result, the interaction energy with H is usually considered to be negligible. This may represent an oversimplification, however, since it assumes the absence of tetragonal distortion, which is not universally accepted (Zhang *et al.*, 1984), and neglects possible trapping at the core.

The local H occupancy of sites in the neighborhood of a dislocation is determined by Fermi-Dirac statistics, reflecting the occurrence of site saturation, as suggested independently by Louat (1956) and by Beshers (1958).

From an expression for the interaction energy such as Eq. (2.2), a distribution of site energies $n(E)$ can be calculated (Kirchheim, 1982). This then allows a simple formulation of the relation between the average H lattice concentration c and the H chemical potential, $\mu=\mu^0+(RT/2)\ln(P_{H_2}/P^0_{H_2})$, with P_{H_2} being the external H_2 pressure and $P^0_{H_2}$ the pressure in the reference state:

$$c=\int_{-\infty}^{+\infty}\frac{n(E)dE}{1+\exp[(E-\mu)/kT]} \ . \tag{2.3}$$

For the case in which almost all of the H is trapped by edge dislocations, one obtains (Kirchheim, 1982)

$$\mu-\mu^0=-(A/2)\sqrt{\alpha\rho\pi/c} \ , \tag{2.4}$$

where α is the saturation concentration of H in the neighborhood of the dislocation and ρ is the dislocation density.

When there are large local concentrations of H in the vicinity of dislocations, H-H interaction must be included in the theoretical treatment. The simplest approximation is obtained by introducing an additional term in the expression for the chemical potential according to the mean-field approximation. This term is considered to be either constant (Kirchheim, 1981) or proportional to the local concentration (Wolfer and Baskes, 1985). In either case, the predicted segregation of H atoms to dislocations leads to extended local regions of large concentration. The formation of such high-concentration regions introduces additional energy terms due to elastic accommodation of the H cloud and the formation of a boundary between the cloud and surrounding matrix (Park *et al.*, 1987). Furthermore, a rearrangement of the matrix atoms could in principle occur, leading to the formation of a new phase, as has been observed for other solutes such as N in Fe (Beaven and Butler, 1980) and O in Si (Bourret and Colliex, 1982). It should be noted, however, that for H in Pd there is no evidence for the formation of the β phase even though an extended zone of segregation occurs at dislocations (Kirchheim *et al.*, 1987).

As indicated above, H interactions at the dislocation core must be treated atomistically rather than by a continuum model. Moreover, the predicted behavior is sensitive to local atomic configuration, and here there is a serious deficiency of information. In lieu of direct experimental information, current understanding of the core structure relies largely on computer simulations, which at present cannot be regarded as entirely definitive. Such simulations have indicated a tendency for vacancy-like defects to form along the dislocation core (Häkkinen *et al.*, 1990), and, in line with the discussion of Sec. II.A, such defects should trap H substantially more strongly than the peripheral strain field.

The mobility of H can be substantially reduced by its attractive interactions with dislocations. These effects are usually treated within the framework of simple trapping models assuming a constant interaction energy (McNabb and Foster, 1963; Oriani, 1970), despite the fact that dislocations provide a spectrum of trapping energies. In a generalized trapping model the distribution of site energies around dislocations can be treated rigorously, but at the price of complexity (Kirchheim, 1988). Variations in saddle-point energies are also conceivable in the neighborhood of dislocations, but the extent of this effect is virtually unknown. The matter is potentially of some importance, since such variations would determine whether dislocations provide short-circuit diffusion paths. Additionally, saddle-point shifts would be expected to alter H transport towards the dislocation core and consequently might contribute to the serrated yielding of metals.

Experimental characterization of the interactions between dislocations and H is made difficult by the small volume fraction of the metal which is disturbed by the defect. Even at the highest dislocation densities of 10^{11} cm^{-2}, the cores are typically saturated at average concentrations above about 1 atomic ppm. Electrochemical measurements of uptake and release are applicable in this concentration regime, however, and have been widely used to observe the influence of dislocations on H solubility and diffusivity. Other utilized probes of H concentration include measurement of H_2 pressure changes above the sample (Flannagan *et al.*, 1976) and small-angle neutron scattering (Kirchheim *et al.*, 1987), although both of these techniques require larger concentrations. An indirect and powerful technique at low H content is internal friction (reviewed by Schiller, 1976), which senses the interaction between H and the moving dislocations. In such experiments, the heights of intrinsic dislocation peaks are decreased by the addition of H, and a new peak (cold-work or Snoek-Koester peak) appears due to the H-dislocation interaction. The interpretation of the Snoek-Koester peak is not simple, however, and a constant interaction energy between the two defects is assumed in all treatments.

Experimental studies of H-dislocation interactions have encompassed a range of metals and alloys, including V, Fe, Pd, Nb, and steels, with the most extensive work having been done on Pd. Several general properties have emerged, all of which are consistent with the theoretical insights developed above. These properties are as follows.

(1) There is strong H binding to dislocation cores. In Pd, for example, the binding energy is about 0.6 eV, with approximately 0.2 eV of that total being ascribed to H-H interactions (Kirchheim, 1981; Rodrigues and Kirchheim, 1983). A similar value of 0.6 eV was obtained by Kumnick and Johnson (1980) for H in Fe. These relatively large energies support the existence of vacancylike defects along the core, in accord with theoretical predictions (Häkkinen *et al.*, 1990).

(2) The concentration of trap sites in the core is approximately 1 to 2 per metal atom, with the core extending to a radius of about one Burgers vector (Kumnick and Johnson, 1980; Kirchheim, 1981; Funk and Schultz, 1985).

(3) Binding energies in the stress field of the dislocation extend continuously from small values to several tenths of an eV. The values are believed to reflect a combination of elastic and H-H interactions. In most studies the trapping in the core and in the surrounding stress field have not been separated, either by failing to gradually saturate the different trap sites or by not applying a multilevel trapping model. In Pd (Kirchheim, 1981) and Fe (Riecke *et al.*, 1985), however, gradual saturation of trap sites has clearly revealed the spectrum of binding energies.

(4) Dense packing of H can occur within the stress field of dislocations at higher host concentrations, leading to a saturation of sites which extends over several nm (Kirchheim, 1981, 1988; Kirchheim *et al.*, 1987). The H behavior in this zone has caused it to be termed a Fermi-Dirac cloud.

Further efforts toward a predictive understanding of H-dislocation interactions should include three key activities. First, quantitative data on the distribution of binding energies should be obtained for a wider array of metals. Second, it is important to develop more accurate information on the structure of the dislocation core. This will ideally entail refined atomic simulations, using the best available potentials, in conjunction with further experimental studies employing such probes as high-resolution electron microscopy and positron annihilation. Finally, the theoretical methods discussed in Sec. III.A, which have rather successfully described the energetics of H in solution and in the vacancy trap, should be extended to the H-dislocation interactions.

D. Internal boundaries

Grain and phase boundaries constitute the second major class of extended defects in crystalline metals, and the interactions of H with these entities are central to the influence of H on mechanical behavior. A predictive understanding of these interactions, however, has proved elusive, primarily for two reasons. First, information on the boundary atomic configurations is incomplete and often imprecise, and without such data the energetics of the H cannot be quantitatively treated. In addition, boundaries in metals often involve nonmetallic species, as in the case of carbide, nitride, and oxide precipitates, and this can introduce the complication of nonmetallic bonding. The situation is more favorable on the experimental side, where a substantial body of data on H binding energies has been obtained. Furthermore, better determinations of boundary structures are in prospect with the advent of advanced computer modeling and a new generation of electron microscopes with resolutions extending below 0.2 nm.

Due to their structural complexity, internal boundaries are expected to exhibit multiple H binding energies. The number of such energies should be small for coincidence grain boundaries and for phase boundaries where there is a well-defined orientational relationship, whereas the energetics of less regular interfaces are probably more complicated. Most experimental data are not sufficiently detailed to resolve this property, but definite indications of multiple energies do emerge from recent work on Pd grain boundaries (Mütschele and Kirchheim, 1987). Theoretical modeling of the H has not progressed to the point of definitively addressing the range of binding energies. There are calculations of segregation energies for other solute atoms, however, which do indicate a distribution of interaction strengths; these studies employed pair potentials, cluster treatments, and embedded-atom potentials (Messmer and Briant, 1982; Vitek and Wang, 1982; Foiles, 1989).

The segregation of solutes at internal boundaries is often detected by inducing interfacial separation and analyzing the exposed surfaces. This direct approach is difficult in the case of H, however, due to the mobility of the solute down to low temperatures. High-resolution secondary-ion-mass spectrometry (SIMS) has been used to observe H segregation at grain boundaries intersecting the specimen surface, although the lateral resolution of the probing beam encompasses many boundary widths (Fukishima and Birnbaum, 1984). The most extensive information has been obtained indirectly by observing differences in H concentration and mobility due to the presence of the boundaries, and approximate binding energies have been extracted in several instances. Table III give a selection of these results.

It is noteworthy in Table III that, for the fully metallic boundaries, the binding energies are relatively small. Indeed, the values are substantially less than those given in Table I for vacancy trapping in the same hosts, presumably indicating the absence of such open-volume defects at the boundaries. There is a striking difference, however, when the boundary contains a nonmetallic phase or segregated species that is amenable to covalent bonding of the H. Then the binding energies range upward from about 1 eV, suggesting the presence of nonmetallic bonding. This interpretation is reinforced by the results for trapping at Al_2O_3 precipitates in Pd. In that study, the terminus of the oxide phase was switched between O atoms and Al atoms by annealing in air or Al vapor, and the large binding energy was observed only when O was present at the boundary (Huang *et al.*, 1988, 1991).

In addition to their trapping of H, internal boundaries are believed to provide paths for accelerated diffusion. Mechanistic understanding and experimental data are both very limited in this area, however. In the case of substitutionally dissolved impurities, accelerated diffusion is well established and ascribed to a reduced vacancy formation energy in the excess volume of the boundary. In contrast, the diffusion of interstitial H does not rely on vacancies, so that reduced saddle-point energies at the boundary are presumably necessary to accelerate the transport. One experimental investigation of grain-boundary diffusion in Ni has yielded rates two or-

TABLE III. Experimental binding energies for H at internal boundaries in metals, expressed relative to H in solution.

Boundary	Binding energy	Reference
Grain boundary in Al	0.15 eV	Edwards and Eichenauer (1980)
Grain boundary in Pd	0.17–0.48 eV	Mütschele and Kirchheim (1987)
Grain boundary in Ni	$\sim$1.3 eV, S at boundary	Fukishima and Birnbaum (1984)
	$0<E\ll 1$ eV, without S	
γ'-fcc bnd. in fcc st. steel	0.10–0.15 eV	Thomas (1981)
γ'-fcc bnd. in fcc Fe-Ni-Co	0.2 eV	Moody *et al.* (1989)
Fe_3C-bcc bnd. in C steel	0.11 eV	Hong and Lee (1983)
TiC-Fe boundary in Fe	$\sim$1 eV	Pressouyre and Bernstein (1978)
Al_2O_3-Pd boundary in Pd	0.9 eV, O at boundary	Huang *et al.* (1991)
	0.3 eV, Al at boundary	Huang *et al.* (1988)
Al_2O_3-Al boundary in Al	0.7, 1.0–1.4 eV	Myers and Follstaedt (1988)

ders of magnitude greater than in the crystalline matrix (Tsuru and Latanision, 1982), whereas other studies have yielded an enhancement factor of about 4 (Lösch, 1987). The difference in these results may arise from a concentration dependence of the effective diffusivity, with the transport becoming progressively more rapid as the deeper trapping centers become saturated. Such an effect has been observed in Pd experiments, where the apparent diffusivity varied continuously from less than the perfect-lattice rate to greater than that rate as the H concentration was increased over several decades (Mütschele and Kirchheim, 1987).

Although a quantitatively predictive understanding of H-boundary interactions in metals is far from realization at present, recent theoretical and experimental advances suggest that large strides are possible in the near future. One key requirement is better information on the boundary structure, which may be achieved through a combination of refined computer modeling and microscopic observations by such techniques as high-resolution electron microscopy. With this structural information, quantitative or at least semiquantitative H-energy calculations should be possible for fully metallic bonding at boundaries by using effective-medium or embedded-atom methods. In cases where the H bonding is covalent, a quantitative theoretical treatment is more difficult. Here the metals community may benefit from the extensive theoretical work on H in semiconductors. Finally, more extensive and quantitative measurements of H binding energies are need in systems having well-characterized boundaries.

E. Isolated metal clusters

Laser vaporization of metal targets and supersonic expansion of the resulting plume give rise to formation of atom clusters that can range in size from two to a few thousand atoms (Jena *et al.*, 1987). The clusters can be mass separated using time-of-flight or quadrupole mass spectrometry. Recent studies of the structural and electronic properties of these clusters reveal remarkable features that are quite unlike the bulk counterparts and depend strongly on particle size. These unusual properties arise predominantly from two causes: first, most of the cluster atoms are at surfaces; and, second, in contrast to crystalline surfaces, local coordination and symmetry can change greatly from one size to another. Since H is attracted to surface sites in preference to bulk sites, such clusters can be expected to exhibit novel H interactions.

Recent experiments on H-cluster interactions have shown that the H can be absorbed when the corresponding crystalline hydride does not exist (Parks *et al.*, 1985; Whetten *et al.*, 1985; Cox *et al.*, 1990). There are also indications that one may be able to trap as many as eight H atoms per metal atom in very small clusters (Cox *et al.*, 1990). For clusters containing more than about 40 atoms, the properties revert to those of crystalline surfaces. Moreover, the reactivity of H varies strongly with cluster size, varying over several orders of magnitude within a narrow size range (Whetton *et al.*, 1985).

These findings pose several fundamental issues: (1) the difference in electronic structure between H interacting with a cluster and H interacting with the corresponding crystal; (2) the binding sites of the H and their relationship to binding energy; (3) the origin of the extreme sensitivity of the interaction to the cluster size; and (4) the question of whether the most reactive clusters are in an excited state or the ground state.

There are at present few theoretical studies of these issues (Upton, 1986; Rao *et al.*, 1991). Since most of the novel features appear in small clusters, however, the well-developed molecular-orbital theory appears particularly well suited to the problem. Indeed, quantitative calculations free of adjustable parameters should be possible. A combined experimental and theoretical effort could lead to an improved understanding and possible technological advances in H storage and catalysis.

III. THEORY OF METALS

A. Electronic theories

The perturbation of metal electron densities by H has traditionally been interpreted in terms of three highly simplified models (Fiks, 1959): the protonic, the hydrogenic, and the anionic. In the protonic model one assumes that the 1s electron of the H atom joins the con-

duction sea leaving a bare proton, and, consequently, the charge Z_H on the H atom is $+1$. In the hydrogenic model, the charge-density distribution of the 1*s* electron is unchanged, and $Z_H=0$. In the anionic model, H is assumed to attract an electron from the conduction sea and form an H^- ion, thereby yielding $Z_H=-1$. Experimental evidence can be cited for and against each of these models. For example, a Hall-type voltage induced by fast H diffusion in Pd in a strong magnetic field was found to be consistent with the protonic model (Verbruggen *et al.*, 1984). On the other hand, Mössbauer experiments in rare-earth hydrides (Viccaro *et al.*, 1979) and x-ray photoelectron spectroscopy (XPS) in transition-metal hosts (Veal *et al.*, 1979) clearly indicate a net transfer of electronic charge from the metal atoms to the H, supporting the anionic model. Finally, Compton-scattering measurements of the electron momentum distribution before and after hydrogenation (Lasser and Lengeler, 1978) are not consistent with any of the simple models. Such findings forcefully illustrate the fact that, due to the delocalization of conduction electrons, simple considerations of H charge states have limited utility in metals. A realistic description requires instead a detailed analysis of the spatial distribution of the electronic charge density around the proton.

Theoretical understanding of the electron charge distribution around the proton has provided to be a challenging problem, and the matter was not properly addressed until a decade ago. The difficulty arises primarily from two H properties, namely, the absence of a core-electronic structure and the small mass. The first of these characteristics results in a strong attractive potential for the electrons that is singular at the origin. Consequently, the electron response is not linear in the perturbing potentials, making simple perturbative techniques unsuitable. The second property, the small proton mass, results in a large zero-point vibration and dynamical coupling to the electronic system. This gives rise to strong and sometimes anomalous isotope effects in the electronic properties. The small mass of H also facilitates diffusion through the metal at lower temperatures, thereby enhancing interactions with intrinsic lattice defects.

Despite these complications, the electronic structure of H as an isolated static impurity in metals is largely considered to be a resolved problem. In contrast, the interaction of H with defects, and the consequences of quantum proton motion such as anomalous isotope dependences, remain key issues for future research.

In the present discussion we review the principal theoretical techniques that are available for treating the electronic structure of H in metals. We discuss their advantages and limitations, first considering the H as a static particle, and later introducing methods that can account for the effects of the finite mass. The central quantity is the perturbed electron density,

$$n(\mathbf{r})=n_0(\mathbf{r})+\delta n(\mathbf{r}) , \tag{3.1}$$

where $n_0(\mathbf{r})$ is the distribution in the perfect host and $n(\mathbf{r})$ is the changed density after the H atom is introduced. Charge neutrality requires

$$\int \delta n(\mathbf{r})d\mathbf{r}=1 . \tag{3.2}$$

The electron densities can be calculated by using the local-density approximation (LDA) of the density-functional theory of Hohenberg, Kohn, and Sham (Hohenberg and Kohn, 1964; Kohn and Sham, 1965). This theory reduces the complex many-body problem to an effective one-particle problem that is more readily treated. The effectiveness of the LDA in describing the electronic properties of metals is now well established. Therefore, in the following, we only discuss results obtained by this approach.

Application of the theory involves the solution of a Schrödinger-like equation,

$$\left[-\frac{\nabla^2}{2}+V_{\text{eff}}(\mathbf{r})\right]\psi_i(\mathbf{r})=\varepsilon_i\psi_i(\mathbf{r}) , \tag{3.3}$$

where V_{eff} is the effective one-particle potential, ψ_i is the wave function of the ith electron, and ε_i is the corresponding eigenvalue. Here we are using atomic Hartree units in which $e=m=\hbar=1$. The effective potential is given by

$$V_{\text{eff}}(\mathbf{r})=\int \frac{n(\mathbf{r}')}{|\mathbf{r}-\mathbf{r}'|}d\mathbf{r}'-\sum_{\nu}\frac{Z_\nu}{|\mathbf{r}-\mathbf{R}'_\nu|} -Z_{\text{I}}\delta(\mathbf{r})/r+V_{\text{xc}}[n(\mathbf{r})] . \tag{3.4}$$

The first three terms in Eq. (3.4) reflect Coulomb interactions of the electrons with, respectively, other electrons, fixed ion cores located at $\mathbf{R}_\nu$, and the proton at the coordinate origin. The quantity Z_ν is the charge on host ion ν, with $Z_\nu=Z$ in a monatomic host. The proton charge Z_{I} is equal to 1, and its potential has the form $\delta(r)/r$ where δ is the delta function. The final term is the exchange-correlation potential determined from the local electron density $n(\mathbf{r})$. The electron density is obtained from a summation over the probability densities for occupied states in the local region,

$$n(\mathbf{r})=\sum_i^{\text{occ}}|\psi_i(\mathbf{r})|^2 . \tag{3.5}$$

Equations (3.3)–(3.5) can be solved self-consistently. When $Z_{\text{I}}=0$ in Eq. (3.4), this procedure yields the electron density in the unperturbed host, $n_0(\mathbf{r})$. Current theoretical approaches are distinguished in large part by the manner in which the electron-nuclear term in Eq. (3.4) is approximated. In the following, we briefly outline these methods.

1. Jellium model

In this simple model (Popovic *et al.*, 1976; Petzinger and Munjal, 1977; Jena and Singwi, 1978; Kahn *et al.*, 1980), the host-atom ionic charges Z are smeared into a

uniform background of positive charge density $n_0 = Z/\Omega_0$, with Ω_0 being the atomic volume. In the absence of H, the electron-density distribution is also uniform and equal to n_0. When H is present, the effective potential in Eq. (3.4) has spherical symmetry about the proton, and the solution of Eq. (3.3) reduces to a relatively simple one-dimensional problem. Under these conditions it is easy to calculate the electron density $n(r)$ about the proton for any specified background density n_0. The results of such a calculation are shown in Fig. 3, where $a_0 = 0.0529$ nm is the Bohr radius, and $1/r_s = a_0 n_0^{1/3}(4\pi/3)^{1/3}$ (Jena and Singwi, 1978).

A key property illustrated by Fig. 3 is the strong localization of the perturbation of electron density by the proton. While $n(r)/n_0$ depends strongly on n_0, the perturbed density is seen in all cases to approach its limiting value within the small distance of $2a_0$. This localization makes possible the more advanced effective-medium and cluster descriptions of the H to be discussed below. Further insight is obtained by evaluating the net charge associated with the proton within a sphere of radius R, which is given by

$$Z_H(R) = -\int_0^R \delta n(r) 4\pi r^2 dr + 1 \ . \tag{3.6}$$

In the vicinity of the proton, $Z_H(R)$ is consistently larger than that for the free H atom (Jena *et al.*, 1979). This extra charge is a result of electron transfer from the metal atoms, and it is confirmed by more sophisticated calculations (Gelatt *et al.*, 1978; Gupta and Freeman, 1978; Puska *et al.*, 1981).

We now discuss the energetics of the H as calculated from the jellium model. Although the results have only semiquantitative significance for real metals, they nevertheless provide important physical insights into the attractive interaction of H with open-volume defects. The energy necessary to embed a H atom in a homogeneous electron gas of density n_0 can be expressed as (Puska *et al.*, 1981; Manninen *et al.*, 1984)

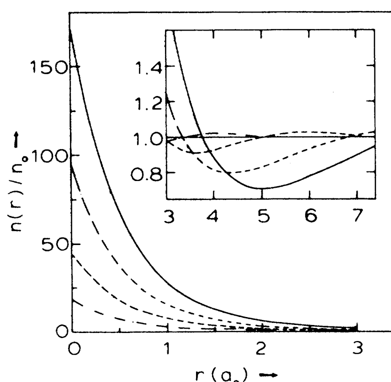

FIG. 3. Normalized electron-density distribution $n(r)/n_0$ around a proton in an electron gas. The normalized density at small radius increases with decreasing electron density or, equivalently, with increasing r_s, and the plotted curves correspond, respectively, to $r_s = 2.07$, 3, 4, and 5. The inset extends the plot to large r.

$$\Delta E^{\mathrm{hom}} = E^{\mathrm{hom}} - E^{\mathrm{at}} \ , \tag{3.7}$$

where E^{hom} is the energy of the atom in a homogeneous electron gas and E^{at} is its energy in free space. The quantity ΔE^{hom} can be computed from the self-consistent solution of Eqs. (3.3)–(3.5), and it is shown as a function of n_0 in Fig. 4. This energy is negative over most of the range of metal densities. Its minimum, however, falls below the solution-site electron density for most metals. As a result, H is expected to be attracted to regions of reduced electron density, such as open-volume defects and surfaces. Further, the strong dependence of the embedding energy on n_0 also indicates that the propensity of metallic hosts to absorb H should vary greatly in concert with their differing interstitial electron densities. This is also consistent with experimental observations.

Although the jellium model provides useful insights, it is too simplified to provide a quantitative description of most metals. Moreover, since this model contains no structural information, one cannot predict H site preferences or calculate host-lattice distortions. The first of these two properties can be extracted, however, by modifying the jellium model so that the effect of the host ions is treated approximately by spherically averaging the host-atom pseudopotentials. This procedure has been applied to H in metals with limited success (Manninen and Nieminen, 1979).

2. Effective-medium theory

Effective-medium theory (Nørskov and Lang, 1980; Stott and Zaremba, 1980) achieves significant improvements over the jellium model without a major loss of computational simplicity. In the effective-medium approach, the electron density at a target location within

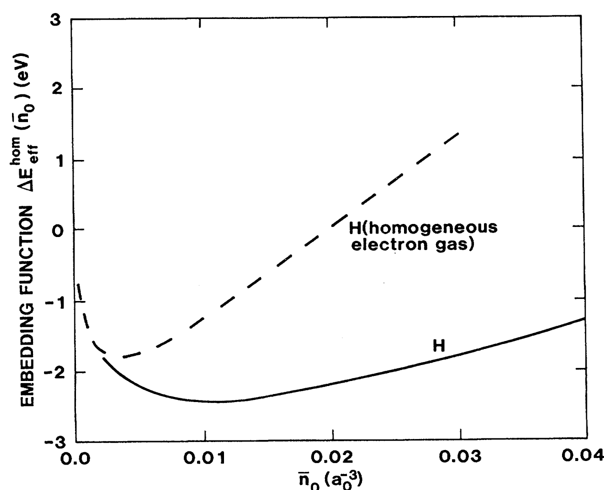

FIG. 4. Hydrogen embedding functions used in the effective-medium theory. The dashed curve represents the uncorrected embedding function for the homogeneous electron gas given in Eq. (3.7), while the solid curve includes corrections for the metal electronic states as reflected in Eq. (3.9).

the metal, before the introduction of H at that site, is obtained from a superposition of free-atom densities $n_{\rm at}$, so that

$$n_0(\mathbf{r})=\sum_{\nu} n_{\rm at}(\mathbf{r}-\mathbf{R}_\nu) . \tag{3.8}$$

Then, as a first approximation, the energy to embed the H atom at $\mathbf{r}$ can be equated to $\Delta E^{\rm hom}(n_0(\mathbf{r}))$, where $\Delta E^{\rm hom}$ is the embedding function calculated for the homogeneous electron gas and shown in Fig. 4. This inherently assumes that the response of the system is determined solely by the unperturbed local electron density at the injection point $\mathbf{r}$. In reality, this simple procedure does not provide a quantitative description of H energetics, so that refinements are necessary. The effective-medium theory accomplishes the correction through two steps (Nørskov, 1982). First, the local electron density at the proton site, $n_0(\mathbf{r})$, is replaced by an appropriately weighted average $\bar{n}_0(\mathbf{r})$ over a small zone about $\mathbf{r}$ where the perturbation of the proton is large. Second, in the case of transition-metal hosts, perturbation theory is used to correct for the hybridization of H 1s electrons with the metal d electrons. The final embedding energy is then given by

$$\Delta E(\mathbf{r})=\Delta E^{\rm hom}_{\rm eff}(\bar{n}_0(\mathbf{r}))+\Delta E^{\rm hyb}(\mathbf{r})+\text{small terms} . \tag{3.9}$$

The embedding function on the right-hand side of Eq. (3.9) is independent of host, and it is shown in Fig. 4. It differs from the jellium embedding function $E^{\rm hom}$ because one of the several perturbation terms can be cast as a universal function of n_0 and has been combined into the embedding term for convenience. The term $\Delta E^{\rm hyb}$, which is smaller than the embedding term but nonetheless significant, must be calculated case by case.

Effective-medium theory has been very successful in describing the energetics of H in metals when the bonding is predominantly metallic. For example, it has yielded quantitative or nearly quantitative binding energies and atom positions for H chemisorption, for H introduction into solution, and for H trapping by vacancy defects, and it has reliably predicted the trends of these properties among the metals (Nordlander *et al.*, 1986). The predictions for vacancy trapping were compared with experiment in Fig. 1, and a similar comparison of chemisorption energies is shown in Fig. 5.

More generally, effective-medium theory is currently the approach providing the most realistic description of H-defect interactions in metals while retaining sufficient computational simplicity to be widely applicable. Its principal limitations are the severe underlying approximations, which limit accuracy, and the absence of information on electronic wave functions. These deficiencies are avoided by the more rigorous band-structure and cluster methods, which will now be discussed. The improvements are achieved, however, at the price of a greatly increased computational complexity, which, at present, makes the treatment of H-defect complexes difficult by these methods.

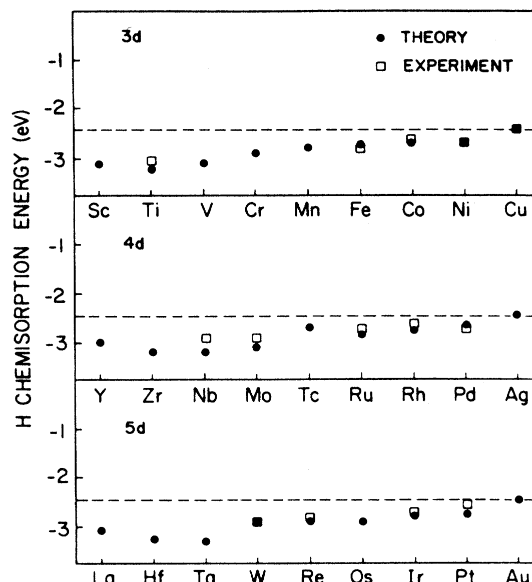

FIG. 5. Hydrogen-atom chemisorption energies from effective-medium theory compared to experiment. The horizontal lines give the contribution of the embedding term in Eq. (3.9).

3. Band-structure methods

These methods exploit the periodicity of the crystal and properly take into account both short-range and long-range effects. The use of Bloch's theorem reduces the numerical task considerably, and quantitative information on the electronic structure and properties of metals can be obtained using this scheme (Moruzzi *et al.*, 1978). The most commonly used band-structure methods are based on the linear augmented plane wave (LAPW) (Anderson, 1975) and the linear muffin-tin orbitals (LMTO), which differ mainly in the construction of the basis functions and electron potentials. These methods are very efficient for perfectly periodic systems such as stoichiometric hydrides (Gelatt *et al.*, 1978; Gupta and Freeman, 1978; Gupta, 1989; Switendick, 1989), where the unit cell is small. In systems where H resides as an impurity, however, the periodicity is lost. Such an irregularity can still be treated within the conventional band-structure scheme, but one must consider a large unit cell, or "super cell," which contains the defect site and a number of surrounding host atoms (Chakraborty *et al.*, 1981). This requirement can be very demanding computationally. Nevertheless, high-speed computers and more efficient codes are enabling some theorists to perform super-cell calculations of H in metals (Jepsen *et al.*, 1980; Sun and Tomanek, 1989), extending even to lattice relaxation and zero-point vibration of the H (Gillan, 1988, 1989). In order to describe H at a defect, however, the size of the cell should be still greater to minimize defect-defect interactions.

Band-structure methods based upon the Kohn-Korringa-Rostoker Green's function (KKK-GF;

Podloucky *et al.*, 1980) have also been used to study defects in solids. The perturbed-crystal Green's function is related to the host Green's function through a Dyson equation involving a defect-perturbed potential. Both the unperturbed and the perturbed potentials are assumed to be of the muffin-tin form, and the perturbation is localized to the region neighboring the defect site. This method is computationally simpler than the super-cell technique, since it involves determining the unperturbed Green's function only once, and the perturbed Green's functions for various impurities can be obtained simply by a knowledge of the perturbing potential. This approach has been successfully applied in treating vacancies and magnetic impurities in transition metals as well as H-metal systems (Akai *et al.*, 1986; Zeller, 1987). Again, however, with presently available computing capabilities, the definitive treatment of H-defect complexes including relaxations and H zero-point vibration appears difficult. Nevertheless, with continuing advances in theory and computing machines, such applications may well become feasible in the future.

4. Cluster models

From earlier calculations such as the one represented in Fig. 3, it is clear that the electronic interactions of H are strongly localized. This property allows cluster models to be used in the study of H-metal interactions (Jena *et al.*, 1979). In such calculations, one chooses a small number of metal atoms, typically about 30, surrounding the H to form a molecular cluster. Both the energetics and the electronic properties of the cluster can then be studied using the standard self-consistent-field, linear-combination-of-atomic-orbitals, molecular-orbital (SCF-LCAO-MO) method. The starting point is to write ψ_i in eq. (3.3) as a LCAO,

$$\psi_i(r)=\sum_{\mu} C_{\mu i}\phi_{\mu} , \qquad (3.10)$$

where the ϕ_μ are orbitals of the atoms forming the cluster. The coefficients $C_{\mu i}$ of the summation are obtained by solving the variational equation (3.3), thereby yielding the electronic wave functions of the system. The total electronic energy is then obtained by combining single-particle energy eigenvalues with charge-density-weighted integrals of electron-electron interaction terms in the Hamiltonian. These calculations can be performed fully self-consistently. When only localized effects are important, the cluster model can yield reliable information on both energetics and electronic properties.

A further noteworthy feature of the SCF-LCAO-MO methods for clusters is that they use not only the conventional local-density approximation (LDA) to the density-functional theory (DFT), but also quantum-chemistry techniques (Hehre *et al.*, 1986). This contrasts with the band-structure methods, where the total energies are usually calculated within the framework of the LDA-DFT. In the quantum-chemistry techniques, the electrostatic and exchange contributions to the potential are calculated in the Hartree-Fock approximation, and correlation is treated either through configuration interaction or through perturbation techniques. When performed with an extensive basis set, these methods can predict energies to a high level of accuracy (Rao and Jena, 1985; Bonacic-Koutecky *et al.*, 1991). Such treatments are computer-intensive, however, and applications have been limited to very small clusters, typically 1–5 transition-metal atoms or about 20 light alkali-metal atoms. Hence most of the modeling of bulk properties via clusters uses either the LDA-DFT or less elaborate, semiempirical quantum-chemical codes.

In assessing the utility of the cluster and band-structure methods for H in metals, it is instructive to compare their predictions for the electron density of states. This is done in Fig. 6, which shows results for the superstoichiometric hydride PdH_2 (Liu, Rao, *et al.*, 1989 and unpublished; Sun and Tomanek, 1989). The consistency is good, with the prominent H-induced states at -7 eV and -13 eV being in close agreement. The energetics of the H-H interaction and the equilibrium H-H separation are also in good agreement, further supporting the validity of the two methods.

The cluster model has also been used to study the pairing mechanism of H in yttrium (Liu, Challa, *et al.*, 1989). In most metals, H atoms precipitate to a super-lattice phase at low temperatures. In rare-earth metals such as Y, however, the H atoms form pairs mediated by a metal atom along the *c* axis (McKergow *et al.*, 1987). The cluster calculations reproduced this property and even predicted the observed temperature dependence of the pairing. Other successful applications have included H chemisorption reactions on Be (Bagus *et al.*, 1983) and on transition metals (Andzelm and Salahub, 1987) and positive-muon hyperfine interactions in ferromagnetic metals (Lindgren and Ellis, 1982).

Cluster methods have not been commonly used to treat H-defect interactions because of the large computational times that would be required. The origin of this difficulty is essentially the same as in the case of the super-cell band-structure methods, namely, the relatively large number of atoms that must be included to provide a realistic description. Nevertheless, it appears very desirable to pursue the extension of both band theory and cluster methods to the simpler H-defect interactions. Such calculations would provide an important added basis for evaluating the energetics obtained from the less rigorous effective-medium theory. In addition, they would provide realistic H-perturbed electron-density distributions in the vicinity of the defect for the first time.

Moreover, even within their current limitaitons, the band-structure and cluster methods should be capable of enhancing the treatment of H-defect interactions through the development of improved energy functionals for the effective-medium theory. At present these functionals are obtained through severe approximations, and a more rigorous analysis of appropriately chosen configurations

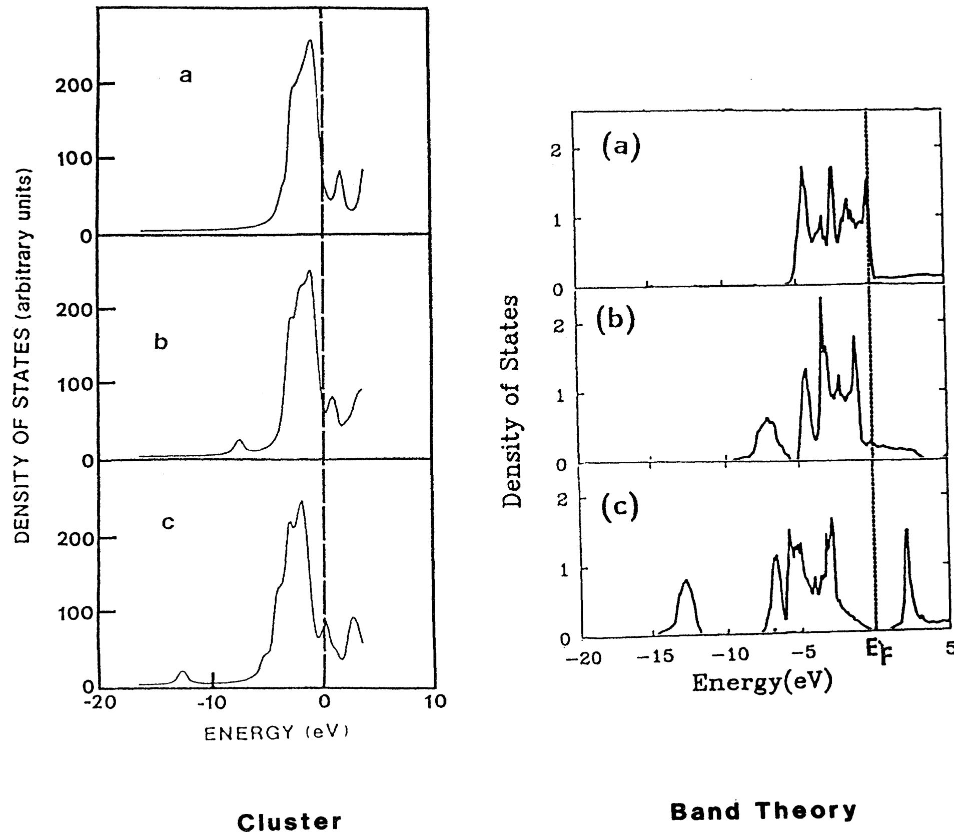

FIG. 6. Density of states in Pd hydrides as calculated using cluster methods and band-structure theory: (a) Pd; (b) PdH; (c) PdH_2.

could provide valuable validation and refinement. For example, a more accurate knowledge of solution energy as a function of host-lattice parameter would provide a valuable test of the spatial derivatives of the potentials. Moreover, similar benefits should be possible for the semiempirical embedded-atom potentials, which are discussed in Sec. III.B in connection with simulations.

5. Proton quantum mechanics

In the above discussions we have used the adiabatic approximation, namely, that the electrons respond to the proton as if it were a static particle of infinite mass. Within this picture the electronic states are identical for the proton, deuteron, triton, and positive muon. This is not in fact the case; rather, numerous isotope effects occur in metal-H systems, and many of these are anomalous. The properties exhibiting such anomalies include H diffusion, Dingle temperatures, vibrational ferquencies, electrical resistivity, Knight shift, and superconducting transition temperature.

An understanding of these isotope effects requires calculations that treat the wave natures of both the electrons and protons in a self-consistent manner. Such a description has still to be achieved, and it is an important goal for future research.

In lieu of a full quantum-mechanical treatment of the proton-electron system, protonic wave functions have been calculated within the context of effective-medium theory. The procedure is to solve a Schrödinger equation for the proton in which the Hamiltonian potential energy is taken from Eq. (3.9). In cases where it is desired to include lattice distortions about the H, the coupled static-displacement and Schrödinger equations are solved self-consistently. This theoretical approach has been used to treat the isotope dependence of self-trapping energies, the spatial distribution of H in transition metals with and without point defects, and even the temperature dependence of such distributions (Manninen *et al.*, 1984; Puska and Nieminen, 1984; Besenbacher, Nørskov, *et al.*, 1985). The results agree well with a wide range of experimental data.

B. Simulations

1. Computational methods

In order to understand and quantify the influence of H-defect interactions on the macroscopic stress response of metals, it is necessary to establish a theoretical connection between the atomic interactions discussed in Secs.

II–III.A and the many-body cooperative processes ocurring on a scale of micrometers. This is usually done through molecular-dynamics simulations, Monte Carlo methods, or adiabatic-displacement treatments, with approximate interatomic potentials and classical equations of motion being used. Two-body potentials have traditionally been employed in such simulations (Lee, 1981), but this approach requires the addition of a "volume-dependent" term in the total energy to reproduce experimental elastic constants. Moreover, it is difficult unambiguously to define an effective "volume" for less symmetric atomic configurations such as those appearing near surfaces and defects. This problem has more recently been avoided by using many-body descriptions of the metallic interactions which are based on density-functional theory. These treatments include a function of electron density which replaces the traditional volume-dependent contribution while being unambiguously determined by the configuration of surrounding atoms.

The most widely used description of the above kind is the embedded-atom method (Daw and Baskes, 1984; Daw, 1989), which is related both to the effective-medium theory discussed in Sec. III.A and to the method of multiple-body potentials (Finnis and Sinclair, 1984). The cohesive energy is expressed as the sum of an embedding energy, which is a function of electron density, and two-body potentials. The total structural energy of the system is then given by

$$E_{\text{tot}}=\sum_i F_i(n_0(\mathbf{r}_i))+\frac{1}{2}\sum_{ij}\phi_{ij}(r_{ij}) \ . \tag{3.11}$$

Here $n_0(\mathbf{r})$ is the electron density at $\mathbf{r}$, the location of atom i, when that atom is absent from the lattice. As in the effective-medium theory, this electron density is approximated by a sum of atomic electron densities from surrounding atoms, so that $n_0(\mathbf{r})$ is given by Eq. (3.8). The pairwise interaction ϕ_{ij} between atoms i and j, separated by a distance r_{ij}, can be regarded as an electrostatic coupling between ion cores. In certain cases it is desirable also to include H-H interactions that occur external to the metal; for example, such an extension is necessary to treat dissociative absorption from H_2 gas. This has been accomplished through the addition of a third energy term (Baskes *et al.*, 1987; Foiles *et al.*, 1987) based on the method of diatomics in molecules (Kuntz, 1976).

The functions F and ϕ have been determined in two ways. One of these procedures is semiempirical and begins with a parametrization designed to provide flexibility while retaining physically realistic behavior. The parameters are then evaluated by fitting to experimental metal properties such as lattice constants, elastic constants, and sublimation energies. For the interactions of H, the fitted properties include energies of solution, of migration, and of chemisorption. The details of this method are given elsewhere (Daw and Baskes, 1983, 1984; Daw, 1989). The second approach extracts the two functions from effective-medium theory without fitting to experiment (Manninen, 1986; Jacobsen *et al.*, 1987).

Before considering the simulation of H interactions at dislocations and grain boundaries, which is the principal concern of this subsection, it is useful to note that the embedded-atom method has also been applied successfully to other H interactions in metals. These processes include the surface reflection of energetic H at energies below 100 eV (Baskes *et al.*, 1987), dissociative absorption of H_2 at thermal energies (Foiles *et al.*, 1987), and H order-disorder transitions on Pd surfaces (Daw and Foiles, 1987). Experimental data are available for comparison in all of these cases, and the simulations are found to be in qualitative or semiquantitative agreement. Moreover, a modified version of the embedded-atom method has recently been developed to include the angular interatomic forces present in semiconductors (Baskes, 1987; Baskes *et al.*, 1989). This computational approach has not been applied to H in semiconductors, but it holds promise for such applications.

One ultimate goal of the simulations of extended defects is to provide a predictive description of their stress-induced evolution in the presence and absence of H. This is a formidable task in the most general case, since it requires an integrated and accurate treatment of energetics, defect structure, and atomic motion for a large number of atoms. Indeed, such a comprehensive treatment has not been achieved in any system. The field has advanced rapidly during the past decade, however, and simulations of selected aspects of the H behavior have reached the point of providing important mechanistic insights. These developments, coupled with the continuing progress in methodology and computer hardware, suggest that the investigation of H embrittlement can increasingly move beyond its currently empirical basis.

2. Dislocations and plastic deformation

Simulations relevant to H at dislocations have been of several types. One recent study addressed the structure of dislocations in Al, using Eq. (3.11) with potentials from effective-medium theory (Häkkinen *et al.*, 1990). A particularly significant outcome of this work is the predicted tendency for vacancy defects to form along the core. This provides a plausible explanation of the strong H trapping at dislocation cores in Fe and Pd, which was discussed in Sec. II.C; in the absence of the pronounced open volume associated with vacancies, dislocation structures are not expected to provide the reduced electron densities necessary to account for the measured binding energy of 0.6 eV.

The binding energy of H at sites near the dislocation core in Ni has been calculated using the embedded-atom method with empirical potentials (Daw *et al.*, 1986). The investigated structure did not include vacancy defects, and under this condition the dominant interaction is due to the compression and tension of the lattice: the predicted binding energy above the slip plane is the negative of the energy below the plane, and, a few angstroms re-

moved from the dislocation core, the binding energies agree well with continuum theory. The strongest predicted trapping of H occurs on the slip plane near one of the partials, and it has a magnitude of ~ 0.05 eV. These results reinforce the view that the H-dislocation binding of 0.6 eV observed in Fe and Pd may involve vacancy defects.

The motion of a dislocation is affected by bound H in two opposing ways. The more straightforward effect is pinning, which reflects the endothermic detrapping necessary to separate the moving dislocation from its H. The second process, termed H-enhanced local plasticity, actually eases the dislocation transport. This phenomenon was recently discovered in deformation experiments, as discussed in Sec. IV.B, and it is believed to occur when the dislocation moves sufficiently slowly for the H to redistribute by thermal diffusion and thereby continuously minimize system energy.

The pinning of a dislocation by H in Ni was simulated by molecular dynamics using Eq. (3.11) and semiempirical embedded-atom potentials (Daw *et al.*, 1986). A slab containing a dislocation was subjected to shear stress, and the resulting dynamical evolution was treated with and without H being present. These simulations encompassed times in the range 10–70 psec, temperatures of 0 and 300 K, interstitial H concentrations of 0, 1, and 10 at. %, and applied shear stresses of $(1.5-96)\times 10^{-4}$ times the shear modulus C_{44}. The effects of the pinning on dislocation motion were found to be pronounced at the lowest stresses and negligible at the highest.

Simulations have also been used to explore mechanistic origins for the observed H enhancement of dislocation motion, as discussed in Sec. IV.B. These continuum calculations used finite-element methods to treat the interactions of strain and associated hydrogen-concentration fields about elastic singularities in a self-consistent manner. The results indicate that the H can weaken strain-mediated interactions among dislocations and between dislocations and precipitates. This shielding effect is hypothesized to reduce the interactive pinning that normally retards dislocation flow.

Still other simulations have exhibited the influence of H on the generation of dislocations from a crack tip. These calculations were performed for a stressed crack in Ni, with and without H in solution, using the embedded-atom method with semiempirical potentials (Daw and Baskes, 1987). The results show that dislocations are emitted from the crack more rapidly when H is present. It is thought that the H facilitates dislocation formation at the tip by lowering the ledge energy.

3. Grain boundaries and intergranular fracture

Grain boundaries constitute the second major class of extended defects involved in deformation, and the influence of H on the strength of these boundaries remains one of the principal issues in H embrittlement. Atomic simulations have begun to make significant contributions in this area. The problem has two aspects—the extent of H accumulation at the boundary, to be discussed in Sec. IV.C, and the reduction of cohesion resulting from a given grain-boundary concentration. The latter property is the one addressed by the simulations discussed below.

Recent theoretical studies have used effective-medium theory to treat a highly idealized situation where fcc-Ni or bcc-Fe splits along a low-index plane with no relaxation or deformation in the separating halves (McMullen *et al.*, 1987). At high H concentrations the calculated boundary weakening is substantial: for the Ni (111) interface, fracture stress is reduced by 45% times the boundary atomic fraction of H. Substantial enhancement of boundary fracturing was also observed in more realistic, molecular-dynamics simulations (Daw and Baskes, 1984; Daw *et al.*, 1986), which treated H-doped Ni using embedded-atom semiempirical potentials. In physical terms, such results reflect the fact that H atoms can find locations of optimally reduced electron density on the fracture surface and thereby reduce their energy relative to the unfractured configuration.

4. Future research

Generally speaking, the simulations discussed in this subsection have qualitatively reproduced major features of the interactions of H with dislocations and grain boundaries. In so doing, they have significantly advanced our mechanistic understanding. The impact would be strengthened, however, by improving accuracy to the point of allowing reliable semiquantitative estimates of rates and magnitudes to be made. For example, the extent of grain-boundary decohesion depends very much on the extent of H segregation to the boundaries, and this is now quite uncertain. In a similar vein, the influence of H on dislocation transport is sensitive to the interaction energetics in both the core and strain fields, and here the simulations depart substantially from available experimental data, with the measured binding energies being larger. Considerable improvements should be possible through an intensified focus on two areas that were already cited in Secs. II and III.A, namely, refinement of the interatomic potentials and better determinations of boundary and dislocation-core structures.

A second common feature of the above simulations is that they do not attempt fully to reproduce plastic flow and boundary fracture, but rather describe particular aspects of the underlying mechanisms. The latter role is extremely useful and perhaps the only feasible one. The difficulties of a comprehensive molecular-dynamics description are illustrated by the fact that the advance of a crack involves perhaps 10^{15} lattice-vibration periods and 10^{9} atoms. Significantly broader treatments might be achieved, however, through the use of hybrid methods. Such procedures as the use of adiabatic displacements, the mating of discrete lattices to a surrounding continuum, and the use of Monte Carlo techniques to incorporate H diffusion appear worthy of consideration.

IV. MECHANICAL RESPONSE OF METALS

Studies of the effects of H on deformation and fraction in recent years are extensive and quite impressive with respect to the range of systems investigated and the amount of materials characterization obtained (Birnbaum *et al.*, 1973; Birnbaum, 1979; Lynch, 1988; Moody and Thompson, 1990). A noteworthy finding is that H embrittlement occurs very widely, more so than was appreciated even a decade ago. Materials previously considered to be insensitive, such as Al and stainless steels, have succumbed at sufficiently high H fugacities and low strain rates (Liu *et al.*, 1980; Briant, 1981; Zeides, 1986; Zeides and Birnbaum, 1990). Moreover, the new intermetallic compounds being developed for aerospace applications appear to be susceptible (Stoloff, 1990).

There is a rather broad consensus that at least three general mechanisms contribute to H-associated mechanical degradation. These are (1) phase transformations such as hydride formation induced by the combined presence of H and stress, (2) H-enhanced plasticity, and (3) weakening of grain boundaries by H. Uncertainty and controversy remain, however, regarding underlying atomic processes and the relative importance of the three mechanisms. The current situation is reviewed in the following subsections from a mechanistic perspective. While phase transitions lie outside the formal scope of the present report, which is concerned with H-defect interactions, they are included because of the competing role they play.

A. Phase changes

A number of metallic systems have exhibited H embrittlement due to stress-induced formation of hydrides and their subsequent brittle fracture. These systems include the group-VB metals Nb, V, and Ta (Eustice and Carlson, 1961; Wood and Daniels, 1965; Sherman *et al.*, 1968; Westlake, 1969; Owen and Scott, 1972; Hardie and McIntyre, 1973; Takano and Suzuki, 1974; Gahr *et al.*, 1977; Grossbeck and Birnbaum, 1977); Zr (Nuttall, 1976; Northrup, 1979); Ti (Nelson *et al.*, 1972; Paton and Williams, 1973; Schöber and Wenzl, 1978; Shih *et al.*, 1988); and alloys based on these metals. The basic requirements for such embrittlement are that the precipitates be stabilized by the presence of H and the crack-tip stress field (Westlake, 1969; Gahr *et al.*, 1977; Flannagan *et al.*, 1981; Narita *et al.*, 1982), and that they be brittle (Mueller *et al.*, 1968; Gahr and Birnbaum, 1980; Birnbaum, 1984). The typical system that exhibits failure by this mechanism also forms stable hydrides in the absence of stress when the H fugacity is sufficiently high. These hydrides, by virtue of their large and positive $\Delta V_{\text{formation}}$, are thermodynamically more stable under the stress and fugacity conditions at the crack tip (Dutton *et al.*, 1977; Simpson and Puls, 1979; Flannagan *et al.*, 1981). Such thermodynamic conditions are present in many additional metal systems where definitive studies of embrittlement remain to be done. Finally, in the particular case of stainless steels, which generally do not form stable hydrides, other types of H-induced phases may possibly cause embrittlement, such as the martensitic phases (Benson *et al.*, 1968; Narita and Birnbaum, 1980; Narita *et al.*, 1982; Rozenak *et al.*, 1990) and fcc "pseudohydrides" (Maulik and Burke, 1975; Narita *et al.*, 1982).

The specific sequence of microscopic processes leading to embrittlement by stress-induced hydride formation may be qualitatively described as follows. Under applied stress, the chemical potentials of the solute H and the hydride are reduced at locations of concentrated tensile stress such as crack tips. Diffusion of H to these elastic singularities and precipitation of hydrides then occur. The kinetics of this process depends on many factors, including the source of the H. The phase change to the hydride is accompanied by a decrease in the critical stress intensity for crack propagation, from $K_{\text{Ic}}^{\text{solid solution}}$ to $K_{\text{Ic}}^{\text{hydride}}$. In addition hydride formation produces a high, compressive, local stress field due to the large and positive $\Delta V_{\text{formation}}$. This reduces the local stress intensity K_{I} caused by the externally applied stress. In effect, the stress-induced hydrides act in a manner similar to "phase transformation toughening" (Shih *et al.*, 1988). Thus there are two countervailing effects: a reduction in the stress intensity and a reduction in the fracture toughness, K_{Ic}. In general, the latter effect dominates, and the decreased K_{Ic} allows rapid crack propagation when the applied stress is only moderately increased. The crack propagates by cleavage until the hydride/solid-solution boundary is reached. At that point the crack enters a ductile phase having a high $K_{\text{Ic}}^{\text{solid solution}}$, and the crack stops until more hydride is formed by a diffusion-controlled process. The process repeats itself, resulting in discontinuous crack growth through the stress-induced hydride phase. Whether the hydride is seen in a post-facto examination of the fracture surface depends on whether the hydride is stable under the conditions of the examination.

The stabilization of hydride phases by stress is mechanistically complex because $\Delta V_{\text{formation}}$ is accommodated not only elastically but also by plastic deformation of the solid-solution matrix (Grossbeck *et al.*, 1976; Makenas and Birnbaum, 1980). The influence of plasticity on the stability of hydrides during formation and reversion (including reversion on removal of the external stress) has been clearly demonstrated. In a few instances, such as that of V-H, the hydride plates are accommodated in an entirely elastic manner, and complete reversion occurs on removal of the external stress (Takano and Suzuki, 1974). Usually, however, accommodation occurs partially by plastic deformation of the matrix, and the hydrides are stabilized above the stress-free solvus by the free energy of the plastic accommodation; such behavior is seen in Nb-H (Grossbeck *et al.*, 1976; Dutton *et al.*, 1977; Grossbeck and Birnbaum, 1977; Simpson and Puls, 1979; Makenas and Birnbaum, 1980; Birnbaum, 1984); in

Ti-H (Shih *et al.*, 1988); and in a number of other systems. The detailed formulation of these processes in thermodynamic terms is complex and still controversial.

Hydrogen-associated failure is competitive with ductile fracture, and it is observed only when the latter process does not intervene. Embrittlement by stress-induced formation of hydrides (or high-concentration solid solutions) is thus observed under conditions where the hydrides can form at a rate sufficient to preclude other forms of failure. In these systems, ductile rupture generally occurs if the strain rate is increased or if the temperature is decreased (Gahr and Birnbaum, 1976); at high strain rates the time available for hydride formation is decreased, while at low temperatures the rate of hydride formation is decreased. Similarly, if the temperature is increased, the stability of the hydride may be sufficiently decreased that it can no longer be stress induced, and hence failure may again occur by ductile processes. The thermodynamics of these processes can be used to elucidate the conditions under which hydride-related embrittlement can occur (Flannagan *et al.*, 1981).

An important special case of H-related second-phase embrittlement may occur during the embrittlement of austenitic stainless steels. This matter remains controversial, and the mechanism is unproven. In a number of cases, H embrittlement of metastable stainless steels, such as types 304 and 316, has been ascribed to H-enhanced transformation of the γ fcc phase to the α' bcc and ε hcp martensites (Benson *et al.*, 1968; Louthan *et al.*, 1973; Briant, 1979; Eliezer *et al.*, 1979; Narita and Birnbaum, 1980; Narita *et al.*, 1982; Rozenak *et al.*, 1990). *In situ* transmission-electron-microscopy (TEM) studies (Narita and Birnbaum, 1980; Rosenak *et al.*, 1990) have identified these martensitic phases in front of the crack tip and along the crack sides. Some researchers, however, have disputed the presence of such martensites on the fractured surfaces (Whiteman and Troiano, 1965; Hanninen and Hakarainen, 1980). Moreover, these phases have not been shown to occur solely in the presence of H, nor has it been established whether they are a cause or simply a consequence of the fracture process. In sum, then, this mode of stainless-steel embrittlement is an issue for further investigation.

While the mechanisms of fracture related to H-induced phase transitions are relatively well understood, a number of important issues still need to be addressed. Among these are

(1) The thermodynamics and kinetics of constrained hydride systems are only partially understood. The effects of elastic and plastic accommodation need to be studied to allow the effects of stress on hydride formation to be understood. The role of the matrix properties on plastic accommodation of the hydrides needs to be explored.

(2) The mechanical properties of hydrides and of the high-H concentration solid-solution phases should be determined over a wide range of temperatures and strain rates.

(3) From thermodynamic considerations a number of additional important systems are probably embrittled by stress-induced-hydride mechanisms, but direct measurements to establish this have not been carried out.

(4) The presence and influence of miscibility gaps and high-concentration H solid solutions have not been established in many systems. In alloys such as the stainless steels, these phases may be of importance in H embrittlement.

B. Plastic deformation

There is now a large body of evidence that H strongly affects plastic deformation in metals in a manner leading to enhanced fracture. This area of investigation has emerged only in the past few years, and while a broad range of related phenomena has been observed, few of these processes are fully understood or universally accepted. Nevertheless, progress toward a unified understanding is being made through the key concept of H-enhanced local plasticity (HELP; Beachem, 1972). In the discussions that follow, this area is addressed in two ways. First, a range of experimental observations are interpreted in terms of the local plasticity enhancement. Then, possible ways in which the H-dislocation interactions can lead to HELP are considered.

The model of local plasticity enhancement by H is essentially as follows. Application of external force to the metal produces local concentrations of tensile stress, notably in the vicinity of cracks. When H is present in solution or in the ambient, its concentration increases in the stress region. This occurs because the slightly enlarged interstitial solution sites are energetically more attractive, as can be inferred from the electron-density considerations of Sec. III or simply by noting that the volume change associated with H uptake is positive. The model then hypothesizes that dislocations move more easily in the presence of the H, leading to a local reduction of the flow stress, which then facilitates crack growth by locally ductile processes. While this concept of enhanced plasticity initially appears to be at variance with embrittlement, there is in fact no contradiction when it is noted that the zone of ductile failure tends to be so highly localized that the total macroscopic deformation remains small. Consequently, from a macroscopic vantage point this type of failure will appear brittle.

The above mechanism is supported by a wide range of experimental results, with the work and discussions of Lynch (1986, 1988) and of Birnbaum *et al.* (Eastman *et al.*, 1980; Matsumoto and Birnbaum, 1980; Matsumoto *et al.*, 1981; Tabata and Birnbaum, 1983, 1984, 1985; Birnbaum *et al.*, 1986; Robertson and Birnbaum, 1986; Shih and Birnbaum, 1986; Bond *et al.*, 1987, 1988; Shih *et al.*, 1988) being particularly relevant. There is agreement between Lynch and Birnbaum *et al.* on the basic thesis that the presence of H increases the plasticity at the crack tip and leads to fracture. There are significant differences, however, in that Lynch views the

phenomenon as a surface effect while Birnbaum *et al.* consider the H effects to occur in the volume of the material as well as near the surface. With this background, we turn now to a consideration of the experimental evidence.

The HELP mechanism holds that localized plastic fracture occurs as a result of H-induced local plasticity at the crack tip. Shear localization due to H has been clearly shown for high purity Al (Zeides, 1986; Zeides and Birnbaum, 1990), steels (Hwang and Berstein, 1982, 1986; Onyewuenyi and Hirth, 1983), and Fe-N alloys (Deve *et al.*, 1989). The detailed mechanism by which this leads to local fracture is not completely understood, however, and the problem is quite complex. In addition to the local decrease in flow stress caused by H in solid solution, H has also been shown to result in serrated yielding (Portevin–Le Chatelier effect) in the temperature range in which H embrittlement is severe (Kimura and Birnbaum, 1990). A relationship between serrated yielding (i.e., a region of negative strain-rate dependence, $d\sigma/d\varepsilon<0$) and shear localization can be expected (McCormick, 1988). Continued localization of shear is expected to lead to fracture by various plastic-failure processes, although the exact mechanism is not known (Deve *et al.*, 1989).

The deformation and fracture of a number of metals and alloys during exposure to H_2 gas has been observed in real time using environmental-cell TEM. The investigated materials include Ni (Eastman *et al.*, 1980; Matsumoto and Birnbaum, 1980; Robertson and Birnbaum, 1986); Fe (Tabata and Birnbaum, 1983, 1984, 1985); Inconel 718 (Robertson *et al.*, 1984; Shih and Birnbaum, 1986); 304 stainless steel (Rozenak *et al.*, 1990); A533b stainless steel (Robertson *et al.*, 1990); 316 stainless steel (Rozenak *et al.*, 1990); Al (Bond *et al.*, 1988); the age-hardened alloys Al 7075 and Al 7050 (Bond *et al.*, 1987); and α-Ti alloys (Shih *et al.*, 1988). Void formation is observed along intense slip bands, and fracture occurs along slip planes in a saw-tooth morphology. In many cases "slits" or elongated microvoids open up along the active slip planes in front of the crack tip. These are then joined to the crack tip by plastic rupture processes. In general, the entire H-enhanced fracture process is one of plastic rupture rather than brittle fracture, consistent with the notion of H-enhanced plasticity. While the *in situ* TEM experiments are carried out on thin specimens (plane stress), similar microstructural features can be resolved on the fracture surfaces of bulk specimens (Eastmen *et al.*, 1980; Lynch, 1986).

Another consequence of the HELP mechanism is that the fracture surface is predicted to be that along which the shear localization occurs. In general, this is the slip plane, as has been observed (Matsumoto and Birnbaum, 1980; Lynch, 1986). In cases where multiple slip is prevalent, however, or where special constraints are imposed by the stressing mode (Vehoff and Rothe, 1983; Vehoff *et al.*, 1987; Lynch, 1988), the macroscopic fracture plane may differ from the slip plane. In these cases an average fracture path may be imposed by the external stress, although the microscopic fracture path will follow the active slip planes.

Dislocation motion was also investigated during the previously cited *in situ* TEM experiments. Observations were made on specimens under stress in which the deformation processes had ceased to operate in vacuum. On adding H_2 gas to the environmental cell, dislocation sources operated and the dislocations began to move. Subsequent removal of the H_2 gas caused a cessation of the dislocation motion, and the cycle could be repeated many times. Hence the effect of the H was to reduce the stress for dislocation motion and consequently for dislocation generation. This H enhancement of mobility was observed for screw, edge, and mixed dislocations, and also for dislocations that were in tangles, in slip bands, and far from other dislocations. The effects were quite general, with similar behavior being observed in fcc, bcc, and hcp crystal structures and in alloys as well as pure metals.

Macroscopic flow stresses were also observed to decrease when H was introduced into solution before deformation, and this effect was again ascribed to H-enhanced dislocation motion. Such behavior was induced by cathodic charging of pure Fe (Matsui, Kimura, and Kimura, 1979; Matsui, Kimura, and Moriya, 1979; Moriya *et al.*, 1979), by plasma charging of Fe (Kimura and Birnbaum, 1987a), and by gaseous charging of Ni (Eastman *et al.*, 1982). Very significant decreases in the flow stresses were observed, particularly after the above cathodic charging of high-purity Fe. These experiments were carefully carried out to minimize dislocations introduced by the H charging treatment. Flow-stress decreases in the Fe were originally interpreted as due to decreases in the energy to nucleate kinks on screw dislocations, thus decreasing Peierls-Nabarro lattice interactions (Matsui, Kimura, and Kimura, 1979; Matsui, Kimura, and Moriya, 1979; Moriya *et al.*, 1979). However, observations of the phenomena using *in situ* TEM environmental-cell techniques, and macroscopic deformation experiments for systems in which there are no strong dislocation-lattice interactions, suggest that this explanation is not correct. Furthermore, the effect is seen for edge as well as for screw dislocations. The generality of the phenomena indicates that an explanation must be based on interactions common to many systems. One such interaction is the elastic interaction between dislocations and H solutes within the metal matrix.

In contrast to the above observations, cases of increased flow stresses due to H have been reported (Bernstein, 1974; Cornet and Talbot-Besnard, 1980). The general procedure used in these experiments is to introduce the H by cathodic charging during deformation. In systems that can form hydrides, or that have miscibility gaps, cathodic charging at too high a current density can result in the formation of a surface hydride (or high-concentration solid solution). This will cause increases in the flow stress due to the surface phase (Kimura and Birnbau, 1987b). At lower current densities, the high H-concentration gradient formed in the near surface region

will cause a high dislocation density to be formed, and this will cause surface hardening (Kimura and Birnbaum, 1987b). At still lower current densities, less severe concentration gradients form, and the stresses associated with these gradients can act as dislocation sources and thereby decrease the flow stress. The intrinsic effect of H solutes is seen only if these artifacts are avoided by the use of very low cathodic current densities at temperatures where the diffusivity is sufficiently high. In general, with the possible exception of the experiments by Kimura *et al.* (Matsui, Kimura, and Kimura, 1979; Matsui, Kimura, and Moriya, 1979; Moriya *et al.*, 1979), these conditions have not been met by cathodic-charging experiments.

A definitive mechanistic understanding of H-enhanced dislocation motion has not been achieved. A promising model, however, postulates that dislocations and other elastic singularities have their strain-mediated interactions reduced by H-associated "elastic shielding" (Sirois *et al.*, 1992). In this mechanism, the mobility of H allows it to diffuse to positions of lowest free energy and to form higher-concentration atmospheres surrounding dislocations, solutes, and precipitates. The binding energies of H at such entities are typically tenths of an eV, as discussed in Sec. III, and this generally allows the atmospheres to form over the range of temperatures where H embrittlement is prevalent. Moreover, when the H mobility is sufficiently high in relation to dislocation velocities, these atmospheres can move with the dislocations in response to applied stresses. This condition is satisfied for most of the systems studied. Shielding of the elastic interactions is then considered to result from continuous adjustments in the H clouds, which minimize the total free energy of the system. For example, as two dislocations approach each other, the H concentration at each point responds to the combined stress fields, thereby reducing the energy increment associated with their impingement. With the consequent reduction of pinning effects, the effective mobility of the dislocations is increased.

The above shielding effect was examined theoretically through self-consistent elasticity calculations using finite-element methods (Sirois *et al.*, 1992). This treatment yielded the configurations of the H atmospheres, the interaction energies, and the forces between the elastic singularities. Representative results are shown in Fig. 7. In general, the predicted effect of H atmospheres at dislocations is to decrease the interactions with elastic defects at short range and to have little effect at large distances. This spatial dependence is a consequence of the H-atmosphere interactions, which vary as $1/r^2$ while the dislocation stress fields vary as $1/r$. The magnitude of this decrease of the interaction stress can be of the order of the dislocation stresses at distances of about 10 Burgers vectors for reasonable H concentrations.

The above considerations indicate that elastic shielding effects should be small at high temperatures where the concentration of H in the atmospheres is reduced, and also small at low temperatures where the atmospheres are not sufficiently mobile. These effects are therefore expected to be more pronounced in the intermediate temperature range and at low dislocation velocities (low strain rates). This is in accord with experimental observations of H embrittlement.

The expected properties of the elastic shielding effects also correspond well to observations of macroscopic softening. In Fe the decrease in the flow stress is greatest at temperatures of about 200 K (Matsui, Kimura, and Kimura, 1979; Matsui, Kimura, and Moriya, 1979; Moriya *et al.*, 1979), is largest at low strain rates, and increases as the number of short-range obstacles, such as solutes, are increased (Tabata and Birnbaum, 1984, 1985). In Ni and Ni-C alloys, the temperature range of H-enhanced dislocation motion is somewhat above that in which serrated yielding is seen (Kimura and Birnbaum,

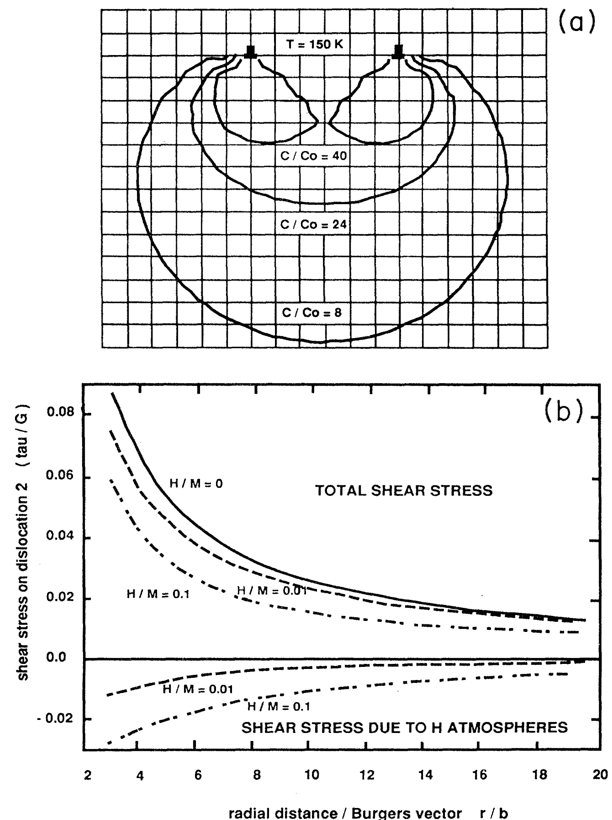

FIG. 7. Influence of H on dislocation-dislocation interactions. (a) calculated contours of enhanced H concentration C/C_0 near two closely spaced edge dislocations. The scale increment is one Burgers vector, b. For well-separated dislocations, the iso-concentration profiles have the classical symmetrical form characteristic of a single dislocation. (b) repulsive force per unit length for two parallel edge dislocations in the presence of various bulk H atomic fractions, H/M. The force is expressed as stress normalized to the shear modulus of the metal. The upper curves show the total force between the dislocations while the lower curves give the attractive component due to the redistributed H atmospheres.

1990), indicating that H atmospheres can move along with dislocations. Furthermore, direct elastic shielding effects at solutes having noncubic displacement fields have been observed using the N anelastic relaxation in Fe (Au and Birnbaum, 1978b).

Hydrogen-associated failure also occurs through weakening of grain-boundary cohesion, as discussed in Sec. IV.C. Distinguishing this effect from the HELP mechanism was at one time thought to be straightforward: if the fracture appeared to follow grain boundaries, the decohesion process was taken to be dominant. Recently, however, studies of apparently intergranular fracture in Fe, Ni, Incoloy 703, and Ti using *in situ* straining of TEM specimens have revealed a more complicated situation (Shih *et al.*, 1988). On the microscopic scale visible by TEM, the fracture was observed to occur through H-enhanced local plasticity, which proceeded in the vicinity of and occasionally along the grain boundaries. These results have been interpreted in the light of high-resolution SIMS measurements on polycrystalline Ni (Ladna *et al.*, 1986) and Ni-V alloys (Robertson *et al.*, 1984), which showed H enrichment in a zone encompassing the grain boundaries. Thus the identification of the dominant failure mechanisms is less straightforward than previously believed, and the HELP process may be more prevalent than grain-boundary decohesion. It should be noted, however, that this remains one of the more controversial aspects of H embrittlement.

Despite the extensive research outlined above, the phenomena and underlying mechanism of H effects on dislocation behavior are not well established. The proposed relationship between H-enhanced dislocation motion and fracture remains unproven, although increasingly strong evidence in its favor can be adduced. Even less certain are the atomic processes by which H eases the dislocation transport. These deficiencies in understanding have considerable technological significance, since many of the important structural materials fall into the category of non-hydride-forming systems where plasticity-related fracture mechanisms are likely to be active. Important issues for further research include the following.

(1) The interactions between dislocations and interstitial H need to be further characterized with respect to energetics and dynamics. Such studies should ideally combine microstructural observations with more detailed measurement of the H-dislocation interaction and improved atomistic simulations.

(2) The above studies should give particular attention to determining the validity of the dislocation-shielding mechanism and quantifying its characteristics.

(3) Embrittlement by the localized-plasticity mechanism should be further tested to establish its validity and generality.

C. Cohesion

One of the first proposed and most commonly cited mechanisms of H embrittlement is decohesion (Steigerwald *et al.*, 1960; Oriani and Josephic, 1974, 1977). This concept associates the embrittlement with a decrease in the atomic bond strength due to the local concentration of H. In its basic form, the mechanism is interpreted in terms of the energy of two half solids as they are separated. This energy can include the influence of elastic distortion of the two half solids, but it does not include inelastic effects. Redistribution of H is allowed in the case of equilibrium separation, whereas during nonequilibrium separation the H distribution is fixed. The fracture or "separation" energy is $2\gamma_f$, with γ_f being the surface-formation energy. Since H has a lower energy in regions of reduced electron density such as surfaces, as discussed in Sec. III, $2\gamma_f$ is smaller when H is present on the fracture surface. This reduction is smaller for rapid, nonequilibrium separation than for equilibrium separation where H redistribution can occur (Hirth, 1980; Hirth and Rice, 1980). Nevertheless, the "cohesive stress," i.e., the maximum force per unit area required to separate the two half solids, is expected to be diminished in both cases.

Although the above effects of H on cohesion are widely acknowledged, their magnitudes under fracture conditions are not well established, and this has contributed to controversy regarding the importance of decohesion in H embrittlement. The following discussion considers available information in this area and also reviews fractographic evidence on the relative roles of decohesion and H-enhanced plasticity.

Table IV summarizes selected energetics pertinent to decohesion in Fe and Ni. Tabulated are estimated fractional changes in the surface energy for equilibrium slow fracture, for nonequilibrium fast fracture, for discontinuous fracture, and for fast fracture along grain boundaries where H segregation has previously taken place. These energies were calculated for H solution concentrations corresponding to equilibrium with H_2 gas at a pressure of 1 atmosphere. The values were estimated from the

TABLE IV. Effects of H on surface energies during fracture.

Metal	Fractional changes in surface energies				
	Equilibrium fracture	Nonequilibrium fracture	Intermittent fracture $\mu/100$	Intermittent fracture $\mu/10$	Intergranular fracture
Ni	0.53	3.2×10^{-4}	3.3×10^{-4}	4.9×10^{-4}	0.21
Fe	0.61	1.2×10^{-5}	1.3×10^{-5}	2.4×10^{-5}	0.25

difference between the energy of H on the surface and that within the unfractured solid, using H surface concentrations that would be characteristic of the conditions for each type of fracture. In the case of "equilibrium fracture," segregation to the free surface was allowed during the slow fracture process (an unlikely occurrence). For discontinuous fracture, the H concentration in front of the propagating crack tip was increased by diffusion and was calculated (Li *et al.*, 1966) assuming hydrostatic stresses of $\mu/100$ and $\mu/10$, μ being the shear modulus. For intergranular fracture, the preexisting grain-boundary concentration was estimated using the grain-boundary segregation enthalpy (Lassila and Birnbaum, 1987). These results suggest that significant decohesion effects can be expected only for equilibrium fracture, which does not occur in practice, and for intergranular fracture, since the predicted local H enrichment is insufficient in other cases. The theoretical many-body simulations of fracture that were discussed in Sec. IV.B are in general agreement with this picture.

Direct experimental confirmation of the reduction in separation energy due to H is not available. Indeed, the nonequilibrium separation energy of the brittle hydride β-$NbH_{0.8}$ was found to be approximately equal to the equilibrium surface energy of Nb (Gahr and Birnbaum, 1980), suggesting the absence of substantial decohesion. It should be noted, however, that the energetics of fracture in this material may not be representative of metals with small H concentrations and strong driving forces for H segregation. More directly pertinent are reported measurements of the equilibrium surface free energy of Ni containing 0.03 at. % H. These data indicated that the H-induced reduction in surface energy is small (Clark *et al.*, 1980). Small-strain parameters such as elastic constants and phonon frequencies are not immediately indicative of the strength of cohesion. Nevertheless, it is interesting to note that these quantities tend to show stiffening of the lattice when H is introduced. For example, the elastic constants and phonon frequencies of the Group-VB metals show this behavior (Magerl *et al.*, 1975; Springer, 1978; Mazzolai and Birnbaum, 1985a, 1985b), even with the large volume increases which alone would decrease the force constants. In the case of fcc metals, the elastic constants decrease with the addition of H (Springer, 1978), but this effect can be explained by the H-associated volume increase.

In order to determine whether fracture actually occurs by the decohesion mechanism or by another mechanism that intervenes, careful fractography and *in situ* studies of the fracture process are required. Such studies were discussed in Sec. IV.B, and in a number of cases they support the mechanism of H-enhanced localized plasticity rather than decohesion. In the decohesion mechanism the fracture is by cleavage, which occurs when the applied stress exceeds the cohesive stress. This cleavage fracture is generally accompanied by plastic deformation (McMahon and Vitek, 1979), which greatly increases the total energy of fracture and hence the macroscopic K_{Ic}. In systems where the fracture occurs transgranularly, failure is expected to be along cleavage planes and to exhibit the fractography of cleavage. The large amount of plastic deformation which often precedes fracture should not have a major effect on the fractography. Since slip is a structure-conservative process, when cleavage occurs after slip it should exhibit all of the major features of a cleavage failure. This is demonstrably true in cases where the cleavage occurs through hydrides, the formation of which is preceded by significant plastic deformation. In general, H-embrittled fracture surfaces (other than those that occur by hydride formation) do not exhibit cleavage fracture surfaces as would be expected from decohesion.

Intergranular fracture by decohesion due to H implies that the fractography should reveal the morphology of the grain interfaces. However, most high-resolution fractography shows much more structure on the H-embrittled intergranular fracture surfaces than is expected from brittle fracture along the grain boundaries. *In situ* TEM observations of the H-related intergranular fracture of a number of systems (Robertson *et al.*, 1984) shows that the fracture occurs mostly along slip planes in the vicinity of the grain boundaries, often crossing the grain boundary to follow slip planes in the adjacent grains. The slip lines and other structural details seen on intergranular facets produced by H embrittlement may correspond in part to the fracture path following slip planes adjacent to the grain boundary rather than following the grain boundary itself. In this case the concept of grain-boundary decohsion hardly appears applicable.

Hydrogen-induced grain-boundary decohesion does appear to be an active fracture mechanism in certain alloy systems where other embrittling species are segregated to the boundaries. An example of this is the Ni-S system (Lassila and Birnbaum, 1987). *In situ* TEM studies in an environmental cell (Lee, Robertson, and Birnbaum, 1989) clearly showed that intergranular fracture was caused by H and that it occurred by crack propagation directly in the grain boundary. This fracture was accompanied by significant plasticity on both sides of the boundary. A similar situation was seen in studies of H embrittlement of Ni_3Al containing dilute B, where the fracture occurred directly along the grain-boundary plane (Bond *et al.*, 1989). In these cases, it does appear that the cohesion along the grain boundary is reduced by the presence of H.

In summary, consideration of energy changes during segregation of H to interfaces and surfaces leads one to expect only a very small H-induced decrease in the separation energy during transgranular fracture, but a substantially larger decrease during intergrangular fracture in those cases where H segregation to the grain boundaries has taken place. Direct experimental characterization of this effect is currently lacking. Such decohesion is competitive with H-enhanced plasticity, and fractography and microstructure studies indicate that the latter process frequently intervenes, even when the fracture ap-

pears to follow grain boundaries. The decohesion mechanism has been unambiguously observed, however, in systems where H and other embrittling solutes cosegregate to boundaries.

There is a compelling need for better understanding of the influence of H on cohesion. This goal should be pursued experimentally in at least three areas. First, more comprehensive work on H-modified elastic constants and phonon-dispersion relations would illuminate the small-strain regime. Second, careful measurements on surface energies under equilibrium and nonequilibrium conditions are needed for a variety of systems. Finally, it is highly desirable to develop new techniques that probe the presently inaccessible large-displacement regions of the lattice potential. One possible approach would utilize the atomic-force microscope. Data of this kind would greatly enhance and validate the theoretical developments considered in Sec. III.

The magnitude of the above H effects is governed by the extent of H enrichment at the region of fracture, and this depends in turn on the energetics of H binding at boundaries. As detailed in Secs. II.D and III.A, substantial experimental and theoretical progress has been made in this area, but much work remains to be done.

Finally, as indicated in Sec. III.B, it is important to develop more realistic simulations of the fracture process, using both discrete-atom and finite-element methods.

V. SILICON

Hydrogen interacts strongly with an extensive array of defects and dopants in crystalline Si, usually causing a qualitative change in the electrical and optical properties of the imperfection. These interactions have a large and growing impact on Si device technology, and this has stimulated a substantial body of research, both basic and empirical, to provide an information base for prediction and control. The more fundamental studies seek to characterize the migration, chemical kinetics, and microscopic structure of the H and its complexes. In Si and other semiconductors, as contrasted to the metals, the solution states and diffusion mechanisms of H are complicated and controversial, and this bears directly on the interactions with defects. Consequently, the present discussion will include treatments of diffusion and the solution condition.

Hydrogen interactions have been investigated far more extensively in crystalline Si than in other semiconductors, both experimentally and theoretically. It is increasingly clear, however, that many of the phenomena identified in Si extend to other diamond-lattice semiconductors, including the zinc-blende compounds. Moreover, the interactions of H in crystalline Si also serve to illuminate the more complicated processes occurring in the amorphous phase. The Si-H system is thus prototypical, and this provides an important added impetus for the research on its properties.

A. Hydrogen-dopant complexes

The experimentally based suggestion (Sah *et al.*, 1983) that H can electrically passivate shallow-acceptor dopants in Si provided a strong stimulus for research on H behavior. It was soon demonstrated that by direct exposure to a H plasma more than 99 percent of substitutional B near the surface could be passivated (Pankove *et al.*, 1983, 1984). Combined spreading-resistance measurements and SIMS profiling demonstrated that the increase in resistivity was accompanied by the migration of H into Si and that the depth of H penetration agreed with the depth of acceptor passivation (Johnson, 1985b). Many experimental studies contributed information on the microscopic nature of the acceptor-H complex. Infrared vibrational spectroscopy (Johnson, 1985b; Pankove *et al.*, 1985; Stavola, Pearton, *et al.*, 1988) and ion-channeling techniques (Marwick *et al.*, 1987; Nielsen *et al.*, 1988) supported a bond-centered structural model (DeLeo and Fowler, 1985a; Pankove *et al.*, 1985) in which the H is positioned along the ⟨111⟩ axis between the B and an adjacent Si, as depicted in Fig. 8.

Hydrogen neutralization of shallow-donor impurities in Si was first revealed with combined resistivity and Hall-effect measurements on *n*-type layers that were inhomogeneously doped by ion implantation (Johnson, Herring, and Chadi, 1986b) and uniformly doped during epitaxial growth (Johnson, Herring, and Chadi, 1987). In both materials, the decrease in the free-electron density after hydrogenation was accompanied by an increase in the effective Hall mobility. This is consistent with reduced ionized-impurity scattering due to neutralization of donor dopants, but not with the generation of physically separate H-associated compensating defects. Total-energy calculations find an energy minimum when the interstitial H atom is situated antibonding to a Si atom that is adjacent to the substitutional donor atom (Johnson, Herring, and Chadi, 1986b; Chang, and Chadi, 1988), as depicted in Fig. 9 for the case of the P dopant. Spectroscopic evidence for such donor neutralization in Si was obtained from IR-absorption measurements and provides support for the microscopic model (Bergman, Stavola, Pearton, and Lopata, 1988).

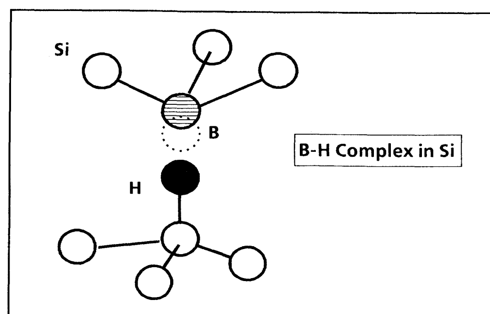

FIG. 8. Structural model for the acceptor-H complex in Si. From Chang and Chadi (1989b).

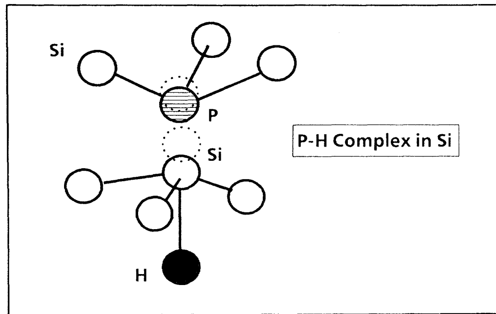

FIG. 9. Structural model for the donor-H complex in Si. From Zhang and Chadi (1990).

Particularly detailed information on the H complexes with shallow group-III acceptors and shallow group-V donors has come from IR vibrational spectroscopy. The measured vibrational frequencies give clues to the identity of a defect complex and to its bonding configuration, and also provide an important benchmark for theoretical treatments of the bonding (Stavola and Pearton, 1991). Moreover, the combination of such measurements with symmetry-breaking uniaxial stress permits the determination of the symmetry and reorientation kinetics of the defect. In the case of the acceptors, H stretching bands have been identified for B-H, Al-H, and Ga-H complexes and lie near 2000 cm^{-1} (Stavola *et al.*, 1987). These vibrational frequencies are in good agreement with theory (DeLeo and Fowler, 1991) for the defect configuration of Fig. 8, engendering confidence in the structural model. The transverse H stretching modes of the acceptor-H complexes have not been found, however; they are presumably located in a low-frequency spectral region where they are difficult to observe, and may be related to poorly understood low-frequency excitations of the complexes.

The donor-H complexes P-H, As-H, and Sb-H give rise to H stretching and wagging vibrations near 1560 and 810 cm^{-1}, respectively (Bergman, Stavola, Pearton, and Lopata, 1988). These data provided the essential spectroscopic confirmation of the existence of the donor-H complexes. Moreover, there is little dependence of the vibrational frequency upon donor species, and this supports the structural model of Fig. 9 in which the H is attached to one of the donor's Si nearest neighbors rather than to the donor itself.

Uniaxial-stress studies of the As-H and B-H complexes show that these complexes have trigonal symmetry (Bergman, Stavola, Pearton, and Hayes, 1988). In the case of the B-H center, stress experiments have been used to produce alignment and then to measure the reorientation kinetics (Stavola, Bergman, *et al.*, 1988). The reorientation occurs through the motion of H between equivalent sites about the B, with an activation energy of 0.19 eV, as shown in Fig. 10. This makes another important contact with theory (Denteneer *et al.*, 1989a). An important remaining question concerns the significance of quantum effects in describing the motion of light H

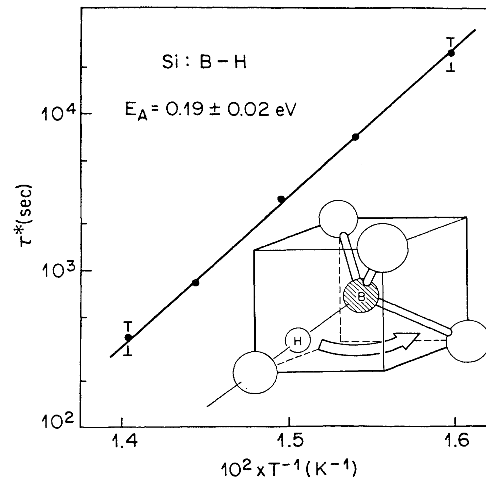

FIG. 10. Temperature-dependent time constant for the decay of stress-induced dichroism in the IR spectrum of the B-H complex. The inset shows the path of H jumps among the bond-center sites (from Stavola, Bergman, *et al.*, 1988).

(Stoneham, 1989).

In addition to the dopant-H complexes, a number of other IR features are introduced by the ion implantation of H into Si (Stein, 1975). These spectra are still poorly understood, although some recent progress has been made in studies by Nielsen *et al.* (1989b).

B. Deep levels and native defects

Lattice defects can arise during growth, during such processing steps as ion implantation, and during service as in the radiation environment of space. The electrical passivation of these damage centers by H provided an early and continuing motivation for the study of H in semiconductors. For example, in 1966 Gray and Brown reported a reduction in the density of electrically active states at the SiO_2-Si interface when the oxidation was performed in wet oxygen, and this effect was recognized as due to the passivation of the interface states by H. Thus one motivation for the study of H in semiconductors is its use in the removal, at least electrically, of defects. Another motivation, and increasing a major one, is the use of H decoration as a tool in studying the defects. Infrared studies in particular, following the pioneering work in Si by Stein (1975), have been very fruitful in this regard and hold considerable promise for the future, as we shall describe.

Experimental studies of H-related defects within crystalline semiconductors have encompassed point, line, planar, and volume imperfections, as discussed in a number of reviews (Pearton, Corbett, and Shi, 1987; Chevallier and Autocouturier, 1988; Corbett, Lindström, Pearton, and Tavendale, 1988; Corbett, Lindström, Snyder, and Pearton, 1988; Deák *et al.*, 1988a; Pearton *et al.*, 1989; Corbett, Pearton, and Stavola, 1990). The point defects include those occupying, or sharing, a single lattice site, such as substitutional impurities and impurity intersti-

tials, vacancies and self-interstitials, and antisite defects in compound semiconductors. It is now recognized that the vacancy and self-interstitial are mobile at room temperature in Si and many other semiconductors, so that the observed defects are products of aggregation or impurity trapping. Aggregates of point defects can occur, resulting in what are still small, essentially point defects, or in line, plane, and volume defects. Dislocations are the most prominent type of line defect; they arise in plastic deformation and have attendant point defects, which contribute to the electrical activity. Grain boundaries may be viewed as arrays of dislocations. There is much interest in H passivation of dislocations and grain boundaries, but knowledge of the atomic configuration and bonding of H at these extended defects remains very limits. (See, for example, Seager and Ginley, 1979; Pohoryles, 1981; Osip'yan *et al.*, 1982; Hanoka *et al.*, 1983; Dubé and Hanoka, 1984; Dubé *et al.*, 1984; Kazmerski, 1985; and Seager *et al.*, 1987.)

It seems clear that the H can interact with the dangling bonds associated with dislocations, thereby affecting the reconstruction of the core and subsequently leaving the structure altered when the H dissociates. A detailed microscopic understanding is lacking, however. The interaction of H with the reconstruction of the dislocation core is supported by the recent observation (Kisielowski-Kemmerich *et al.*, 1990) that H aids dislocation motion in Si at high temperature. Further, it is well known (Corbett *et al.*, 1989) that H causes embrittlement of Si at low temperatures, and recently (Zhang and Haasen, 1989) the influence of H on the brittle-to-ductile transition has been studied. These mechanical effects of the H have striking parallels to the phenomena reported in Sec. IV for metals.

The interaction of H with interfaces has been investigated in detail for two cases, the Si-SiO_2 interface and the bare Si surface. The Si-SiO_2 (100) and (111) interfaces contain a technologically important dangling bond, which has been shown by electron paramagnetic resonance (EPR) to reside on a Si atom at the Si side of the interface (Brower, 1989). This electrically active center is passivated by the formation of a Si-H bond with dissociation energy 2.5 eV, as demonstrated in further EPR experiments (Brower, 1988, 1990; Brower and Myers, 1990). Dangling bonds on the Si (100) and (111) bare surfaces are also passivated by formation of Si-H, and these interactions have been extensively examined through IR spectroscopy, low-energy electron diffraction (LEED), scanning tunneling microscopy, and thermal release from external surfaces and internal surfaces (Chabal *et al.*, 1983; Schulze and Henzler, 1983; Chabal, 1986; Gupta *et al.*, 1988; Koehler *et al.*, 1988; Jansson and Uram, 1989; Boland, 1990; Higashi *et al.*, 1990; Sinniah *et al.*, 1990; Mortensen *et al.*, 1991; Reider *et al.*, 1991; Wise *et al.*, 1991; Myers *et al.*, 1992). The strength of the Si-H bond is again found to be near 2.5 eV (Myers *et al.*, 1992).

Hydrogen interacts with dilute oxygen impurities in Si in ways that have important technological consequences but are not well understood. The O is believed to have at least two paths of precipitation. The homogeneous-precipitation process apparently leads to the O-related thermal double donors observed upon annealing at 450 °C. Hydrogen enhances the formation rate for these thermal donors near 400 °C (Fuller and Logan, 1957; Brown *et al.*, 1988; Stein and Hahn, 1990); the underlying mechanism is incompletely understood, but recent theoretical calculations indicate that it may involve H-assisted O hopping (Estreicher, 1990). Once formed, these electrically active centers can be passivated by H at lower temperatures (Johnson and Hahn, 1986; Pearton, Chantre, *et al.*, 1986). In contrast, heterogeneous precipitation of O at lattice imperfections leads to the formation of amorphous SiO_x precipitates and to carrier recombination centers, which again can be H passivated. Hydrogen introduced by ion implantation has also been related to shallow donors at $E_c-0.026$ eV, where E_c is the energy at the bottom of the conduction band (Schwuttke, 1971; Ohmura *et al.*, 1972, 1973; Gorelkinskii *et al.*, 1974; Kimerling and Poate, 1974; Obodrikov *et al.*, 1976; Gorelkinskii and Nevinnyi, 1983); in view of their energy, these are presumably single donors. It is not clear whether O precipitation is involved in these defects, as it appears to be in the 450 °C thermal donors. There is not a dramatic difference in the occurrence of these centers between Czochralski and float-zone Si, whose O contents are greatly different. In view of the dramatic radiation-enhanced diffusion of O that has been observed (Oates *et al.*, 1984; Pflueger *et al.*, 1985), however, the possibility of O involvement remains. We expect that eventually the role of H in all these processes will be clarified, leading to a much improved understanding of the defects themselves.

Ion implantation of H produces marked electrical and optical changes in semiconductors. The defect structures produced by the collisional displacements tend to be simple, since the energy transferred is on the average small. Implantation of H into Si at room temperature an energy of 300 keV leads initially to deep H-related centers and then to the formation of shallow donors when the material is annealed in the range 300–500 C. Comparative studies using H and He implantation served to determine which of the defect centers were H related (Irmscher *et al.*, 1984). After room-temperature implantation, this work identified five electron traps at $E_c-0.01$ eV, $E_c-0.13$ eV, $E_c-0.32$ eV, $E_c-0.41$ eV, and $E_c-0.45$ eV, respectively, and one hole trap at $E_v+0.28$ eV, where E_v is the energy at the top of the valence band. Proton implantation of a sample at 80 K produced a H-related level at $E_c-0.18$ eV, which was tentatively assigned to either a $(V\cdot H)$ complex or an $(I\cdot H)$ complex, where V denotes the vacancy and I the Si self-interstitial. The levels found following the room-temperature implantation were also found following implantation at 80 K and subsequent annealing to room temperature. Svensson *et al.* (1990) carried out similar experiments at

low implantation fluences and found H-related centers at $E_c - 0.32$ eV and $E_c - 0.45$ eV. Implantation of *p*-type Si with 7 MeV H created four H-related electron traps observed (Mukashev *et al.*, 1979a) after annealing to 500 °C.

Electron irradiation should result in even simpler defects than proton implantation, since the average collisional interchange of energy is substantially smaller in the former case. Comparisons of irradiation with 5-MeV electrons on Si grown in either H_2 or Ar revealed H-related electron traps at $E_c - 0.08$ eV and $E_c - 0.20$ eV and a hole trap at $E_v + 0.10$ eV. Comparison of the thermal recovery of defects observed in both H-grown and Ar-grown crystals also showed a pattern of annealing that seems to be general: the recovery temperature of the defects in the H-grown samples, as determined from electrical measurements, converged to the range of 180–200 °C for *p*-type and to 250–270 °C for *n*-type material, in contrast to the recovery temperature of the same defects in Ar-grown crystal, which recover 80–150 °C higher. The same tendency was found for defects produced by thermal-neutron irradiation of float-zone Si that had been grown in H (Du *et al.*, 1985). In these studies, the $(V \cdot O)^-$, $(V \cdot P)^-$, and $(V \cdot V)^-$ centers were observed, and the presence of H reduced the apparent annealing temperature for the $(V \cdot O)^-$ center from 350 °C to 250 °C. These results are believed to reflect H passivation of the defects at a temperature below the onset of their thermal annihilation. The thermal-neutron irradiations also produced a H-related level at $E_c - 0.20$ eV, and this was attributed to a vacancy-H complex. Subsequent annealing at 250 °C yielded a new level at $E_c - 0.35$ eV, and it was attributed to a vacancy-H-O complex.

We noted that the presence of H causes a lower recovery temperature. It has also been observed that the presence of H causes a lower apparent damage-production rate for irradiations at room temperature; this is seen, for example, in the case of the $(V \cdot O)^-$ center. This is believed to indicate either a passivation of the defects by the H or competing formation of H-related defects. Judging from the high-temperature measurements of H diffusion and permeation (Van Wieringen and Warmoltz, 1956; Myers, 1988) and studies of the diffusion profiles of H in Si (Capizzi and Mittiga, 1987; Kalejs and Rajendra, 1989; Mathiot, 1989; Seager and Anderson, 1990a); H should be quite mobile at room temperature, but would normally be trapped; the extent to which irradiation can free trapped H has not been established, but this process clearly may be important.

Following Stein's pioneering work (1975), many H-related IR bands have been observed in implanted Si in the Si-H bond-stretching frequency region around 2000 cm^{-1}, and others have been found in the bond-bending and bond-wagging regions (Gerasimenko *et al.*, 1979; Cui *et al.*, 1979, 1982, 1984; Mukashev *et al.*, 1979b, 1989; Ma *et al.*, 1981; Zhang and Xu, 1982; Bai *et al.*, 1985; Qi *et al.*, 1985; Shi *et al.*, 1985; Nielsen *et al.*, 1989a). One can envision a chemically driven partial dissociation of H-saturated multivacancy defects that will result in Si-H, Si-H_2, and Si-H_3 configurations in crystalline Si, but that alone will not explain the multiplicity of bands (and presumably of defects). Broad absorption bands have also been observed in amorphous Si and attributed to Si-H, Si-H_2, and Si-H_3. In discussing the H-related spectra in substituted silane molecules, Lucovsky (1979) showed that the frequency correlated with the electro-negativity of the neighbors of the Si to which the H is attached. It was then shown (Sahu *et al.*, 1982) that this correlation could be put on a quantum-chemical basis, in that the frequency of these bands depends on the bond character (i.e., the amount of *s*- and *p*-mixing) of the Si-H bond, with the bond character determined by both the chemical environment of the defect and the associated strain. With this approach the vibrational stretching frequency of many configurations was predicted (Lucovsky, 1979). Strong support for this approach was provided by experiments (Qi *et al.*, 1985) showing an agreement between experiment and the predicted frequency for vibration of an Si-H complex with an adjacent O atom. The specific structure of that defect, however, and those of the many other defects remain to be worked out.

A central problem in establishing the structure of the above H-defect centers is that both vacancy-related and interstitial-related defects can have the same bond character, leading to ambiguity in identifications based on IR spectroscopy alone. Moreover, until recently, theoretical work has reflected this same ambiguity (Singh *et al.*, 1977, 1978; Deák, *et al.*, 1988b; DeLeo and Fowler, 1988; Frolov and Mukashev, 1988). Now, however, both experiment and theory appear to discriminate between these two types of defects; should these results be confirmed by subsequent work, this could be a major breakthrough in the use of H to decorate defects. The experimental advance was that of Mukashev *et al.* (1989), who found that the H-D isotope dependence and the temperature dependence of the IR bands indicate a difference between the bands lying above and below 2000 cm^{-1}. These authors suggested that bands above 2000 cm^{-1} are due to vacancy-related defects, while bands below 2000 cm^{-1} are predominantly interstitial related. This same trend is observed in recent theoretical work by Deák, Heinrich, Snyder, and Corbett (1989), which led those authors to suggest specific models for a number of the bands. Should these studies lead to unraveling the fate of interstitial defects in Si, it would be a major advance. We note also that Mukashev *et al.* (1989) observed H-related changes in the vibrational frequency of the Si-O-Si part of the $(V \cdot O)$ center apparently corresponding to H occupying one and two of the Si dangling bonds of the defect; these frequency shifts were the same as those occurring when an electron occupies the dangling-bond part of the defect and are consisting with the theoretical view that the H of a dangling bond has a net negative charge. Again this work suggests the exciting promise of using H decoration to investigate the structure of defects.

C. Hydrogen-induced defects

It has been demonstrated that hydrogenation of Si can produce extended structural defects appearing as platelets with (111) orientation (Johnson, Ponce, *et al.*, 1987; Jeng *et al.*, 1988; Johnson *et al.*, 1992). These defects can be induced in single-crystal Si by exposure to monatomic H downstream from a H plasma. Although plasma damage could conceivably enhance the rate of generation of these defects or cause other defects, the evidence continues to support the conclusion that the platelets are H induced and H stabilized. Hydrogen-induced electronic defects have also been detected in hydrogenated Si by means of luminescence spectroscopy and deep-level transient spectroscopy (Johnson, Ponce, *et al.*, 1987).

It has been proposed that the above platelets form when a number of H atoms in bond-center sites interact through their associated distortions to create an extended planar defect (Johnson, Ponce, *et al.*, 1987). Calculations on such a defect have been performed (Corbett *et al.*, 1989; Ortiz *et al.*, 1990; Zhang and Jackson, 1991), and it was found that the strain interaction will stabilize the planar configuration. Hydrogen atoms bond in the same orientation on a succession of Si atoms without forming a molecule, and thereby form an incipient crack, a prototype of a defect causing the brittleness of Si grown in H_2 gas.

D. Charge states of migrating hydrogen

The charge state of isolated H within Si is an important issue because of its influence on migration and, equally significant, its effect on the rate of trapping reactions with charged dopants. There is now evidence that H can exist in Si as an amphoteric center with positive, neutral, and possibly negative charge states; for simplicity the associated H-Si complexes are designated as H^+, H^0, and H^-. The distribution of the H among these states, and hence its diffusion rate and reactivity, should depend on the position of the Fermi level. At this point we cite experimental evidence for the various charge states; discussion of theory, and the closely related matter of atomic bonding configurations, will be deferred to Sec. VIII.B.

The deep-donor level yielding H^+ was hypothesized to interpret experimental results for H diffusion and shallow-acceptor neutralization in *p*-type Si (Johnson, 1985a; Tavendale *et al.*, 1985; Capizzi and Mittiga, 1987; Pantelides, 1987). Strong support for the existence of such a deep-donor level was obtained from the study of H immobilization in Si *p-n* junctions, as discussed in Sec. VI.E. Other hydrogenation data (Seager and Anderson, 1988), electron-paramagnetic-resonance detection of atomic H (Gorelkinskii and Nevinnyi, 1987), and muon spin resonance (Kiefl and Estle, 1991) all point to a stable H^0 state.

In *n*-type Si, H neutralizes shallow-donor dopants (Johnson, Herring, and Chadi, 1986b, 1987), and theory suggests (Johnson, Herring, and Chadi, 1986b; Chang and Chadi, 1988) that this arises from the formation of a complex involving the dopant and H^-. It was only recently experimentally inferred (Tavendale, Pearton, and Williams, 1990; Zhu *et al.*, 1990) that H can migrate in Si as a negatively charged species. The evidence is the combined observation of a strong electric-field dependence in the rate of removal of (P·H) complexes during bias-temperature stress of hydrogenated Schottky-barrier diodes and the resulting spatial redistribution of neutralized donors. It should be noted, however, that this interpretation has recently been questioned, and an alternative interpretation of the experimental data has been suggested (Seager and Anderson, 1990b; Seager *et al.*, 1990). As a result the existence of H^- within crystalline Si remains controversial. The presence of H^- would imply that, in addition to the previously determined deep-donor level, there also exists an acceptor level for H in the Si band gap.

E. Hydrogen dimerization

The depth profile of H that results from its diffusion through a *p-n* junction in single-crystal Si at moderate temperatures can be highly structured, with features that depend on the reverse bias applied during H diffusion (Johnson and Herring, 1988). In n^+-*p* junctions subjected to plasma hydrogenation at 200 °C, a prominent peak appeared in the distribution at the edge of the bias-dependent depletion layer in the *p*-type material, as seen in Fig. 11. The resulting H concentration greatly exceed-

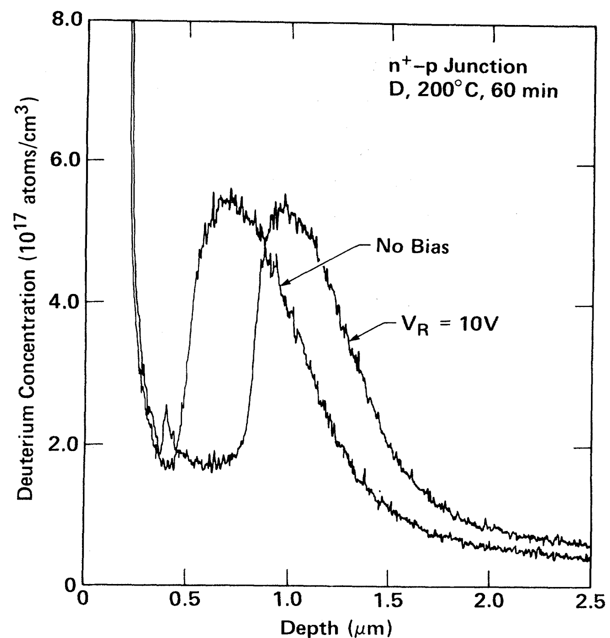

FIG. 11. Deuterium depth profiles in n^+-*p* junction diodes, with and without a reverse bias V_R during the plasma deuteration treatment. The junctions were formed by implanting P into *p*-type (1×10^{17} B/cm^3) Si, followed by furnace annealing, to electrically activate the dopants. From Johnson and Herring (1988).

ed the local B concentration, which was approximately 1×10^{17} cm^{-3}. Most of this H accumulation was found to be in the form of highly immobile neutral entities. It was then proposed that these entities were H pairs, H_2. Formation of H_2 by the conventional reaction $2H^0 \rightarrow H_2$, however, is incapable of accounting for the bias-dependent structure in the depth profiles. It was consequently inferred that the competing reaction $H^+ + H^0 \rightarrow H_2 + h^+$, with h^+ denoting a free hole, becomes dominant in p-type regions, at least at 200 °C.

The stable, immobile species that is found in p-type Si after hydrogenation at 200 °C does not form appreciably in moderately doped n-type Si (Johnson and Herring, 1989a). This was shown by observing the effect of subsequent vacuum annealing on the depth profile of the H; the results suggest instead the presence of a mobile but charge-neutral hydrogenic species. The presence of neutral monatomic H in such high concentrations would have to be reconciled, however, with the universal failure, to date, of attempts to observe the electron-spin resonance of this species at or above room temperature. One could try to avoid these difficulties by postulating that most of the H is in the form of neutral diatomic complexes. However, these could not be the stable "molecules" found in the p-type material, since the latter are highly immobile; rather, one must postulate a different, metastable complex, $H_2{}^*$. A possible microscopic model has been proposed by Chang and Chadi (1989a), whereby a Si-Si bond is replaced by two Si-H bonds, as discussed in Sec. VIII.B.3.

F. Hydrogen migration

It is possible to obtain considerable information about H in Si from studies of its diffusion. The transport is rather complex because monatomic H can exist in multiple charge states—notably H^+ and H^0 in p-type material and H^0 and perhaps H^- in n-type material—and because the H appears to be present in a number of different configurations including atomic, diatomic, and bound to a defect or impurity. Simple diffusion of H in a material satisfies Fick's equation, which for a constant diffusion coefficient D and fixed surface concentration $[H]_0$ has the solution (Carslaw and Jaeger, 1959)

$$[H]=[H]_0 \operatorname{erfc}[x/(4Dt)^{1/2}] , \tag{5.1}$$

where x is the depth within the specimen and t is the diffusion time. A consequence of this equation is that the mean diffusion depth is proportional to $(Dt)^{1/2}$. In Si, however, the shape of the H depth profile and its scaling with time often depart greatly from these predictions due to the complications enumerated above.

In the case of p-type Si, results from numerous diffusion experiments have been interpreted in terms of the following reactions:

$$H^+ + B^- \rightarrow (H\cdot B) , \tag{5.2}$$

$$H + (H\cdot B) \rightarrow (B\cdot H\cdot H) , \tag{5.3}$$

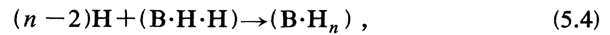

$$(n-2)H + (B\cdot H\cdot H) \rightarrow (B\cdot H_n) , \tag{5.4}$$

$$H + H \rightarrow (H\cdot H) . \tag{5.5}$$

Equation (5.2) reflects the Coulombic interaction between the charged B and a charged H. Equations (5.3) and (5.4) then describe the capture of additional H atoms by a B; the diffusion profiles suggest that this process extends to $n \sim 8-16$, and there is direct evidence for an additional, weakly bound H in current-voltage measurements (Lindström *et al.*, 1989). Theoretical studies have suggested that such H agglomeration may occur at least in part without the formation of H_2 molecules, in the manner discussed in Sec. V.C, leading to the formation of H-stabilized platelets (Chang and Chadi, 1989a; Corbett *et al.*, 1989; Ortiz *et al.*, 1990). Further theoretical work (Korpas *et al.*, 1990, 1991) is being carried out on the agglomeration process for $n < 8$ at a B site in Si. Finally, Eq. (5.5) describes direct molecule formation.

Diffusion in n-type Si has been proposed to include the following reactions:

$$H^- + P^+ \rightarrow (H\cdot P) , \tag{5.6}$$

$$H + P \rightarrow (H\cdot P) , \tag{5.7}$$

$$H + (H\cdot P) \rightarrow P + (H\cdot H) , \tag{5.8}$$

$$(2n)H + P \rightarrow P + (H\cdot H)n , \tag{5.9}$$

$$H + H \rightarrow (H\cdot H) . \tag{5.10}$$

Equations (5.6) and (5.7) indicate the reaction of a single H with the donor P, with Eq. (5.6) expressing the possibility of a Coulombic interaction. The available diffusion data in bulk Si do not require this reaction; i.e., there is no evidence of a negatively charged H in n-type Si in the resistivity range 0.1–100 Ω cm. Johnson and Herring (1989b) and Tavendale, Pearton, and Williams (1990), however, have found evidence of H^- in drift experiments; so the Coulombic reaction may occur. Where the energy levels of the states of H are located remains an important question. Equation (5.8) indicates that a second H may reactivate the P, a process included to account for the observed incomplete deactivation of the dopant (Stavola *et al.*, 1987; Bergman, Stavola, Pearton, and Hayes, 1988; Bergman, Stavola, Pearton, and Lopata, 1988) and the fact that the diffusion profile does not show the plateau associated with impurity trapping in B-doped Si.

It has been found that the simpler diffusion profiles, such as those observed in 1 Ω cm p-type and 100 Ω cm n-type Si, can be fitted with physically reasonable parameters; for example, the deduced capture radii for the dopant trapping processes discussed above are in the nanometer range. It has also been observed, however, that the parameters obtained in fitting an isolated part of the profile are not unique (Borenstein *et al.*, 1990). Nevertheless, there are grounds for optimism that a definitive parametrization can be achieved, particularly since some of the values are expected to be common to multiple experimental conditions.

There is considerable scatter in the published data for diffusion of H in Si (Pearton, Corbett, and Shi, 1987; Corbett, Lindström, Snyder, and Pearton, 1988; Pearton et al., 1989; Corbett, Pearton, and Stavola, 1990). Part of this results from the common presumption that the diffusion profile is described simply by Eq. (5.1) and that as a consequence the mean diffusion depth is proportional to $(Dt)^{1/2}$. In the presence of molecule formation and impurity trapping, however, these properties do not hold, and a more realistic treatment that explicitly includes the various reactions is required.

G. Future research

In general it can be said that great progress has been made in phenomenologically identifying the many interactions of H in Si. The mechanistic understanding of these processes is far less developed, however, and quantitatively predictive models of energetics and kinetics are virtually nonexistent. Focused fundamental research is especially important in the following four areas.

(1) Microscopic probes such as IR vibrational spectroscopy, ion channeling, and EPR should be used in conjunction with electrical measurements to characterize the structure and bonding of a wide range of H-defect centers. The considerable success that has been achieved for H centers associated with shallow donors and acceptors is indicative of the level of understanding that can be realized.

(2) The energetics of the H-defect interactions should be determined more quantitatively. This is central to the selection and thermal stability of the states, and it provides an important point of comparison with theory. There are important technological ramifications as well, since the thermal stability of H passivation is emerging as a decisive factor in its usefulness to device technology.

(3) A more definitive understanding of the multiple H solution states in Si is very desirable. This issue is central to all of the H interactions in Si.

(4) A realistic description of the kinetics of H diffusion and trapping should be developed. Such a formalism provides the essential connection between the atomic interactions and macroscopic properties.

VI. GERMANIUM

Germanium was the first crystalline semiconductor in which a number of shallow acceptor and donor complexes were unambiguously proven to contain H. This series of discoveries began in the 1970s, when several laboratories conducted research with the aim of producing ultrapure Ge single crystals for radiation-detector applications. For large-volume (10 to 200 cm^3) fully depleted Ge p-i-n diodes, which were to be used as charge-sensitive gamma-ray detectors, the net dopant concentration, equal to the difference N_A-N_D between acceptor and donor concentrations, was required to be $\lesssim 10^{10}$ cm^{-3}. Such a small net concentration can be obtained throughout large crystal volumes only with a purity level of approximately one electrically active center in 10^{12} Ge host atoms.

To date, a large number of novel acceptor and donor levels have been discovered and studied in this high-purity material. These levels are not related to the elemental impurities of the third or fifth group of the periodic table. We shall begin with a brief review of all these acceptors and donors. Many of them are impurity complexes and most contain H. The neutral impurities Si, C, and O are "activated" by H to form the monovalent shallow acceptors A(H,Si) (Hall, 1974, 1975; Haller et al., 1980), A(H,C) (Haller et al., 1980), and the shallow donor D(H,O) (Hall, 1974, 1975; Joós et al., 1980), respectively. A similar donor D(Li,O) had been found independently in the course of O studies (Haller and Falicov, 1978, 1979). Kahn et al. (1987) showed that the acceptors A(H,Si) and A(H,C) consist of trigonally distorted complexes that are randomly aligned along the four $\langle 111 \rangle$ axes. The donor D(H,O) exhibits an unusually sharp set of optical transition lines, which led to the notation "S" in early studies (Seccombe and Korn, 1972). An isotope shift of 51 μeV in the ground state of D(H,O) upon substitution of H with deuterium (D) was the first direct proof of the presence of H in the center (Haller, 1978). D(H,O) has a complicated 1s-state manifold, which has been explained in terms of the tunneling of the H ion between four equivalent real-space positions along the $\langle 111 \rangle$ axes.

The study of the incompletely passivated multivalent acceptors Be, Zn, and Cu in Ge has provided especially interesting physics. Crystals doped with the double acceptors Be and Zn at concentrations of 10^{14} to 10^{15} cm^{-3} have been developed in recent years for far-IR photoconductive-detector applications (Haegel, 1985; Haegel and Haller, 1986). In Ge:Be and Ge:Zn crystals containing H, one finds the shallow single acceptors A(Be,H) and A(Zn,H) (McMurray et al., 1987). Kahn et al. (1987) have shown that these two acceptors have trigonal symmetry, like A(H,Si) and A(H,C) discussed above. In Ge:Cu crystals, which played an important role as photoconductive material in the past, one can generate $A(Cu,H_2)$ acceptors (Kahn, 1986; Kahn et al., 1986). This semishallow monovalent acceptor complex consists of a substitutional Cu impurity that binds two interstitial H atoms.

In dislocation-free pure Ge crystals grown in a H_2 or D_2 (deuterium) atmosphere, one always finds an acceptor with an energy level at E_v+80 meV (Haller, Hubbard, Hansen, and Seeger, 1977). This acceptor has been assigned to a divacancy-H complex. As an effective hole trap it renders ultrapure, dislocation-free Ge crystals useless for radiation-detector applications. Radiation-detector Ge typically contains 100–1000 dislocations/cm^2 in order to provide sinks and thereby to suppress the formation of vacancy clusters and divacancy-H complexes.

Besides the electrically active complexes discussed

above, there is indirect evidence for the existence of neutral complexes. In close analogy to the observations in Si and several III-V materials, it appears that H passivates deep and shallow acceptors. Because of the small concentrations of these neutral centers, all attempts to detect them directly with IR vibrational spectroscopy or EPR have been unsuccessful.

It is noteworthy that H activation of neutral impurities in Ge was the first evidence of the electronic activity of H. All earlier attempts to detect physical or chemical effects of H in a semiconductor had failed. Several years after the discoveries in Ge, H "passivation" of shallow acceptors, i.e., the formation of a neutral complex consisting of a shallow acceptor and a H atom, was discovered in Si (Pankove *et al.*, 1983; Sah *et al.*, 1983). Since then, passivation of numerous shallow and deep impurities in Ge (Haller *et al.*, 1981; Haller, 1986), Si (Pearton, Corbett, and Shi, 1987), and a number of compound semiconductors has been studied and reported (Haller, 1989; Pajot, 1989). So far, H activation has been detected only in Ge. This is not necessarily an indication that activation does not occur in other semiconductors as well. One must remember that the concentrations of A(H,Si), A(H,C), and D(H,O) in Ge are very small indeed, and that the extraordinary purity of the host crystal facilitated their discovery.

Electrically active, H-containing centers are particularly interesting because their electronic structure may be influenced by the atomic configuration of the impurity complex. The reduced symmetry of an impurity complex can create splittings of the ground and of the bound excited states, leading to rich electronic dipole transition spectra in the far IR. Perhaps the most important advantage of electrically active centers is the fact that they can be studied with a wide range of sensitive techniques including variable-temperature Hall effect, photoconductivity, and far-IR high-resolution spectroscopy. Using photoconductivity techniques, concentrations of shallow levels as low as 10^6 cm^{-3} can be studied. The investigation of fully passivated dopants, on the other hand, is limited to less sensitive methods that require defect concentrations in excess of 10^{15} cm^{-3}.

A. Ultrapure germanium

In numerous trials with crystal-growth ambients that included vacuum, N_2, Ar, He, and H_2, only the H_2 environment yielded radiation-detector material with outstanding charge-collection properties. The superiority of H_2 was originally thought to result mainly from its purity and reducing action. It is now believed, however, that H passivates the majority of residual deep traps that are created either by impurities or by native defects. Early studies of H permeation in single-crystal Ge by Van Wieringen and Warmoltz (1956) and later by Frank and Thomas (1960) showed that H is a fast diffuser with a relatively low solubility, the latter quantity being between 10^{14} and 10^{15} cm^{-3} near the melting point. In a tritium (T) radiotracer experiment, Hansen *et al.* (1982) used a self-counting p-i-n diode to show that such concentrations of T remained trapped in ultrapure Ge when the crystal was cooled from the melting point to room temperature.

The number of characterization techniques that are sufficiently sensitive for this material and that are also useful in determining the impurity species and defect structure is small. Variable-temperature Hall-effect measurements in the Van der Pauw (1958) configuration allow the determination of $N_A - N_D$. The degree of compensation ($N_{\rm Minority}/N_{\rm Majority}$) is larger than 0.1 in typical ultrapure crystals, and such values do not permit an accurate extraction of minority impurity concentration from Hall-effect freeze-out curves (Blakemore, 1987). Moreover, ultrapure Ge becomes extrinsic only below approximately 180 K, which means that electrical measurements must be performed below this temperature if impurity effects are to be distinguished.

Radioactive-tracer experiments have yielded unique information in the study of ultrapure Ge. A number of crystals were grown in ^{14}C-coated silica crucibles and were subsequently studied with autoradiography (Haller *et al.*, 1982) and with selfcounting and spatially resolving radiation detectors (Luke and Haller, 1986). These measurements established a lower limit for C dissolved in Ge of 10^{14} cm^{-3}. They further showed that C is dispersed in crystals grown in a N_2 atmosphere but forms some clusters in crystals grown in a H_2 or D_2 atmosphere. This difference is still not understood.

Small amounts of T_2 were added to the H_2 growth atmosphere of some crystals. Radiation detectors fabricated from these crystals measure the energy distribution of the electrons created in the T decays inside the crystal (Hansen *et al.*, 1982). These studies set a lower limit on the H concentration between 10^{14} and 10^{15} cm^{-3}.

It is important to emphasize how small the concentrations of the various impurity complexes in ultrapure Ge are. Many of the powerful techniques including SIMS, Rutherford backscattering spectrometry (RBS), ion channeling, EPR, nuclear magnetic resonance (NMR), and IR vibrational spectroscopy are too insensitive to be useful for the study of these novel centers. For the study of the electronic structure of acceptors and donors present at the typical low concentrations, one uses photothermal ionization spectroscopy (PTIS) (Lifshits and Nad', 1965; Haller and Hansen, 1974a, 1974b; Kogan and Lifshits, 1977). This low-temperature technique combines a photo-stimulated transition of a hole (electron) from the 1s-like ground state to a bound excited state with a phonon-assisted transition from the bound excited state into the valence (conduction) band, as depicted in Fig. 12. There exists an optimum temperature range for PTIS in which the phonon density is sufficiently large to ionize bound carriers from an excited state to a band, but ionization from the ground state is still negligible. Once the hole (electron) has reached the valence (conduction) band, it increases the conductivity of the crystal. This

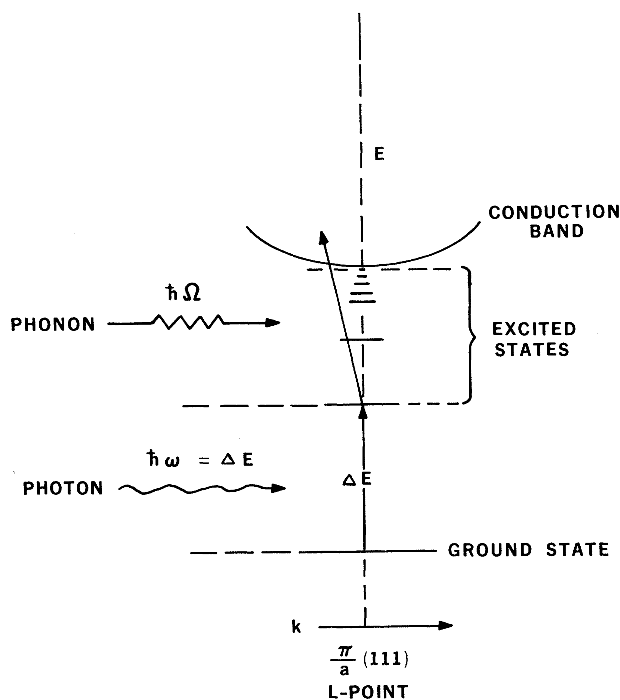

FIG. 12. The two-step ionization process which is the basis of PTIS.

conductivity increment is then measured as a function of the energy of the exciting IR photons.

B. Shallow-level complexes containing hydrogen

These complexes share a similar structure consisting of a substitutional impurity binding one H atom in its vicinity. Extensive far-IR spectroscopy has shown that the symmetry of these complexes is trigonal (Kahn *et al.*, 1987). This leaves essentially two choices for the position of the H atom: interstitial in one of the four antibonding directions, or located in one of the four bonds about the impurity.

The monovalent acceptors A(H,Si) and A(H,C) appear in ultra-pure Ge crystals grown from silica and graphite crucibles, respectively. A(H,Si) is generated through rapid thermal quenching ($\geq 150\,°C/s$) of a small sample from a temperature of about 425 °C (Hall, 1974, 1975). This acceptor complex dissociates at room temperature with a time constant of minutes. Substitution of D for H leads to the acceptor A(D,Si) with a 21 μeV deeper ground state. This isotope shift is direct evidence of the presence of H in the center (Haller, 1978). A(H,C) is present in as-grown crystals and dissociates around 200 °C. The maximum concentrations of these two acceptors in standard ultrapure Ge lie between 10^{11} and $5\times10^{11}\ cm^{-3}$, depending slightly on the crystal-growth conditions and the position in the grown crystal. It is important to recognize that only a very small fraction of the total concentrations of H, Si, or C participate in the formation of these electrically active complexes.

The centers A(Be,H) and A(Zn,H) form in crystals that are grown in a H_2 atmosphere and doped with Be and Zn, respectively (McMurray *et al.*, 1987). Both centers are stable to temperatures of about 650 °C, significantly higher than the dissociation temperatures of A(H,Si) and A(H,C). Assuming first-order reaction kinetics, Haegel (1985) determined the prefactors ν and the dissociation energies E for both centers. She found $\nu[A(\mathrm{Be,H})]=3\times10^{8}\ s^{-1}$, $E[A(\mathrm{Be,H})]=2.1\pm0.6$ eV, $\nu[A(\mathrm{Zn,H})]=3\times10^{12}\ s^{-1}$, and $E[A(\mathrm{Zn,H})]=3.0\pm0.3$ eV. Table V summarizes the 1*s*-state properties of the four static trigonal centers described in this subsection. It is interesting to note that the average value of the energy of the 1*s*-state in all four cases lies very close to the theoretical energy of effective-mass-like acceptors (Baldereschi and Lipari, 1976).

Recently, Denteneer *et al.* (1989a) performed calculations based on density-functional theory in the local-

TABLE V. Properties of acceptor complexes with two 1*s*-like levels in Ge.[a]

Acceptor complex	Level designation and binding energy (meV): Ground state	Excited state	Energy splitting (meV)	Average energy (meV)
A(H,Si)	$A(\mathrm{H,Si})_2$ 11.66	$A(\mathrm{H,Si})_1$ 10.59	1.07	11.13
A(H,C)	$A(\mathrm{H,C})_2$ 12.28	$A(\mathrm{H,C})_1$ 10.30	1.98	11.29
A(Be,H)	$A(\mathrm{Be,H})_1$ 11.29	$A(\mathrm{Be,H})_2$ 10.79	0.50	11.04
A(Zn,H)	A(Zn,H) 12.53	b		

[a]This list includes only those acceptor complexes with hole-binding energies in the range 8.4–12.6 meV. Although some species might possess more than two 1*s*-like levels, no more than two have been detected for those included here.
[b]A second 1*s*-like level has not been detected but is believed to exist.

density approximation for the acceptor A(H,Si) in Ge. They found a small H binding energy of approximately 50 meV and large barriers between the energy minima for the location of the negatively charged H ion. The energy minima are located in the antibonding directions near the T_d interstitial sites. These theoretical results are in good agreement with major experimental findings, i.e., the low thermal stability of A(H,Si) and its static trigonal structure.

Germanium crystals that contain the substitutional triple acceptor Cu (Hall and Racette, 1964), in conjunction with H, exhibit in PTIS a series of broad lines that belong to an acceptor with a ground state at 17.81 meV above the top of the valence band (Haller, Hubbard, and Hansen, 1977). PTIS studies over a range of temperatures have shown that this acceptor has a 1s-state that is split into a large number of components that are closely spaced (Kahn *et al.*, 1987). When thermally populated, each of the components of the 1s-state manifold acts as an initial state for optical transitions of the bound hole to one of the effective-mass-like excited states. This in turn explains why the lines of this center appear broad.

Partial substitution of H with D or T in the above center leads to additional series of lines that are all sharp, indicating an unsplit 1s-ground state. Spectra with and without the isotopic substitution of D are shown in Fig. 13. In crystals containing only Cu and D, one series of transition lines is observed that originates from a level at

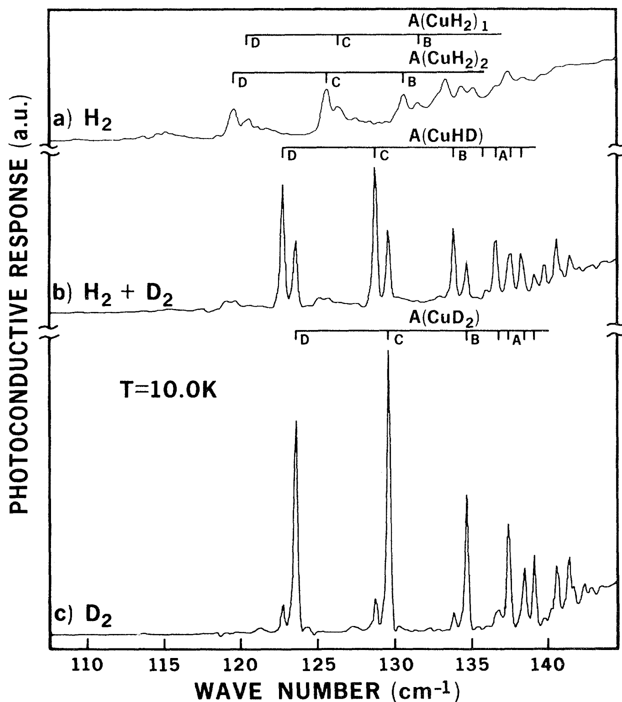

FIG. 13. PTIS spectra of Cu-dihydrogen acceptors in samples grown under different hydrogen isotopes: (a) pure H_2, showing the complex spectrum of $A(CuH_2)$; (b) a 1:1 mixture of H_2 and D_2, showing $A(CuH_2)$, A(CuHD), and $A(CuD_2)$ in a 1:2:1 ratio; (c) nearly pure D_2, showing $A(CuD)_2$ and a trace of A(CuHD).

18.20 meV above the valence band. In crystals containing H and D in equal concentrations, one observes not only the spectra related to H or D alone, but also an additional spectrum of an acceptor level at $E_v + 19.10$ meV, as seen in Fig. 13. The existence of this third series can be explained only if we assume that each Cu acceptor binds two H isotopes, forming $A(Cu,H_2)$, A(Cu,HD), and $A(Cu,D_2)$. This explanation has been reinforced with crystals containing most combinations of H, D, and T (Kahn *et al.*, 1986).

The difference between the 1s-ground state of $A(Cu,H_2)$, which is split into many closely spaced components, and the various combinations containing D and T has been attributed to a difference in symmetry. Uniaxial-stress studies indicate that $A(Cu,H_2)$ has full tetrahedral symmetry. This can be understood in terms of rapid tunneling of the H, which in turn explains the splitting of the ground state. In centers containing the heavier isotopes, tunneling ceases and the ground state is no longer split. The Devonshire (1936) model, which treats the energy levels of a hindered rigid rotor, qualitatively explains these observations. The model shows how the motion of a rotor changes from rotation to libration as the moment of inertia increases.

Rapid thermal quenching of standard ultrapure Ge samples from 425 °C generates A(H,Si). During annealing near room temperature of this acceptor complex, a donor complex D(H,O) forms. The maximum concentration of this complex reaches a few times 10^{11} cm^{-3} (Hall, 1974, 1975). Substitution of H with D leads to a ground-state shift of 51 μeV, a direct proof of the presence of H in the center (Haller, 1978).

Two experimental observations have made this donor a much debated impurity complex. First, D(H,O) produces extremely sharp lines that do not split under stress (Joós *et al.*, 1980). Second, at very high stress a new set of lines appears at lower energies. Besides these two basic features, a number of additional properties of D(H,O) have been revealed. Temperature-dependent PTIS studies by Navarro *et al.* (1986) have shown that the 1s-like state is split into several components. The spectroscopically determined splittings between the various 1s-state components do not correspond to the energies in the Boltzmann factors determined from variable-temperature PTIS studies. The differences have been explained in terms of nuclear-tunneling-induced splitting in the ground state and in the bound excited p-like states.

C. Deep-level centers and dislocations

The existence of H-vacancy centers in Ge was evidenced rather early (Haller, Hubbard, Hansen, and Seeger, 1977) by the observation of carrier trapping in ultra-pure, dislocation-free material and by the discovery of an acceptor level at $E_v + 80$ meV when the crystal had been grown in H_2. This level was observed in Hall-effect measurements, and it produces a strong, single-peak signature in deep-level transient spectroscopy (DLTS). Fur-

ther, thermal quenching and annealing experiments showed that the acceptor is subject to annihilation and regeneration through dissociation and recombination reactions; its maximum concentration is about 10^{13} cm^{-3} and is much smaller than the total H concentration. These findings, coupled with considerations of defect concentrations and defect mobilities in solidified Ge, led to the proposition that the acceptor level is due to a divacancy-H complex, V_2H. The reversible concentration are then explained by the reaction

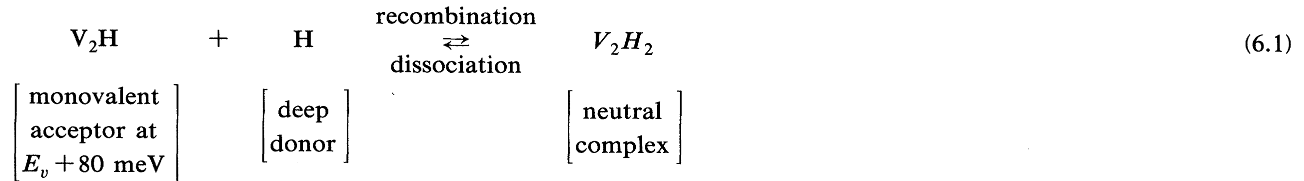

$$\underset{\begin{bmatrix}\text{monovalent}\\ \text{acceptor at}\\ E_v+80\text{ meV}\end{bmatrix}}{V_2H} \quad + \quad \underset{\begin{bmatrix}\text{deep}\\ \text{donor}\end{bmatrix}}{H} \quad \underset{\text{dissociation}}{\overset{\text{recombination}}{\rightleftarrows}} \quad \underset{\begin{bmatrix}\text{neutral}\\ \text{complex}\end{bmatrix}}{V_2H_2} \tag{6.1}$$

This reaction has been studied quantitatively in the recombination direction; the dissociation proceeds, for all practical purposes, instantaneously. Efforts have been made to obtain symmetry information on the V_2H center using DLTS with uniaxial stress and PTIS, but these were unsuccessful.

A number of deep-level impurities have been passivated by H, including Cu, Ni, Cd, Te, Zr, Ti, Cr, and Co (Pearton, Corbett, and Shi, 1987). Most of these studies have been qualitative, however, and important work remains to be done if the effects of hydrogenation are to be understood mechanistically. Moreover, additional impurities such as Au, Pd, Pt, and Fe are probably subject to H interactions.

In view of the large number of H interactions with point defects and impurities, it is not surprising that H binds to dislocations as well. Two kinds of studies have reported on H-dislocation interaction: DLTS studies on ultrapure Ge diodes and EPR investigations on a variety of Ge crystals. Hubbard and Haller (1980) demonstrated that the strength of a dislocation-related broad DLTS peak band was proportional to the dislocation density. In the same study, it was shown that crystals grown in a H_2 atmosphere generated broad, dislocation-related DLTS peaks at lower temperatures than crystals grown in N_2. With today's knowledge, we interpret this difference as reflecting partial passivation of the dislocation-generated levels in the band gap. Using dislocation-rich pure Ge crystals, Pearton and Kahn (1983) showed that a dislocation-related broad band in DLTS decreased in intensity upon plasma hydrogenation. This information is consistent with full passivation of dislocation bands by H. The DLTS studies of the effects of H on dislocation-related energy bands are qualitative, however, and do not provide microscopic information on the dislocations or the H sites.

In a very detailed EPR study, Pakulis and Jeffries (1981) and Pakulis (1983) investigated a large number of ultrapure Ge crystals that were grown in vacuum or in H_2 or D_2 atmosphere. Several of the samples were dislocation free. The sensitivity of EPR was greatly enhanced through the use of large cylinders of Ge. Besides the well-known shallow-donor-related lines, a large number of spin resonances related to dislocations were found in optically pumped samples. In H-free crystals, these resonances showed normal absorption character. In crystals grown in H_2 or D_2, however, the sign of the resonances switched. The reason for this reversal is not understood, but it is presumably related to the detection of the spin resonances by electrical measurements instead of the usual magnetic detection. Pakulis and Jeffries (1981) were able to identify two sets of lines. Four broad lines were aligned along $\langle 111 \rangle$ while a set of 24 sharp lines were aligned along $\langle 111 \rangle$ with a 1.2° distortion in all six $\langle 110 \rangle$ orientations. The authors explained their EPR data in terms of dangling bonds associated with variants of the 60° dislocations. The dangling bonds of a given dislocation point approximately along one of the $\langle 111 \rangle$ orientations. The small 1.2° tilt of the dangling bonds could either be due to an intrinsic distortion or be the result of a Peierls-like instability (Peierls, 1965).

D. Future research

Hydrogen has been shown to react with a wide range of imperfections in Ge, paralleling in many respects the more extensively investigated behavior of H in Si. The mechanistic understanding of these interactions remains quite limited, however, to an even greater degree than in Si, and this provides extensive opportunities for future fundamental research. The extraordinary purity and the control over crystal synthesis make Ge especially valuable for experiments that should be performed without interference from nearby defects and impurities. Areas warranting particular attention include the following.

(1) We have seen that H passivates, partially passivates, and even activates dopants in the Ge lattice. Most of these complexes have trigonal symmetry, but we do not know if H resides in the bonding or the antibonding position. To arrive at the exact structure of the various complexes is of considerable importance.

(2) The tunneling behavior of H in defect and dopant centers is a fundamental unresolved issue. We do not understand why H tunnels in some impurity complexes and not in others, and theory has given little guidance in this area. Significant progress can be made by identifying and characterizing additional tunneling centers. We expect

that partially passivated multivalent acceptors and perhaps donors offer the best prospects for finding such centers in Ge, Si, III-V and II-VI semiconductors, and their alloys. Theoretical work in this area should be encouraged.

(3) Very little is known about the states of isolated H in Ge. Results from muon spin resonance indicate two preferred locations which, for the case of Si, have been identified as the tetrahedral interstitial site and the bond-centered site. From the very strong similarity of the results in Ge and Si, we may conclude that these two sites are the preferred location for H in Ge as well. The relative populations of these centers, however, remains an outstanding issue.

(4) Electric-field-drift experiments on H ions can give mobility and charge state information. Such experiments have been very successful in Si and should be repeated in Ge. The higher reverse-leakage currents in the smaller-bandgap Ge diodes may pose experimental difficulties, but these considerations should not deter efforts to obtain such crucial information.

(5) The fundamental diffusion and permeation experiments from the '60s should be repeated. Today's improved crystal quality and instrumental sensitivity will allow measurements to be extended to substantially lower temperatures. It would be particularly significant if data could be obtained that directly show the formation of H_2 or impurity complexes.

VII. COMPOUND SEMICONDUCTORS

Hydrogen is readily introduced into III-V semiconductors where it forms stable complexes with a wide range of defects and dopants. This often has the effect of eliminating the electrical activity of the affected center; for example, as will be discussed, all of the shallow donor and acceptor impurities can be passivated. Technological applications exploit this passivation to improve materials properties, isolate devices, and fabricate device structures. Perhaps even more important is the unintentional introduction of H during semiconductor growth and processing; such H might migrate during device operation and thereby alter device characteristics. These considerations have motivated intensive efforts to understand the formation and properties of the H-defect complexes. While present knowledge is very limited from a fundamental viewpoint, combined experimental and theoretical studies are making rapid progress. The compound semiconductors are both more complicated and less studied than Si, and the range of issues needing attention is correspondingly greater.

Many of the principal techniques used to probe the microscopic properties of defects are not applicable to H-containing complexes because these passivated centers are usually not electrically active or paramagnetic. Infrared absorption, however, has proved especially effective in this area. The vibration of the light H in complexes occurs at frequencies well above intrinsic lattice absorption and in a range where sensitive photoconducting detectors are available. As a result the limits on detection are typically below 10^{16} H/cm^{-3}. In addition to the H vibrations, the perturbed local modes of the passivated dopant impurity can also be studied. Once a vibrational fingerprint has been identified for a defect complex, it can be used to study the stability and chemical reactions of the complex. Infrared absorption is also well suited to the application of uniaxial-stress techniques that provide information about defect symmetry and dynamics. Further, the vibrational characteristics provide a benchmark for theoretical treatments of the complexes.

A. Shallow donors in gallium arsenide

It is now well established that the donor impurities Si, Ge, Sn, S, Se, and Te can be passivated by association with atomic H (Chevallier, Dautremont-Smith, Pearton, *et al.*, 1985; Chevallier, Dautremont-Smith, Tu, and Pearton, 1985; Chung *et al.*, 1985; Pearton, Dautremont-Smith, *et al.*, 1986). In the case of Si-doped GaAs, for example, H-plasma hydrogenation causes a strong reduction in carrier concentration in the near-surface region, with the depth of the modification being inversely dependent on the initial Si doping level. At least some of the carrier removal in a thin layer ≤ 50 nm from the surface may be due to plasma-bombardment effects, but, from comparison with electrolytic H-insertion experiments, it is clear that donor neutralization at greater depths is due to H passivation. The passivation depth also varies as the square root of the plasma exposure time, indicating a diffusion-controlled process. Moreover, SIMS profiling of deuterated samples as a function of annealing temperature shows a rapid redistribution of the D at about 400 °C where the donor activity is restored. There is direct evidence for drift of H as a positively charged species in GaAs (Tavendale, Pearton, Williams, and Alexiev, 1990), and there are further indications that its properties are similar to those in Si, where mobile H^0, H^+, and possibly H^- occur as discussed in Sec. V (Pearton, Dautremont-Smith, Lopata, *et al.*, 1987). Assuming that this is the case, donor passivation in n-type GaAs can be represented by the equations

$$H^0 \rightarrow H^- + e^- \;, \tag{7.1}$$

$$S^+ + H^- \rightarrow (S^+H^-)^0 \;, \tag{7.2}$$

for the representative case of S donors.

The donor neutralization is caused by the formation of a H-donor bond utilizing the extra donor electron (Chevallier, Dautremont-Smith, Pearton, *et al.*, 1985; Pearton, Dautremont-Smith, *et al.*, 1986). This mechanism has support from a number of other experiments, and it is believed that the alternative model of compensation of the donors by separate H centers can be ruled out. The electron mobility in n-type samples increases upon hydrogenation but is restored to its initial value by annealing, and this is attributed to the reversible transformation of ionized donors into neutral complexes by the H (Jalil *et al.*, 1986). In addition, after hydrogenation, Si-

implanted GaAs samples exhibit a drastic reduction in the intensity of the luminescence lines belonging to recombination at the Si donors (Weber, Bantien, *et al.*, 1986; Weber, Pearton, and Dautremont-Smith, 1986). This reduction in luminescence intensity cannot be explained by the creation of nonradiative centers or new compensating acceptors, but it is in accord with the formation of H-donor bonds.

While all of the important donor dopants in GaAs have been passivated by H_2-plasma exposure, characterization by IR absorption has only been reported for H complexed with the two Ga-site donors Si and Sn. The study of GaAs:Si_{Ga}-H by Pajot, Newman, *et al.* (1988) is the most complete; it includes data for the stretching and wagging modes of H and D in the complex, their dependence upon Si isotope, and also data for the local mode of Si_{Ga}. The activation energy for release of the H from the complex was also examined and found to be 2.1 eV (Pearton, Dautremont-Smith, *et al.*, 1986). The H and D stretching spectra are shown in Fig. 14. It should be noted that the bands are at lower frequency than the H stretching band of acceptor-H complexes and that there are distinct sidebands observed due to the isotopes of Si; the lower frequency indicates a relatively weak bond to the H, and the sidebands indicate that the H is attached directly to the Si atom. The Si_{Ga}-H complex also exhibits a wagging mode, which is believed indicative of H in an antibonding configuration. Finally, there is a vibration at 384 cm^{-1} due to the isolated Si_{Ga} donor whose intensity is reduced upon plasma exposure. This body of IR data, with the further support of uniaxial-stress results and theory to be discussed below, provides a strong case for a configuration in which H is attached directly to the Si_{Ga} atom in an antibonding direction, as depicted in Fig. 15(b), rather than the bond-center arrangement shown in Fig. 15(a).

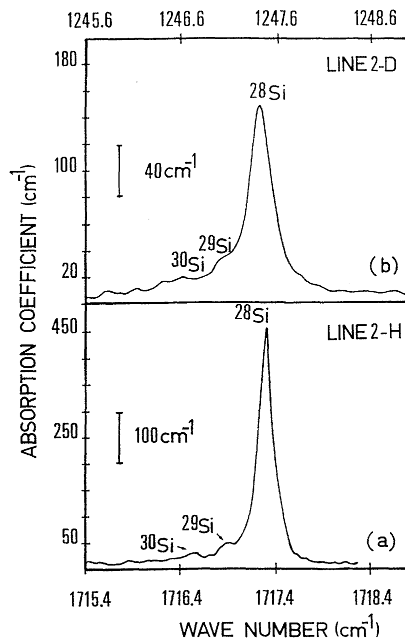

FIG. 14. Infrared-absorption spectra measured at 6 K for (a) the H stretching mode of the Si_{Ga}-H complex and for (b) the D stretching mode of the Si_{Ga}-D complex in GaAS (from Pajot, Newman, *et al.*, 1988).

Pajot (1990) has also examined the H stretching and H wagging modes of the Si_{Ga}-H complex under uniaxial stress. The stretching mode at 1717 cm^{-1} shows the trigonal splitting pattern expected for a nondegenerate mode under stress. The wagging band at 896.8 cm^{-1} is doubly degenerate without stress; the stress lifts both the orientational degeneracy and the vibrational degeneracy and gives a more complicated splitting pattern than the nondegenerate stretching mode. These results confirm the mode assignments and symmetry of the complex in detail and are fully consistent with the antibonding configuration proposed for this defect.

The Si_{Ga}-H complex has been treated theoretically by Briddon and Jones (1989), who calculated the electronic structure and total energy for a cluster of 56 atoms using a self-consistent, local-density-functional pseudopotential method. The antibonding H site shown in Fig. 15(b) was found to be greatly favored over the alternative, bond-center configuration of Fig. 15(a), in agreement with the conclusions from experiment. Moreover, the calculated vibrational frequencies are in fair agreement with IR measurements. The Si atom is also predicted to relax away from the As atom on the C_3 axis of the complex and into a more planar configuration, as represented in Fig. 15(b).

Stretching and wagging modes have also been observed for the Sn-H (or D) complex. The presence of the wagging mode indicates that Sn-H has an antibonding configuration. There is also a pronounced lowering in the vibrational frequencies when compared to those of the Si-H bond, and this difference is very similar to that between Sn-H and Si-H stretching frequencies in molecules. Hence GaAs:Sn-H is suggested to have an antibonding configuration with H attached directly to the Sn. The experimentally determined activation energy for H dissociation from the complex is 1.46 eV (Kozuch *et al.*,

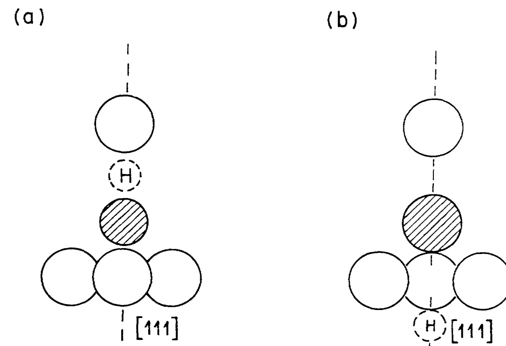

FIG. 15. Dopant-H structures in GaAs. (a) the bond-centered (BC) configuration of H complexed with a Ga-site shallow dopant; (b) the alternative, antibonding (AB) configuration of the H. The shallow dopant is shaded and the open circles represent As atoms.

1990).

It is interesting to compare the donor dependence of IR-absorption spectra obtained from donor-H complexes in the Si and GaAs hosts. In Si the frequency shift for a change of donor is much smaller, as observed, for example, between P and Sb. This is because in Si the H is not attached directly to the donor as in GaAs, but rather is bonded to a neighboring Si atom. The configuration still has H at an AB site, however, so that the mode frequencies and stress characteristics are similar for the two hosts.

B. Shallow acceptors in gallium arsenide

All of the investigated shallow-acceptor species in GaAs, namely, Be, Mg, Zn, Cd, C, and Si_{As}, are passivated by association with atomic H (Johnson, Burnham, *et al.,* 1986; Pan *et al.,* 1987; Pearton, Dautremont-Smith, Tu, *et al.,* 1987). The only reported reactivation energy is for Zn, where a value of 1.6 eV was measured. For the Ga-site acceptors Mg, Zn, Be, and Cd, the passivation mechanism appears to be the formation of an As-H bond, as first proposed by Johnson, Burnham, *et al.* (1986), rather than direct H-dopant bonding. This leaves the acceptor threefold coordinated, in analogy to the mechanism of acceptor passivation in Si. Under the assumption that H is in a positive charge state in *p*-type GaAs, with a donor level in the upper half of the band gap, one can write for the passivation of Zn acceptors (Tavendale, Pearton, Williams, and Alexiev, 1990)

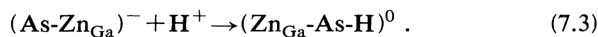

$$(\text{As-Zn}_{\text{Ga}})^- + \text{H}^+ \rightarrow (\text{Zn}_{\text{Ga}}\text{-As-H})^0 \ . \qquad (7.3)$$

The H is most likely in a bond-centered site under these conditions. In the special case of the Si_{As} acceptor in GaAs, there appears to be formation of a Si-H bond with the H located between neighboring As and Ga atoms, i.e., still in a bond-centered site. The passivation of Si_{As} acceptors can be written

$$(\text{Ga-Si}_{\text{As}})^- + \text{H}^+ \rightarrow (\text{Ga-Si}_{\text{As}}\text{-H})^0 \ . \qquad (7.4)$$

Infrared-absorption spectra have been reported for H complexed with acceptor dopants on both the Ga and As sublattices. The first Ga-site acceptor complex to be discovered was GaAs:Zn-H, but we focus on GaAs:Be-H because more is known about this defect. Indeed, it has become the model system for H complexed with Ga-site acceptors. In the absence of H, a local mode due to substitutional Be is observed. Upon passivation, this mode decreases in intensity and a new band appears at higher frequency. The frequency of the new mode has a small dependence upon the mass of the H isotope. These data prove that the Be and H have formed a close pair and interact at least weakly.

The frequency of the H stretching band for the Be-H complex (Stavola *et al.*, 1989), and the Zn-H complex as well, is close to the frequency of As-H bonds in molecules; this is consistent with the H being attached primarily to an As neighbor of the Be atom. The suggested configuration is then the bond-centered arrangement shown in Fig. 15(a). The B-H complex in Si is known to have a similar structure. This picture is reinforced by IR-absorption spectra from GaAs:Be-H obtained at a temperature of 15 K during application of uniaxial stress; the pattern is characteristic of a defect with trigonal symmetry. At temperatures above about 120 K, the H can hop between the four bond-center sites about the As. This H-jumping process is similar to what has been observed for the B-H complex in Si and suggests similar pathways for H motions in the two complexes.

Briddon and Jones (1989) have performed *ab initio* calculations for the bond-center configuration of the Be-H complex. The Be-H and As-H bond lengths are calculated to be 0.185 and 0.154 nm, respectively. The Be-As distance has been greatly expanded to accommodate the H. For their largest cluster, Briddon and Jones calculate a H stretching frequency of 2018 cm^{-1}. This result is in excellent agreement with the experimental value of 2037 cm^{-1}.

Much less is known about the As-site acceptors in GaAs. Stretching vibrations have been identified for GaAs:Si_{As}-H and GaAs:Ge_{As}-H. For Si_{As} the local-mode region for Si has also been examined to prove that the H-related vibration is due to H complexed with Si_{As} and not some other Si-related defect that is also present in such samples. It was suggested that the complex also has a bond-center configuration but with the H attached to the acceptor. Recent calculations by Briddon and Jones (1989) support this configuration.

Lastly, the GaAs:Mg-H complex shows only a very sharp, weak absorption in the H stretching region. The reason for its vibrational characteristics being different from the other Ga-site acceptors is not known (Pajot, 1990).

C. Dopants in other compound semiconductors

1. AlGaAs

Both donors and acceptors in AlGaAs are passivated by association with atomic H; this has been observed for the donors Si, Te, and Se and the acceptors Si and Mg (Pearton, Dautremont-Smith *et al.*, 1986; Chevallier and Aucouturier, 1988). Isochronal-annealing studies of Si-doped, H-passivated $Al_{0.3}Ga_{0.7}As$ showed that both the shallow donor and the *DX* center associated with Si recover their electrical activity at about 400 °C, corresponding to an activation energy of ~2.0 eV. There has been little systematic study of shallow-impurity neutralization in AlGaAs, although in most respects it behaves similarly to donor and acceptor passivation in GaAs. It will be interesting to see the effect of increasing Al composition on the characteristics and thermal stability of the dopant deactivation.

2. GaP

The only published report of dopant passivation by H in GaP has come from Weber and Singh (1988; Singh and Weber, 1989). These workers observed passivation of the S donor, the Ga-site acceptors Cd and Zn, and the P-site acceptor C; the intensity of the acceptor-related lines was strongly reduced after plasma exposure, as was the bound exciton line related to the S donor. In addition, the hydrogenation reduced the concentrations of electrically active N and N-N pairs; the substitution of N for P in GaP causes a strong relaxation around the impurity (Jaros and Brand, 1979; Weber and Singh, 1988; Singh and Weber, 1989), and this distortion apparently attracts the H. It is not clear whether H acts to relieve the strain around the N or whether there is formation of a polarized N^{-}-H^{+} complex. In the case of the N-N complex, the degree of passivation depends on the pair separation, with preferential bonding of H to the closer pairs. The thermal stability of shallow-impurity passivation in GaP is somewhat higher than for the corresponding cases in GaAs.

The passivation mechanisms for shallow-level dopants in GaP are presumably similar to those in GaAs. Therefore, the passivation of the S donor is probably the result of the formation of a S-H bond, whereas acceptor passivation may be due to H at a bond-centered site forming a P-H bond and leaving the Cd_{Ga} and Zn_{Ga} threefold coordinated. In the case of the C_P acceptor, the H may again be at the bond-centered position, attached to the C but weakly interacting with the neighboring P atom. We note at this point that no significant passivation was detected for the Mg_{Ga} acceptor. This is a surprising result whose explanation is not clear.

3. InP

The hydrogenation of InP poses special problems because of the degradation of the surface upon exposure to atomic H. It is therefore necessary to provide a simultaneous overpressure of P, or alternatively to protect the InP surface with an encapsulating layer that limits loss while being permeable to atomic H; such protective layers have included InGaAs (Antell *et al.*, 1988; Chevallier *et al.*, 1989; Dautremont-Smith, 1989; Lopata *et al.*, 1990) and SiN_x. A third alternative is direct proton implantation at low energies and at fluxes small enough to avoid surface degradation (Omeljanovsky *et al.*, 1989).

Early experiments showed a slight degree of passivation of Sn donors in InP, and a further report of donor passivation has appeared recently (Crookes *et al.*, 1990). A much stronger degree of acceptor deactivation is observed. Both Zn and Mn acceptors have been reported to be passivated by H (Antell *et al.*, 1988; Omeljanovsky *et al.*, 1989). In one case the source of H was AsH_3 present during the epitaxial growth in an InP-InGaAs structure (Pan *et al.*, 1987). The thermal stability of Zn passivation has been the subject of preliminary investigation only, but these studies showed an activation energy for reactivation of ~ 1.8 eV. There was a direct correlation of in-diffused D concentration and penetration depth with the depth and efficiency of Zn passivation. In the case of *n*-type InP doped with Sn or Si, the amount of D incorporated was approximately an order of magnitude below the donor concentration (10^{17} cm^{-3}), and donor passivation was not observed for plasma exposure temperatures as low as 75 °C (Dautremont-Smith *et al.*, 1989). In contrast, acceptor passivation was very strong, with usually a two-to-three-order-of-magnitude reduction in active hole concentration after plasma exposures between 125 and 250 °C.

Pajot *et al.* (1989) found sharp IR lines at 2288 cm^{-1} in hydrogenated InP(Zn), which shifted to 1665 cm^{-1} upon isotopic substitution with D. These are in the frequency range expected for P-H stretching bonds, and therefore the acceptor-passivation mechanism is probably the same as for GaAs; that is, the atomic H occupies a near-bond-center position and is predominantly bonded to a P atom, leaving the Zn threefold coordinated.

D. Point and extended defects

Clerjaud *et al.* (1987) have observed IR absorption by several H-passivated centers in as-grown bulk crystals of GaAs and InP which had not been deliberately H charged. Apart from its scientific significance, this is one of many examples of unintentional hydrogenation. Interpretation of these complexes is more difficult than for intentional passivation studies because the identities of the interacting defects or impurities are not independently known. Nevertheless, lines at 2001 and 2202 cm^{-1} in GaAs and InP, respectively, have been provisionally ascribed to H associated with the two vacancy centers V_{Ga} and V_{In}; supporting evidence includes the appearance of the InP line in H-implanted material and uniaxial-stress measurements showing that both centers have trigonal symmetry.

Ion implantation of H simultaneously produces numerous vacancies and self-interstitial atoms, and consequently this treatment provides a means of studying the interactions between H and point defects. Recently Stein (1990, 1991) performed IR-absorption measurements as a function of temperature on GaAs following H ion implantation at 80 K. Immediately after implantation the principal H-associated band is at 2029 cm^{-1}; this absorption is ascribed to an As-H bond, based in part on its occurrence also in H-implanted InAs. When the temperature moves above approximately 200 K, the As-H band decays and is replaced by a band at 1834 cm^{-1}, which had previously been identified as due to Ga-H (Newman and Woodhead, 1980; Pajot, Chevallier, *et al.*, 1988; Wang *et al.*, 1990); the Ga-H center then disappears near 500 K. The structures of these H-defect complexes have not been definitively established. Nevertheless, based on comparisons of the observed annealing behavior with current ideas concerning radiation-damage recovery in Ga-As, Stein has hypothesized that both complexes con-

sists of closely spaced self-interstitial-vacancy pairs with the H bonded to the interstitial component; the lower-temperature center is then (V_{As},I_{As}-H) while the entity annealing at 500 K is (V_{Ga},I_{Ga}-H).

Hydrogen also plays an important role in passivating interfacial defects in heteroepitaxial layers such as GaAs-on-Si (Pearton, Wu, *et al.*, 1987) and GaAs-on-InP (Chakrabarti *et al.*, 1990). The electrical and optical properties of the GaAs layers upon hydrogenation become more like those of homoepitaxial material. Also, H plays a key role in a new dry etching mixture, $CH_4/H_2/Ar$, which has demonstrated low-damage etching of III-V semiconductors (Pearton *et al.*, 1990). Hydrogen passivation of both dopants (Moehrle, 1990; Pearton *et al.*, 1990) and deep levels (Pearton and Tavendale, 1982) occurs during such etching.

E. Hydrogen migration and solution states

The solution states and diffusion of H are poorly understood in GaAs and the other compound semiconductors, and the degree of uncertainty exceeds even that discussed for Si in Sec. V. Unresolved issues include the charge states of isolated H, its preferred lattice sites, and the occurrence of H dimerization. Moreover, reported diffusion-coefficient measurements in GaAs exhibit considerable variation, presumably as a consequence of the sensitivity of the effective mobility to host conditions and the mode of charging; for example, the reported diffusion activation energies include 0.62 eV for a relatively high donor concentration of 3×10^{18} cm^{-3} (Zavada *et al.*, 1985), 1.38 eV (Chevallier *et al.*, 1988), 2.2 eV for implanted H in n^+ GaAs (Raisanen *et al.*, 1988), and 0.83 eV in semi-insulating GaAs (Omeljanovsky *et al.*, 1988).

Dautremont-Smith (1988) has reviewed the influence of doping and H-plasma exposure conditions on the transport of H in GaAs. The driving frequency of the plasma is a relevant parameter in these considerations because of its influence on the ion energies: as the frequency is increased from the KHz range to tens of MHz, the upper extent of the energy range typically decreases from hundreds to tens of eV (Bruce, 1981). Still further reduction in the ion energy is achieved by exposing specimens downstream from microwave plasmas. The diffusion and associated passivation characteristics noted by Dautremont-Smith include the following.

(1) The diffusion depth is greater in *p*-type GaAs than in *n*-type material for the same plasma conditions: at 250 °C in a 30-KHz plasma, the difference is about a factor of 3.

(2) The diffusion depth from a 30-KHz discharge into *n*-type GaAs increases weakly with decreasing donor concentration, whereas in *p*-GaAs the diffusion appears to be enhanced by increased levels of acceptor doping.

(3) Deuterium diffusion is inhibited and the degree of acceptor (donor) passivation decreases when a thin n^+ region is present at the surface of $p(n)$-type material.

(4) Low-frequency plasma exposures produce about an order of magnitude greater depth and greater peak concentration for the same exposure time and temperature than does indirect microwave-plasma exposure in both *n*-type and *p*-type GaAs.

(5) For low-frequency plasma exposure, the depth of electrical passivation in both *n*-type and *p*-type material is much less than the depth of H diffusion, and the concentration of H far exceeds the donor or acceptor concentrations. In contrast, for high-frequency or microwave plasmas there appears to be a closer correlation between the electrical and atomic depth profiles.

The observed differences between *n*-type and *p*-type GaAs can be interpreted in terms of the different charge states of H in these materials. If H has a donor level in the upper half of the band gap, then it will be in a positive charge state in *p*-type GaAs. This inhibits the formation of molecules and leads to a faster diffusivity than in *n*-type material. At plasma exposure temperatures below 200 °C there should be essentially complete compensation of acceptors by an ion pairing reaction similar to that postulated to occur for acceptors in Si. The passivation is completed with formation of the neutral complex due to the Coulombic attraction of the negatively charged acceptor and positively charged H. At temperatures above 200 °C, the passivation is unstable, and rapid diffusion of the H can occur as H^+. The greater diffusion depth at 250 °C in samples of higher acceptor doping levels is a result of this instability, of the inhibition of molecule formation, and of the fact that more D was incorporated initially because of its higher solubility in the presence of more negatively charged acceptors. By contrast, in *n*-type GaAs, the H will be neutral, or possibly in a negative charge state if it has an acceptor level near midgap, and consequently it may readily form H_2 molecules that are nonreactive and expected to be relatively immobile. These molecules may be created by direct attachment of two neutral H atoms, or alternatively by the combination of H^0 with H^- accompanied by the emission of an electron in *n*-type material. There is direct evidence for the existence of H in a positive charge state from its motion in a reverse-biased Schottky diode fabricated on hydrogenated *p*-type GaAs. At this point, however, there has been no direct evidence for a negative charge state for H in GaAs.

The states of isolated H in GaAs have been theoretically treated by Briddon and Jones (1989) using a self-consistent local-density-functional method in a 56-atom cluster. Calculations were performed for two H sites, one the tetrahedral interstitial position with Ga nearest neighbors and the other a bond-center site. For H at the tetrahedral site, the relaxations of the neighboring atoms were found to be small, and there is a level in the lower half of the band gap. For H at a bond-center site, there is a large relaxation of the neighbors, the Ga-As bond length being increased by 42%. In this case there is a level in the upper half of the gap. The total energy for H at the bond-center site was found to be 0.2 eV greater

than for H at the tetrahedral site. The authors note that this energy difference is sufficiently small to make it difficult to determine the true minimum energy configuration. They suggest that, as in Si, the H is probably stable at the tetrahedral site in n-type GaAs and at the bond-center site in p-type GaAs.

F. Future research

The compound semiconductors are exhibiting a rich and expanding variety of H-defect interactions with important ramifications for device technology. Fundamental understanding of these interactions is extremely limited at present, but the successes that have already been achieved show that considerable strides are possible with the coordinated application of microscopic probes and electrical measurements. Areas worthy of particular attention include the following.

(1) The search for H complexes in the compound semiconductors should continue. The range of these entities is potentially much greater in the compounds than in elemental semiconductors because of the two sublattices, yet the level of exploration has been much lower than in Si.

(2) Only a very small fraction of the identified H complexes in the compounds have been structurally characterized, and this is an important area for focused research. Uniaxial-stress measurements in particular have been performed for only a very few defects. As an example of the gaps in information, no As-site acceptor in GaAs has been examined. If IR features due to As-site donors in GaAs are identified in the future, stress studies to determine their symmetry would be of particular interest.

(3) There is much work to be done on the motions of H in defect complexes. Thermally activated reorientation has been examined for GaAs:Be-H and the 2001-cm^{-1} line in as-grown GaAs. It would be of interest to characterize the possible reorientation of H in the other structure types, such as for H at an antibonding site. In a few defects in Ge and Si, the H moves by tunneling at low temperature; a basic question is whether such behavior occurs in the III-V materials.

(4) There has been almost no work done on H-related complexes in III-V alloys. The only data is for the wagging mode of Si-H in n-type AlGaAs.

(5) Thermal stability has been well determined for only a few H complexes in Si, and there are no reliable measurements in III-V materials. Although the kinetics of dissociation often are complicated, this is an important area for future study from both fundamental and technological perspective.

(6) Ion implantation of H at low temperatures has the potential of producing a variety of interesting H-defect complexes, as well as isolated H, which could be probed with such tools as EPR and IR spectroscopy.

(7) There has been only one set of calculations for H-related complexes in the III-V compound semiconductors, so that this field is wide open. Calculations of the structures of many complexes have not yet been attempted. Total-energy surfaces of the type we are used to seeing for H in Si do not exist for the compounds. A study of the possible pathways for H motions has not been attempted.

(8) The solution states and diffusion mechanisms of H in compound semiconductors are poorly understood, despite the fact that these properties underlie all of the H interactions. The fundamental issues are very much the same as in Si, namely, the charge states, the location of energy minima and saddle points, and the possible formation of immobile molecular H. This area should be emphasized in both experimental and theoretical research.

VIII. THEORY OF SEMICONDUCTORS

The computational, quantum-mechanical study of defects in semiconductors continues to evolve from the treatment of simple, high-symmetry substitutional impurities to complex aggregate (multiple) defects. Many of the known aggregates have H as a constituent (Pearton, Corbett, and Shi, 1987; Pankove and Johnson, 1991). Since the H atom lacks a core, its valence electron is bound as tightly as those of many heavier elements, such as the s and p valence states of Si. As a result H reacts strongly with the semiconductor host atoms, not only disrupting normal bonds to form interstitials, but also competing for bonds with other defects and thereby forming complexes.

The band structure of a semiconductor is characterized by a fundamental band gap, which is about 1.1 eV in the case of Si. The disruption of the crystal potential due to the insertion of an impurity atom alters the valence and conduction bands, producing resonances and antiresonances, and frequently introducing an electrical level into the band gap. The "shallow-level" defects, such as substitutional B or P in Si, produce delocalized states and energy levels in the gap close to band edges; they are well described by effective-mass theory. The "deep-level" defects, on the other hand, are characterized by rather localized states and most frequently by energy levels deep within the band gap.

The phenomena that involve atomic motion require the calculation of total energies as functions of atomic positions. First and foremost, such capabilities are needed to establish the equilibrium geometry for each defect charge state. Although "electrical level positions" can be estimated from the single-particle energies, a proper treatment requires the calculation of the total energies for the fully relaxed defect system in two charge states; i.e., the level position is the difference between these energies. The adiabatic energy surface provides an estimate of diffusion and reorientation barriers, and second derivatives of the energy can be used to produce vibrational frequencies. Other defect characteristics that require total-energy calculations are metastability and bistability, negative effective U, and anharmonic contributions to the vibrational frequencies.

A. Computational methods

Most of the computational treatments of defects in semiconductors rely on approximations to the defect environment that fall into one of three categories: cluster, supercell, and Green's function. In a cluster approach, the defect and its environment are simulated by a finite fragment of the solid, or "cluster" (DeLeo *et al.*, 1984; Estreicher *et al.*, 1985; Estreicher, 1988). The cluster is usually terminated by H atoms and treated as a molecule directly or by the recursion method. In the supercell approach, an unterminated cluster ("supercell") is periodically reproduced so that translational symmetry can be invoked (Denteneer *et al.*, 1989b). The Green's-function approach is the most cumbersome method; however, in principle, it best simulates the defect and environment. In this approach the solution relies on a defect potential that is nonvanishing only over a rather limited range, a fortunate characteristic of many defect systems (Williams *et al.*, 1982).

Once the above framework has been established, any electronic-structure method appropriate for molecules can, in principle, be applied to the solid. Currently, in treating the properties of defects in solids, there are two families of state-of-the-art self-consistent theoretical approaches that are used (Van de Walle, 1991). On one hand are the techniques based on the density-functional (DF) theory, where the many-electron system is replaced by an effective-particle model. This approach is exact if applied to the ground state and if the exchange-correlation potential is known. The host atoms are described using *ab initio* pseudopotentials. In practice, the vast majority of the calculations performed so far have used the local-density approximation (LDA), with a variety of parametrized functions being used to approximate the unknown exchange-correlation potential.

On the other hand, a number of methods borrowed from quantum chemistry are used to calculate properties of defects in clusters. Several of these methods are semiempirical, including the complete neglect of differential overlap (CNDO), the intermediate neglect of differential overlap (INDO), the modified neglect of differential overlap (MNDO), and the modified intermediate neglect of differential overlap (MINDO and MINDO/3). In addition, there is the approximate *ab initio* method called partial retention of diatomic differential overlap (PRDDO), and finally the *ab initio* Hartree-Fock (HF) approach with small and large basis sets. Electron correlation is normally neglected, but exchange is fully accounted for. It should be noted that large-basis-set *ab initio* HF calculations followed by extensive configuration interaction treatment are nonrelativistic but otherwise exact.

Furthermore, there has been a resurgence of interest in tight-binding methods; these are now reported with total-energy capabilities, which are of critical importance. References to these methods will be provided as they are discussed in the context of H in semiconductors.

Proponents and opponents of each of the above approaches argue about limited cluster size versus defect-defect interactions in neighboring supercells (in particular for charged defects), about the neglect of electron correlation versus the use of extrapolated functions for the unknown exchange-correlation potential, and about localized Slater-type orbitals versus finite plane-wave basis sets with some cutoff radius. It is clear that each approach has strengths and weaknesses. In situations where the absolute minimum of a potential-energy surface (PES) is deep and well defined, all methods usually agree on the equilibrium structure. There is often disagreement, however, regarding metastable states, potential barriers, electronic structures, vibrational frequencies, and other features.

B. Interstitial hydrogen

1. Experimental information

Most of the experimental information on the configuration of isolated interstitial H in crystalline semiconductors comes from positive muons. The muon is a light pseudoisotope of the proton with mass $m_\mu \simeq m_p/9$ and lifetime $\tau_\mu \simeq 2.2$ μs. This lifetime is longer than the 10^{-10} s necessary for a muon to thermalize in the lattice. Since the techniques and data obtained have recently been reviewed (Patterson, 1988; Estle *et al.*, 1990; Kiefl and Estle, 1991), only the results most relevant to the present discussion will be summarize here. In addition to muon-related data, a hydrogen EPR center labeled AA9 was observed in Si (Gorelkinskii, and Nevinnyi, 1987). This defect is identical to the stable paramagnetic center (Mu^*) observed by muon spin rotation (μSR) and muon level-crossing spectroscopy (μLCR). Finally, lattice location experiments based on the nuclear reaction $\mathrm{D}(^3\mathrm{He},p)^4\mathrm{He}$ were performed in Si (Picraux and Vook, 1978; Nielsen, 1988).

Three muonium centers are observed at low temperatures in undoped diamond and in Si, Ge, GaP, and GaAs. About two-thirds of the incoming muons form "normal muonium" ($\mathrm{Mu} \equiv \mu^+ e^-$), a paramagnetic center with an isotropic hyperfine interaction. The contact spin density at the muon is smaller than that of the free atom, indicating a delocalized wave function. The ratio of this contact density to the free-atom value is 0.83 in diamond, 0.45 in Si, 0.63 in SiC, 0.53 in Ge, and 0.65 in GaP and GaAs. Ten to thirty percent of the muons form "anomalous muonium" (Mu^*), also paramagnetic, but characterized by a highly anisotropic hyperfine tensor which is symmetric relative to one of the $\langle 111 \rangle$ axes of the diamond or zinc-blende lattice. The contact density at the muon is nearly zero in all hosts where Mu^* is observed, and the unpaired electron density resides almost entirely on two nearest neighbors to the muon. Recent μLCR experiments have shown (Kiefl *et al.*, 1988) that Mu^* in *c*-Si is located at a relaxed bond-centered (BC) site (Fig. 16). These experiments confirmed a molecular-orbital model (Symons, 1984; Cox and Symons, 1986; Cox, 1987) and

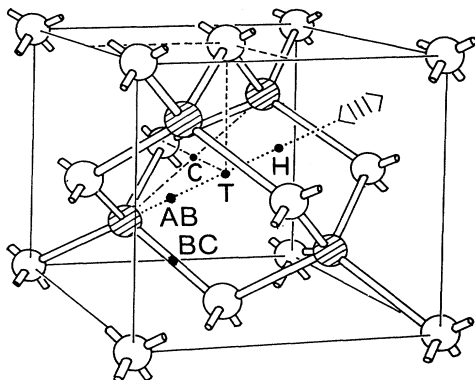

FIG. 16. Interstitial sites in the diamond lattice. The four nearest neighbors to a T site are shaded. The M site (not shown) is midway between two adjacent *C* sites. Note that the BC configuration for any interstitial impurity involves typically 30 to 40 % outward relaxation of the bond, which is not shown.

theoretical predictions (Estle *et al.*, 1986) for Mu*. The remaining muons (typically 10%) contribute to the μSR line occurring at the Larmor frequency for a bare muon. This center is not paramagnetic. It is labeled "μ^+," but could be due to Mu^- as well. Very little is known about μ^+.

In diamond, Mu is stable up to about 400 K, then converts to Mu*, which remains stable up to at least 1000 K. The experiments thus unambiguously demonstrate that the stable species in diamond is Mu*, while Mu is metastable. Further, Mu is not mobile at low temperatures in diamond. Since it has an isotropic hyperfine tensor, Mu can only be localized at the tetrahedral interstitial (T) site.

A Mu$\rightarrow$Mu* transition was also observed in Si, but only in irradiated samples. In Si and Ge, Mu is highly mobile even at very low temperatures, suggesting that Mu is rapidly moving between interstitial sites in such a way as to average out any anisotropy. Three Mu and one μ^+ (but no Mu*) signals have been seen in the 6H and 3C polytypes of SiC. The Mu* signal also is missing in various group II-VI (ZnO, ZnS,. . .) and I-VII (CuCl, CuBr, . . .) semiconductors.

2. Isolated hydrogen in silicon

Theoretical work for H in semiconductors has recently been reviewed (Pearton, Corbett, and Shi, 1987; Pearton, Stavola, and Corbett, 1989; Van de Walle, 1991). The emphasis here will be on the areas of agreement and disagreement. The most recent work will also be discussed. After it was realized that the most stable state of interstitial H in diamond (Claxton *et al.*, 1986; Estle *et al.*, 1986, 1987) and Si (Estle *et al.*, 1987; Estreicher, 1987) is at the BC site, a number of theoretical methods were employed to locate all the minima of the PES, to predict diffusion paths and barrier heights, and to determine the electronic structures, vibrational frequencies, charge states, and other properties of interstitial H in *c*-Si.

a. Neutral H

All of the calculations based on the HF methodology agree on the main features of H^0 in Si, namely, that the lowest-energy state occurs for H at the BC site, that there is also a metastable configuration, and that the barrier for diffusion between adjacent BC sites is larger ($\simeq 1$ eV) than the one between adjacent metastable sites ($\simeq 0.5$ eV). Parameter-free approximate *ab initio* and *ab initio* HF calculations (Estle *et al.*, 1986; Estreicher, 1987) predict that the BC site is lower by 0.9 eV than the metastable T site (Fig. 16). At the latter site, the H wave function is roughly atomic. The barrier for diffusion between adjacent T sites is less than 0.6 eV. These results are supported by the *ab initio* HF calculations of Vogel *et al.* (1989) and Amore Bonapasta *et al.* (1988, 1989). Using the MINDO/3 method, Deák *et al.* (1988b; Deák, Snyder, Lindström, *et al.*, 1988) also obtain the lowest energy for H^0 at the BC site, but find the metastable state to be at the antibonding (AB) site, 0.92 eV higher (Fig. 16). The BC-to-BC barrier height is estimated to be 0.8 eV, and the barrier for diffusion between adjacent AB sites is 0.4 eV. Finally, DeLeo *et al.* (1988) performed MNDO calculations and found H to be slightly off-center at the BC site. Their barrier for BC-to-BC diffusion was about 1 eV.

Calculations performed at the DF level predict qualitatively different properties for H^0. Chang and Chadi (1989a, 1989b) find that the T site is lower than the BC site by 0.25 eV, and that the BC site is metastable. The activation energy for diffusion between adjacent T sites is low (0.3 eV). The calculations of Van de Walle *et al.* (1988, 1989) predict the lowest energy to be at the BC site, but find no metastable configuration. The barrier for BC-to-BC diffusion is lower than 0.2 eV. Both DF approaches find that H^0 has weakly negative-U properties, i.e., that the reaction $2H^0 \rightarrow H^+ + H^-$ is exothermic, even in intrinsic Si.

It should be noted that the MNDO (DeLeo *et al.*, 1988) and DF (Van de Walle *et al.*, 1988, 1990) calculations described above use different transition points (i.e., reaction pathways) for determining activation energies for diffusion between BC sites. In the DF calculations, the host Si atoms are forced instantaneously to follow the intermediate positions of the H impurity. The reverse is done in the MNDO calculations. This point will be addressed below.

The hyperfine frequencies measured by μSR and μLCR provide accurate information about the spin-density distribution at a muon and in its neighborhood. At the BC site, a muon (or proton) is at or very near a node of the wave function. As a result, the calculated contact density is very small and the relative error large. Experimental values are tricky to reproduce, since the effects of the zero-point motion of a muon are significant

in a region where the spin density oscillates near zero. Uncorrelated HF wave functions always are approximate and often lead to overestimates of spin densities.

The various HF calculations for H^0 at the BC site predict average spin densities in rather good agreement with experiment (Estle *et al.*, 1987; Estreicher, 1987; Deák *et al.*, 1988b; Deák Snyder, Lindström, *et al.*, 1988; DeLeo *et al.*, 1988; Amore Bonapasta *et al.*, 1988, 1989; Vogel *et al.*, 1989). At the T site, these calculations always show a roughly atomic wave function (Estreicher *et al.*, 1986; Estreicher, 1987; Vogel *et al.*, 1989) that is much more localized than that observed experimentally. On the basis of molecular-orbital arguments, Mu has been proposed (Symons, 1984; Cox and Symons, 1986; Cox, 1987) to be rapidly tunneling between the four AB sites around the T site. Partial bonding to each Si atom would be responsible for lowering the spin density.

The spin densities obtained from DF calculations are superior to the HF ones. Van de Walle (1990) recently performed such calculations for Mu in Si and achieved excellent agreement with experimental data for Mu (or H) at the BC site as well as at the T site. It should be noted, however, that the same calculations predict (Van de Walle *et al.*, 1988, 1989) the latter to be a local maximum of the PES, the only minimum for neutral interstitial H being at the BC site.

b. Charged states

The relative stability of H^0 and H^+ or H^- has not been determined at the HF level. In the case of H^0 at the BC site, the odd electron is in a nonbonding orbital. Removing this electron tends to slightly stabilize this configuration and shorten the length of the bridged Si-H-Si bond. This has been studied by Deák *et al.* (1988b) and DeLeo *et al.* (1988). Chu and Estreicher (1990) have identified bond-centered H^+ (that is, Mu^{*+}) as the diamagnetic μSR species μ^+.

At the DF level (Van de Walle *et al.*, 1988, 1989; Chang and Chadi, 1989a, 1989b), H^+ is predicted to be the stable form of isolated H in *p*-type Si, at the BC site, with a BC-to-BC diffusion barrier of 0.1 to 0.3 eV. In *n*-type material, the stable configuration would be H^- at the T site, with an activation energy of 0.25 eV (Van de Walle *et al.*, 1988, 1989) or 0.3 eV (Chang and Chadi, 1989a, 1989b). The BC site would be metastable in the case of H^-, about 0.5 eV above the T site (Van de Walle *et al.*, 1988, 1989). Buda *et al.* (1989) performed molecular-dynamics simulations of high-temperature diffusion for H^+. They found that H^+ diffuses from BC to BC via low-density regions (T and H sites shown in Fig. 16) rather than via the predicted (Van de Walle *et al.*, 1988, 1989) lowest-energy path near the C site.

c. Discussion

There is little direct experimental information about the behavior of isolated interstitial H, except in the case of muons (Patterson, 1988). The observation of two paramagnetic species in *p*-type, *n*-type, and intrinsic Si, and the fact that the intensity of the Mu and Mu* signals is to a large extent temperature and doping independent, argue against the predicted (Van de Walle *et al.*, 1988, 1989; Chang and Chadi, 1989a, 1989b) negative-U properties of H. Recent hydrogenation data (Seager and Anderson, 1988, 1990a; Anderson and Seager, 1990) in *n*-type and *p*-type samples show that, on the average, some 90% of H is in the neutral charge state. The observed Mu→Mu* conversion observed in irradiated Si is a strong indicator of metastability for the Mu state. Further, the high anisotropy of Mu* as well as that of its analogous hydrogen EPR center (AA9) unambiguously demonstrate that the barrier for diffusion between BC sites must be large enough to prevent even a muon from rapidly hopping between neighboring BC sites, thus averaging out the anisotropy.

On the other hand, the metastable center, Mu, is mobile even at low temperatures in Si. Old (Van Wieringen and Warmoltz, 1956) and recent (Abrefah *et al.*, 1990) high-temperature diffusivity data for atomic H, valid in the range 970–1200 °C, show an activation energy close to 0.5 eV. The validity of extrapolating these data to low temperatures has been the subject of considerable debate (Pearton, Corbett, and Shi, 1987; Pearton, Stavola, and Corbett, 1989). Recently, however, data consistent with such extrapolations have been obtained by Myers (1988) down to 600 °C. Further, it was recently shown that numerical solutions of transport equations (Kalejs and Rajedra, 1989) fit the diffusion data at 150 °C only if an extrapolation of the high-temperature diffusivities is used to represent the diffusion of H in the absence of traps. Finally, recent room-temperature hydrogenation data (Seager and Anderson, 1988, 1990a; Anderson and Seager, 1990) in *p*-type and *n*-type Si are consistent with a unique activation energy of 0.6 eV, and the diffusivity is close to the one extrapolated from the high-temperature values.

3. Hydrogen dimers

The Albany group (Corbett *et al.*, 1983; Shi *et al.*, 1984) performed MNDO calculations and found that the H_2 molecule forms and is preferred by 1.6 eV to two isolated interstitial H atoms at M sites. The molecule is at the T site with its axis along a $\langle 111 \rangle$ direction. The barrier for diffusion of H_2 between adjacent T sites, via the hexagonal interstitial (H) site, is high (2.7 eV). Similar conclusions had been reached on the basis of CNDO calculations (Mainwood and Stoneham, 1983). However, MINDO/3 calculations later predicted that H_2 is actually higher by 0.24 eV than two H at distant BC sites (Deák *et al.*, 1988b; Deák, Snyder, Lindström, *et al.*, 1988). More extended studies were recently conducted at the same theoretical level (Deák, Heinrich, Snyder, and Corbett, 1989) with a larger number of configurations. The lowest-energy state, labeled $H_{BC}H_{AB}$, consists of a

nearly BC interstitial and a nearly AB H interstitial. This configuration is 0.26 eV lower than two isolated BC H interstitials, i.e., 0.5 eV lower than the H_2 molecule in Si. While the BC site for H corresponds to a 3-center, 2-electron bond [Fig. 17(a)], the $H_{BC}H_{AB}$ configuration is reminiscent of two 2-center, 2-electron bonds [Fig. 17(b)].

A variety of configurations involving two H interstitials have been considered by Chang and Chadi (1989a, 1989b). They performed DF calculations with *ab initio* pseudopotentials using 18-atom supercells. The lowest-energy configuration corresponds to a H_2 molecule at the T site oriented along a $\langle 111 \rangle$ or a $\langle 100 \rangle$ direction. A metastable species labeled $H_2{}^*$, identical to the $H_{BC}H_{AB}$ species in Fig. 17(b), is only 0.4 eV higher, while two H atoms at adjacent BC sites in the (111) plane are much higher in energy, 2.2 eV above H_2.

Finally, DF calculations using 32-atom supercells were performed by Van de Walle *et al.* (1988, 1989). They also find the H_2 molecule to have the lowest energy. In the ground state, H_2 is at the T site, oriented along a $\langle 100 \rangle$ or $\langle 111 \rangle$ direction (with little energy different between them), with a H-H bond length of 0.086 nm, i.e., some 15% longer than in free space. A bond length of 0.085 nm was also reported by Chang and Chadi (1989a, 1989b). Recent calculations at the *ab initio* HF level (Korpas *et al.*, 1990, 1991) predict this bond length to be about 5% shorter in Si than in free space.

4. Hydrogen vibrations

Many H-related IR bands are seen in semiconductors (Gerasimenko *et al.*, 1978; Cardona, 1983; Pearton, Corbett, and Shi, 1987; Tatarkiewics and Stutzman, 1988). In Si, most of the frequencies are roughly within 10% of 2000 cm^{-1} and correspond to Si-H stretches, often perturbed by the nearby presence of a defect. Some frequencies are associated with partially or fully H-passivated vacancies, whereas others correlate with the concentration of impurities such as O or B, etc. A few additional lines in the vicinity of 800 cm^{-1} are associated with wagging modes.

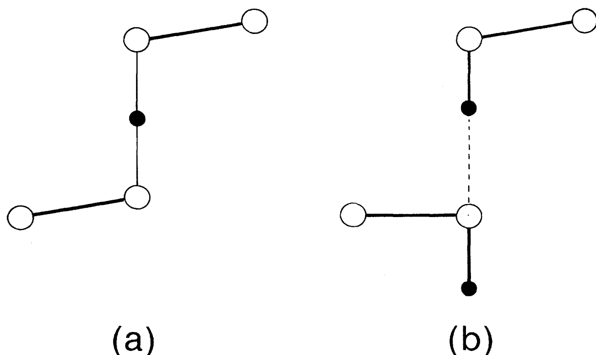

FIG. 17. Qualitative comparison between (a) the BC configuration for one H atom in the Si lattice, and (b) the $H_{BC}H_{AB}$ or $H_2{}^*$ configuration for two H atoms. The latter configuration is energetically close to the H_2 molecule at the T site (see text).

Theoretical investigations of Si-H vibrations are extremely involved because of the accuracy required to distinguish among a dozen IR bands clustered within some 100 cm^{-1}. No method has been tested extensively enough to be reliable in this regard. Large-scale studies of the discrepancies between hundreds of calculated and measured frequencies have been conducted for a variety of *ab initio* and semiempirical HF methods. Large-basis-sets *ab initio* HF frequencies for two-electron bands at equilibrium are systematically higher (Bock and Redington, 1988, and references therein) than the experimental ones by about 10%. Such calculations are prohibitively expensive for many of the configurations of interest here. Frequencies calculated at lower levels of *ab initio* HF theory show larger and less systematic variations relative to experiment (Schröder and Thiel, 1985). Systematic studies at a uniform theoretical level have been attempted using empirical methods (Singh *et al.*, 1977; Shi *et al.*, 1982). Similar studies with well-tested, first-principles techniques need to be conducted.

Deák, Heinrich, Snyder, and Corbett (1989) calculated at the MINDO/3 level the stretching frequencies associated with H at the BC site [Fig. 17(a)] and in the $H_{BC}H_{AB}$ or $H_2{}^*$ configuration [Fig. 17(b)]. They obtained 872 cm^{-1} for the BC site, in close agreement with the value calculated by DeLeo *et al.* (1988). In the $H_2{}^*$ configuration, the frequencies are calculated to be 2039 and 1942 cm^{-1} for the "BC" and the "AB" H atoms, respectively (Deák, Heinrich, Snyder, and Corbett, 1989). Very different frequencies have recently been calculated within the DF formalism by Van de Walle *et al.* (1988). They report 1945 cm^{-1} for H^0 at the BC site, with a Si-H bond length of 0.163 nm, and 2210 cm^{-1} for H^+ at the BC site, with a Si-H separation of 0.159 nm. However, H in bridged bonds, such as H at the BC site (a 3-center, 2-electron bond), is expected to have much lower force constants than H in single bonds, such as the shorter bonds in the $H_2{}^*$ structure.

5. Interstitial hydrogen in other hosts

a. Diamond

In the case of H^0 in diamond, there is almost uniform agreement (Mainwood and Stoneham, 1980; Shahu *et al.*, 1983; Estreicher *et al.*, 1986) that the PES has a deep minimum at the T site with a large barrier for diffusion along T-H-T paths (Fig. 16). (Although the CNDO calculations of Mainwood and Stoneham predict a shallow minimum for H close to the H site, the CNDO method is very approximate, and calculations at much higher levels of molecular-orbital theory have since been performed.) *Ab initio* HF calculations (Estreicher *et al.*, 1986) with polarized basis sets predict a barrier height of 1.3 eV. A configuration of still lower energy than the T site was found at the BC site using minimal-basis-set *ab initio* HF (Claxton *et al.*, 1986), PRDDO and large-basis-set *ab in-*

itio HF (Estle *et al.*, 1986, 1987), and DF theory (Briddon *et al.*, 1988). There is general agreement as well in the above studies concerning the amount of lattice relaxation necessary to accommodate bond-centered H (about 40%). In contrast to bond-centered H in other semiconductors, the bond length in the bridged C-H-C bond is almost identical to that in a single C-H bond, resulting in an unusually large (Briddon *et al.*, 1988) stretching frequency (3132 cm^{-1}) for H in such a configuration. The measured values of the contact and dipolar parameters for Mu* have been reproduced (Hoshino *et al.*, 1989; Vogel *et al.*, 1989). The BC site is substantially lower in energy than the T site, being calculated as 2.4 eV (Estle *et al.*, 1987) or 1.9 eV (Briddon *et al.*, 1988).

Finally, the relative energies of several configurations involving two H interstitials have been calculated using a DF approach with *ab initio* pseudopotentials (Briddon *et al.*, 1988). The lowest energy corresponds to an H_2^* configuration analogous to the one discussed in the case of Si [Fig. 17(b)]. The second-lowest-energy configuration corresponds to two H at distant BC sites (+2.0 eV), followed by the H_2 molecule at the T site (+3.3 eV).

b. Germanium

Few calculations have been published for H in Ge, but the available information suggests (Denteneer *et al.*, 1989a; Maric *et al.*, 1990) that the situation is very similar to that of H in Si. The BC site probably is the absolute minimum of the PES. The equilibrium geometry and hyperfine parameters for H at the BC site have been calculated (Vogel *et al.*, 1989) and are in good agreement with μSR data (Patterson, 1988; Estle *et al.*, 1990; Kiefl and Estle, 1991). A metastable configuration at the T site has been predicted (Vogel *et al.*, 1989), with a diffusion activation energy of 0.49 eV.

c. Weakly ionic compound semiconductors

In contrast to group-IV semiconductors, which are purely covalent, compound semiconductors are partly ionic. As a result there are two inequivalent T sites: T_{le} has four less-electronegative (le) nearest neighbors while T_{me} has four more-electronegative (me) nearest neighbors. Further, the two nearest neighbors to the BC site are inequivalent as well.

Systematic studies of the properties of neutral interstitial H in zinc-blende BN, BP, AlP, and SiC have been conducted at the approximate *ab initio* HF level (PRDDO) in clusters containing 44 host atoms (Estreicher, Chu, and Marynick, 1989; Chu and Estreicher, 1990). In all cases, three minima of the PES have been found: near the BC site and at the two T sites. At the BC site, H can be strongly bound to the le atom while the odd electron primarily resides in a nonbonding orbital on the me atom, or vice versa; the preferred configuration depends on the relative strength of the le-H and me-H bonds and on the relative stability of the odd electron in the nonbonding orbital on the le or me atom. In the cases of BN, BP, AlP, and SiC, H is primarily bound to the le atom (B, Al, Si) while most of the unpaired electron density resides on the me atom (N, P, C). The same was found in an *ab initio* HF study of H in GaAs (Maric *et al.*, 1989). The spin-density distributions for H at the BC site in BP is shown in Fig. 18.

The more stable of the two T sites for H^0 is always the T_{le} site. This was also found to be the case in GaAs (Briddon and Jones, 1989). At this site, the electronic wave function of H overlaps with the four positively charged nearest neighbors, which delocalizes the wave function and stabilizes the interaction. At the T_{me} site, H is surrounded by the four negatively charged atoms. Its electronic wave function is repelled, leading to a higher contact density and energy.

In compound semiconductors the BC site is not always the lowest in energy. Further, the barriers (calculated with PRDDO) between the BC and the T_{le} sites are substantially lower than for C or Si. The energy difference between the BC and the T_{le} sites and an upper limit to the barrier height between these two sites are given in Table VI.

C. Interactions with impurities and defects

Hydrogen is very chemically reactive with imperfections in crystalline semiconductors. In Si, for example, it passivates dangling bonds at defects, at grain boundaries, and at single or multiple vacancies; it also removes the electrical activity of shallow acceptors (B, Al, Ga, In, Tl) and donors (P, As, Sb, Bi), and it can partially or fully

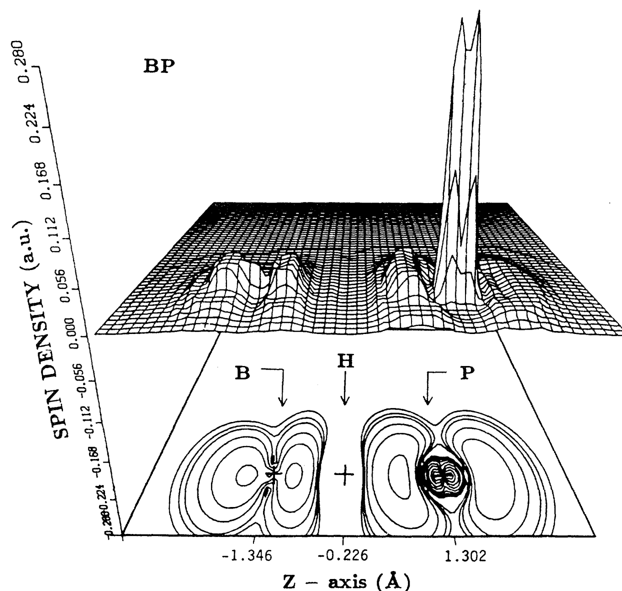

FIG. 18. Unpaired-spin-density distribution for H at the BC site in BP calculated at the PRDDO level.

TABLE VI. Calculated energy difference between interstitial H at the BC and the T_{le} sites, and upper limit on the barrier between these sites. At the BC site, both first and second nearest neighbors to the H were allowed to relax. No relaxation was included for H at the T site. The results are from Chu and Estreicher (1990) except the value for GaAs, which is from Briddon and Jones (1989).

Host	$E(\text{BC})-E(\text{T}_{le})$ (eV)	$\text{BC}\rightarrow\text{T}_{le}$ barrier (eV)
C	−2.70	2.4
Si	−1.45	2.0
BN	−1.24	1.0
BP	−0.45	1.5
SiC	+0.09	1.6
AlP	+0.36	1.5
GaAs	+0.2	

passivate double and triple acceptors (e.g., Be, Cu). Hydrogen also interacts with C, O, the vacancy-O pair, O-associated thermal donors, transition-metal impurities, and other defects. In addition, it tends to "cluster" in the neighborhood of H-passivated B or P in Si and to form platelets. Important progress is being made in the theoretical treatment of these interactions, but large gaps in understanding remain.

1. Hydrogen-vacancy complexes in silicon

Central to H-vacancy (H-V) defects, and, in fact, to all H-related defect complexes, is the interaction between H and a host-atom dangling bond. In Si, the rich IR spectrum in the range 1900–2200 cm^{-1} for stretch modes and 500–1000 cm^{-1} for bending modes is a consequence of the many possible arrangements of H attached to Si dangling bonds (Cardona, 1983; Pearton, Corbett, and Shi, 1987; Pankove and Johnson, 1991). The specific problem of one-to-four H atoms in a single vacancy has been addressed by a number of theoretical studies, including Frolov and Mukashev (1988), DeLeo *et al.* (1984a), Grekhov *et al.* (1983), Pickett (1981), and Singh *et al.* (1977). The results are all consistent with stable H_1-V to H_4-V complexes with the H_4-V center being electrically inactive.

2. Hydrogen complexes with group-III and group-V impurities in silicon

The interaction of H with shallow donors and acceptors in Si is currently the focus of much theoretical research. In the case of group-III and group-V dopants, the H disrupts the fourfold coordination of the substitutional impurity so that it moves off-center and becomes threefold coordinated with Si atoms. Of course, this threefold coordination is the natural chemical tendency for these elements. The earliest evidence for these complexes came from resistivity and SIMS measurements. The most definitive characterization, including the identification of C_{3v} symmetry, emerged from IR vibrational spectroscopy. Dissociation energies have also been measured, and evidence for metastable configurations has been reported. (For a comprehensive review, see Pankove and Johnson, 1991.)

The currently accepted models for the defects are shown in Fig. 19, where H-B and H-P are used to represent the group-III and group-V cases. (In the local-density calculations, P is found to relax in the direction opposite to that shown, as will be discussed shortly.) Note that H is stable at the BC site between the Si and the acceptor in H-B, and stable at the antibonding site of the Si opposite to the donor (Si-AB) in H-P. Based on explorations of the energy surface, it would not be surprising if all the C_{3v} sites (BC, Si-AB, and X-AB where X is the impurity) were locally stable with the exception of the acceptor-AB site (B-AB). Calculated atomic positions, site energies, and vibrational frequencies are given in Table VII (below) for H-B and in Table VIII (below) for H-P.

a. H-B pair

In all cases H causes the B and ⟨111⟩ Si neighbor to move apart, B toward the center of the triangle of neighboring Si atoms. The most conspicuous difference between computational results is the H-Si distance, which is about 0.16 nm in the local-density cases and closer to the natural molecular distance in the other calculations (Table VII). The 0.16 nm result indicates a H balanced between B and Si, while the 0.14–0.15 nm result indicates a H attached primarily to the Si and only weakly interacting with the B. The relative site energies vary among the calculations as well. The dissociation energy

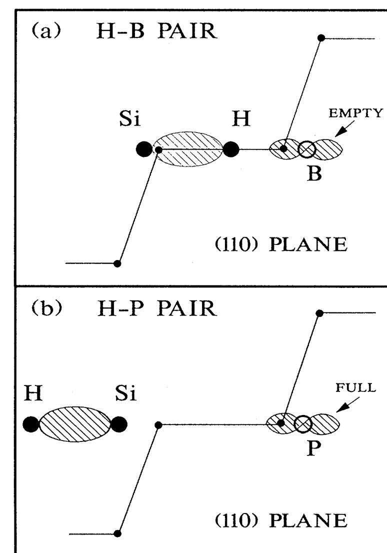

FIG. 19. Geometries of the H-B (a) and H-P (b) pairs in Si from the calculations of DeLeo and Fowler (1985a, 1985b) and DeLeo, Fowler, and Sudol (1990), respectively. The smaller circles indicate unrelaxed lattice sites, and the shaded regions represent electronic states involved in the H interactions.

TABLE VII. Calculated properties of the H-B pair in the BC configuration in Si, including H-induced displacements, interatomic distances, energies of other H sites relative to the lowest-energy BC configuration, and vibrational frequencies. Displacements are considered to be positive in the direction away from the BC site. Frequencies are given for axial vibration (A_1) and for perpendicular, twofold-degenerate vibration (E).

	DeLeo[a]	DeLeo[b]	Amore B[c]	Chang[d]	Denteneer[e]	Estreicher[f]
			Distance (nm)			
B displ.	0.059	0.055	0.048	0.047	0.042	0.049
Si displ.	0.018	0.016	0.022		0.024	0.026
Si-H dist.	0.150	0.156	0.146	0.163	0.165	0.144
B-H dist.	0.163	0.151	0.159		0.136	0.166
			Energy (eV)			
H at Si-AB		1.5	2.45	0.86	1.20	1.64
H at B-AB	1.30	1.7	3.12	0.31	0.48	3.50
			Frequency (cm^{-1})			
H-A_1	1880	1815		1820	1830	
H-E		810				

[a]DeLeo and Fowler (1985a, 1985b, 1986).
[b]DeLeo and Fowler (1989).
[c]Amore Bonapasta *et al.* (1987, 1988, 1989).
[d]Chang and Chadi (1988).
[e]Denteneer *et al.* (1989).
[f]Estreicher, Throckmorton, and Marynick (1989).

for H-B was crudely estimated by DeLeo and Fowler (1985a, 1985b) to be about 1.5 eV. In addition, the reorientation barrier for H in the H-B complex was computed by Denteneer *et al.* (1989b) to be 0.2 eV; by comparison, an experimental value of 0.19 eV was obtained by Stavola, Bergman, *et al.* (1988).

It is important to note that these calculations are based on significant approximations and, further, that only a very restricted subset of the possible reaction pathways have been explored. Moreover, often the treated reaction paths are not the best choices, but rather are those which are computationally convenient (for example, Si atoms that instantaneously follow the motion of a H as it migrates). An additional point is that, in order to properly understand the motion of the H, its low mass relative to that of the other atoms must be recognized in the calculation. This is accomplished naturally in the new high-temperature quantum-molecular-dynamics methods, although it is not clear how to include tunneling contributions (Car and Parrinello, 1985).

The vibrational frequency associated with the H stretching mode has been measured and found to be about 1900 cm^{-1} (Johnson, 1985b; Pankove *et al.*, 1985; Stavola *et al.*, 1987). The predicted stretching frequencies shown in Table VII are close to this experimental value, and all share the characteristic of being lower than the isolated Si-H frequency. This might *a priori* be considered rather surprising, since confinement generally increases frequencies. It was proposed by Pankove *et al.* (1985) that this is the result of a three-body effect involving the Si-H-B chain. This model was later supported by the calculation of DeLeo and Fowler (1985a, 1985b).

Among the curious vibrational features of H-acceptor complexes in Si is a low-frequency mode for H-Al occurring at 78 cm^{-1}, which was found by Stavola, Pearton, *et al.* (1988); the involvement of H is demonstrated by the fact that the frequency decreased by a factor of $\sqrt{2}$ upon isotopic substitution of D. Moreover, evidence was found for a similar mode associated with the H-B pair. It is indeed difficult to envision such a low-frequency vibration for an impurity as light as H; so far, computations have not produced even a bending-mode frequency that low. Another interesting anomaly is the large isotope shift seen in the D frequency on going from ^{10}B-D to ^{11}B-D, but not seen between ^{10}B-H and ^{11}B-H, as reported by Pajot, Chari, *et al.* (1988). This effect was subsequently explained by Watkins *et al.* (1990) as a Fermi-resonance effect (Fermi, 1931): the fundamental, longitudinal mode of the D interacts strongly with the second-harmonic, transverse mode of the B due to an accidental near match in frequencies.

As a final caution, there is recent evidence from the calculations of DeLeo and Sudol (1990) that computed vibrational frequencies for BC H atoms are exceptionally sensitive to the assumed locations of the Si atoms opposite to the H (e.g., those attached to the B for the H-B pair). This is perhaps not surprising, since the frequency is determined by the balance of frequency-increasing confinement and frequency-decreasing three-body effects.

b. H-P pair

The H-P pair exhibits a different set of complications. Again, the local-density calculations produce the largest

Si-H separation. They also produce a P-displacement direction that is opposite to that of the Hartree-Fock-like (non-local-density) methods (Table VIII), with the P found to move toward the neighboring Si along the ⟨111⟩ direction. The impact of this difference on computed frequencies will be discussed shortly.

The computed relative site energies are not very useful, particularly since experimental estimates are not available, but in all cases the results are consistent with metastable BC and P-AB sites.

The experimentally determined stretching-mode frequency of 1555 cm^{-1} (Bergman, Stavola, Pearton, and Lopata, 1988) is most closely reproduced by the local-density calculations, with the others being considerably higher. The higher-frequency predictions from the Hartree-Fock-like methods seem to result indirectly from the large displacement of the ⟨111⟩-Si, which "puckers" through the triangle of neighboring Si atoms. This Si forms something between sp^2 to sp^3 bonds with a H on the interstitial side (Fig. 19). In local-density calculations, H seems to form a weak bond to the Si atoms, and this would tend to produce a lower frequency by itself. Moreover, the presence of a P moving toward the ⟨111⟩-Si further reduces the frequency according to reported local-density calculations. The local-density calculations also predict a metastable configuration with little Si and P relaxation and with H near the tetrahedral interstitial site. This configuration produces a mode at about 400 cm^{-1} (Chang and Chadi, 1988; Denteneer *et al.*, 1990; Zhang and Chadi, 1990). This other site was explored and found to be unstable in the calculations of DeLeo and Sudol (1990).

As a final note, recent studies of the time dependence of hydrogenation profiles (Seager and Anderson, 1988, 1990a) show that the diffusing species has a finite lifetime. The new trapping sites correlate with the dopant concentration, indicating that H is trapped near already passivated B and P dopants. Similar conclusions have been reached on the basis of SIMS data (Corbett, Pearton, and Stavola, 1990).

3. Hydrogen complexes with group-II and group-VI impurities in silicon

Computational treatments of H complexes with group-II and group-VI impurities in Si have not been as extensive as those of single acceptors and donors. A few recent, notable calculations are discussed.

Equilibrium geometries have been calculated for H_2-O (Gutsev *et al.*, 1989) and H_2-S (Yaspir *et al.*, 1988) at a vacancy in Si, and the results are quite similar; both O and S are found to be displaced from the site of the missing Si in a ⟨100⟩ direction, with the H atoms tying up the opposite Si dangling bonds (Fig. 20). The H_2-S defect was predicted to be electrically inactive, however, while H_2-O was reported to have a fully occupied level in the gap. Furthermore, substitutional O is off-center even in the absence of the H, whereas the S is caused to move off-center by the presence of the H atoms. (This explains

TABLE VIII. Calculated properties of the H-P pair in the Si-antibonding configuration in Si, including H-induced displacements, interatomic distances, energies of other H sites relative to the lowest-energy Si-AB configuration, and vibrational frequencies. Displacements are considered to be positive in the direction away from the BC site. Frequencies are given for axial vibration (A_1) and for perpendicular, twofold-degenerate vibration (E).

	Johnson[a]	Zhang[b]	Denteneer[c]	Amore B[d]	Estreicher[e]	DeLeo[f]
			Distance (nm)			
P-origin		−0.018	−0.014	0.009	0.019	0.054
Si-origin		0.066	0.059	0.063	0.074	0.074
Si-H dist.	0.16	0.169	0.166	0.141	0.140	0.144
P-Si dist.		0.284	0.280	0.307	0.328	0.363
			Energy (eV)			
H at BC		1.23	0.45	0.19	1.33	1.48
H at P-AB	0.41	0.67	0.35	2.37	0.92	0.62
			Frequency (cm^{-1})			
H-A_1	2145	1290	1460	2149		2140
H-E		715	740	908		630

[a]Johnson, Herring, and Chadi (1986a).
[b]Zhang and Chadi (1990).
[c]Denteneer *et al.* (1990).
[d]Amore Bonapasta *et al.* (1989).
[e]Estreicher, Throckmorton, and Marynick (1989).
[f]DeLeo, Fowler, Sudol, and O'Brien (1990).

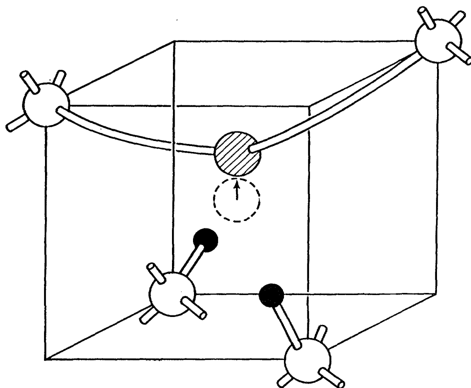

FIG. 20. H_2-S pair geometry. From Yapsir *et al.* (1988).

why the O is an acceptor and not a double donor like the S.) The computed results for the H-S pair have the H attached to one of the two Si dangling bonds. In the H-O system, however, the H is found to attach strongly to the O.

The prototypical H-double-acceptor pair is H-Be, which has been demonstrated by experiment to be a tunneling system (Muro and Sievers, 1986). The local-density calculations of Denteneer *et al.* (1989a), however, suggest a H stable between next-nearest-neighbor Si atoms which are nearest neighbors to the Be (i.e., H at the "C-site" in Fig. 16); this system has C_{2v} symmetry. A barrier for reorientation was found to be 0.1 eV. Thus there is at present a difference between experimental observations and theoretical predictions. In studies by Artacho and Yndurain (1989) and independently by DeLeo, Fowler, and Sudol (1990), the Be was found to behave somewhat like O, twofold coordinating with the neighboring Si atoms. The H then "ties up" one of the two Si dangling bonds and is oriented almost along the $\langle 111 \rangle$ direction.

In studies of tunneling systems such as H-Be, it is important to consider not only the barrier, but also the "reduced mass" appropriate to the tunneling motion (Watkins, 1989). This is quite small if only a H is moving, but can be quite large if its motion is accompanied by the displacements of neighboring host atoms. In the treatment of Denteneer *et al.* (1989a), a H-Be reorientation that involves little Si participation has been identified, but with a barrier of 0.4 eV.

4. Hydrogen complexes in compound semiconductors

In the local-density cluster calculations of Briddon and Jones (1989), the BC site was found to be the stable location for H in the H-Be (H-acceptor) pair in GaAs. This is analogous to the H-acceptor complexes in Si. The H-Si (H-donor) complex in GaAs was also treated. The Si-AB site is found to be the stable location for H. Here, the Si atom is the donor, whereas it is the host atom in Si; hence Si-AB in GaAs is analogous to P-AB in Si. Frequency calculations also have been reported by this group, and they are in good agreement with experiment.

5. Interactions of hydrogen with interstitial oxygen

Oxygen is one of the most common impurities in crystalline Si. It is found in concentrations of the order of 10^{18} cm^{-3} in Czochralski-grown samples. Interstitial O bridges a Si-Si bond (Kaiser *et al.*, 1956; Hrostowski and Alder, 1960; Corbett *et al.*, 1964; Bosomworth *et al.*, 1970) and has a diffusion activation energy (Stavola *et al.*, 1983) of 2.56 eV. This energy is much too large to explain the formation kinetics of the O-related thermal donors (TD's) (Stein *et al.*, 1986; Claybourn and Newman, 1987). It has recently been observed (Brown *et al.*, 1988; Brown *et al.*, 1990; Stein and Hahn, 1990) that atomic H greatly enhances the formation of TD's. Unrelated studies also have concluded that H is strongly attracted to interstitial O and forms complexes in its neighborhood. In μSR experiments (Patterson, 1988), the diamagnetic ("μ^+") and the normal muonium (Mu) signals are absent in CZ samples, leaving only the BC species, Mu*. Further, several IR-absorption lines corresponding to Si-H stretching vibrations have been reported to be O related (Qi *et al.*, 1985).

The interactions between interstitial H and interstitial O have recently been studied using the approximate *ab initio* HF method of PRDDO (Estreicher, 1990). The results show that H "pushes" interstitial O from one BC site to the next and takes its place. This procedure requires an activation energy of 1.25 eV, i.e., much less than is required for O alone to perform a jump, and much less than is needed for H alone to get from the T to the BC site at the same theoretical level (Estreicher, 1987). It is estimated that the proposed mechanism enhances the diffusivity of interstitial O by some 7 orders of magnitude at 400 °C. Several configurations involving O-H bonding have also been examined and were found to be significantly higher in energy than the combination of H and O at neighboring BC sites.

D. Future research

Hydrogen is present in all semiconductors, and it is highly reactive, forming complexes with most impurities and defects in the lattice. The known trapping centers include lattice defects, vacancies, substitutional acceptors and donors, O, transition-metal impurities, H itself, and many others. The ability of H to suppress (or stimulate) the electrical and optical activity of impurities makes it a sometimes desirable, sometimes undesirable agent; in either case, however, a theoretical understanding of the underlying interactions is very important. The variety and complexity of the H states, within the lattice as well as in traps, has made their characterization virtually impossible by experimental methods alone; the complementary role of theory has proved to be crucial.

Modern supercomputers are allowing the use of large

clusters and supercells in theoretical calculations, and the number of approximations is becoming smaller. Techniques are now available to treat the energetics of stable and metastable configurations, and this yields diffusion paths, barrier heights, and vibrational frequencies. The electronic wave functions are also accessible, and these provide charge and spin densities as well as hyperfine parameters. Unfortunately, no single method is powerful enough to provide all of this information. We therefore suggest that a full range of electronic-structure methods be applied to these problems. This includes recently developed tight-binding methods with total-energy capabilities (Tomanek and Schluter, 1987). Sophisticated methods can provide "bench marks" for the semiempirical techniques. Furthermore, emphasis should be placed on applying quantum-molecular-dynamics (MD) methods to problems of diffusion and reorientation. Where MD is not used, careful examination of reaction pathways is required. Such calculations are difficult and require large amounts of computer time and storage. It is also crucial for the existing "state-of-the-art" techniques to be extensively tested in order to establish definitively their strengths and, more importantly, their weaknesses; identifying problems and their origins is the only means of achieving more general and accurate methodologies. Some of the specific problems that need to be addressed are as follows.

(1) It is generally agreed that H^0 and H^+ are stable at the BC site in *c*-Si. There is no clear consensus, however, regarding the relative stability of the various charge states, the metastability of H^0, and the diffusion paths and barrier heights. The various authors also disagree on the most stable state for two interstitials in the lattice, and hence on what is the first step towards the formation of extended H-associated structures such as platelets. Even less is known about H in compound semiconductors, especially those having the wurtzite structure.

(2) The equilibrium structures of H-passivated, shallow single acceptors and donors in Si have been determined by various groups, and a consensus has been reached. Not understood, however, is the apparent clustering of H in the vicinity of already passivated B and P. Furthermore, very little is known about the partial or total passivation of double and triple acceptors in Si. Finally, when one goes beyond Si to other semiconductor hosts, considerably less is known.

(3) Curious phenomena worthy of study include low-frequency modes for the H-acceptor systems, relatively low-frequency stretching modes for the H-donor systems, possible H-acceptor and H-donor metastability or bistability, and tunneling motion in H-double-acceptor complexes in Si.

(4) The role of H in enhancing the formation rate of thermal donors in Si is not sufficiently understood. Only one theoretical examination of this problem is available, and the calculations are limited by the size of the clusters needed to treat multiple defects simultaneously. More generally, the interactions between H and the other most common impurities, such as O, C, and N, are poorly understood.

(5) Hydrogen has also been observed to interact with transition-metal impurities, but the properties of the associated complexes have not been theoretically resolved.

IX. SUMMARY

Hydrogen is interstitial and highly mobile in most solids, and it interacts strongly with a wide range of matrix imperfections. Binding energies relative to the solution state extend to about 1 eV in metals and may reach several eV in covalent materials, and as a result these interactions remain prominent to hundreds of degrees Celsius. Recognized consequences for materials science are extensive and growing, and they range from mechanical degradation of metal alloys to the passivation of electrically active states in semiconductors and dielectrics. The need to predict and control such phenomena provides a strong impetus to understand the underlying atomic processes at a fundamental level. Further, studies of H-defect interactions are an avenue to broader understanding of the solid state, and one that is comparatively accessible to theory because of the relative simplicity and localization of electronic states. From yet another perspective, the low-temperature mobility and high reactivity of H and the availability of sensitive probes for its isotopes make this element attractive as a probe of defects in solids, especially as the defect reactions are increasingly understood.

Hydrogen interactions with defects in solids have been widely investigated, and important advances have been made in both experimental characterization and theory. Nevertheless, the ultimate goal of a quantitatively predictive understanding remains largely unattained. In order to facilitate further progress, the authors of this review undertook to assess current understanding and to identify key directions for future research. We concentrated on the fundamental mechanisms of H-defect interactions, with macroscopic manifestations being treated as outgrowths of the atomistic considerations. Additional focus was achieved by emphasizing the regime of low H concentration and by concentrating on two classes of materials where there has been extensive research, namely, crystalline metals and crystalline semiconductors. Basic H interactions in these systems are broadly prototypical of metallic and covalent materials and provide a foundation for understanding more complicated phenomena occurring at high H concentrations.

In metallic systems, experimental and theoretical research has yielded a near-quantitative description of static H potentials that is applicable to solution states, to well-characterized structural irregularities such as vacancies and strain fields, and to metallic impurities. There remains a strong need, however, to treat the energetics of the H impurity in a manner closer to first principles and thereby to obtain more consistently accurate potentials. In support of this theoretical development it is desirable

to obtain more experimental information on the atomic configurations and binding energies of H at point defects and at defect-solute complexes. Moreover, the theory is far less advanced with respect to detailed electronic wave functions and the dynamic wave function of the proton, and these are areas where qualitative advances are needed. While a comprehensive description of H-defect interactions in metals is unlikely to be achieved in the near term by a single theoretical approach, considerable progress appears possible through a combination of effective-medium methods, cluster models, and band-structure treatments.

The interactions of H with dislocations, grain boundaries, and precipitate margins in metals have generally not been well characterized at the atomic level. A key difficulty is imprecise knowledge of the detailed structures of these extended defects, especially those of boundaries and dislocation cores. Microstructural studies coupled with theoretical modeling are needed to address this deficiency. The prospects for realistic structural modeling are enhanced by the recent development of embedded-atom and effective-medium potentials, which appear to provide substantially improved positional energies compared to two-body forces while retaining computational simplicity. It should also be noted that important progress is being made in the experimental determination of H binding energies at extended defects, and similar data for a broader range of systems are needed. In the case of certain metal-nonmetal interphase boundaries, there is now strong evidence of covalent H bonding, and this is likely to require alternative theoretical methods of the kind employed for semiconductors.

An area of still less fundamental understanding is the influence of H-defect interactions on the deformation of metals under stress. While it was once generally believed that H embrittlement in the absence of phase transitions is largely a consequence of grain-boundary weakening, the extent of H segregation to these boundaries and the consequences for cohesion have not been definitively measured or calculated for the embrittled materials. Moreover, an alternate embrittlement mechanism has emerged with the observation of H-accelerated dislocation motion leading to localized plasticity enhancement. The technological impact of these issues has recently grown with the finding that advanced aerospace alloys as well as conventional steels and titanium alloys are subject to H embrittlement. There is now the possibility that the mechanisms of embrittlement may be illuminated from an atomistic perspective through molecular-dynamics simulations using the improved embedded-atom or effective-medium potentials. Comparisons between such calculations and appropriately chosen deformation experiments are an important area for future research.

Hydrogen in crystalline semiconductors is bound to an extensive array of defects and dopants, modifying and often neutralizing the associated electrical and chemical activity and substantially affecting defect evolution. Such reactions have been known for some time in Si and Ge, and recent work suggests that they are similarly abundant in compound semiconductors. The electrical effects are of considerable importance in device technology, due both to the unavoidable presence of H in processing and to the possibility of controllably passivating unwanted defect centers. Hydrogen has also been observed to cause mechanical embrittlement of semiconductors, presumably as a result of interactions with extended defects, and even to generate new defects. These effects have not been well characterized and are poorly understood at present. Most of the known H-trapping reactions in semiconductors were discovered through electrical measurements, which typically serve to identify the associated dopant or impurity but not to determine the structure of the complex. In selected cases, however, probes such as infrared vibrational spectroscopy have been combined with theoretical analysis to intrepret the atomic configurations and bonding in considerable depth.

Hydrogen states in semiconductors exhibit great variety and complexity, largely due to the directional covalent bonding and the existence of several charge states, and a comprehensive understanding is far from realization. Even the solution condition in the defect-free lattice, which underlies all of the defect interactions discussed here, consists of multiple H charge states and, perhaps, immobile dimers. Hydrogen in solution within Si has received considerable experimental and theoretical attention, and substantial progress has been made in characterizing the associated states. The picture remains incomplete, however, even at a qualitative level. Moreover, analogous studies in Ge and compound semiconductors are in a very early stage. Therefore further experimental and theoretical work on H solution states in semiconductors should be a central element of future research.

The array of defects and dopants known to bind H in semiconductors is very large and growing, but in relatively few cases is there a definitive picture of structure and bonding. Experimental and theoretical tools to address this deficiency are nevertheless available, as demonstrated by notable recent successes in microscopic characterization. For example, the ground-state configurations of group-III acceptor-H complexes and group-V donor-H complexes in Si have been experimentally determined and theoretically predicted. The methods used in such studies are broadly applicable and hold promise for a rather general understanding of H-defect interactions. This, then, is another area warranting further attention. Ideally, these studies will parallel further development of the advanced, self-consistent theoretical approaches that have emerged with the availability of supercomputers.

The binding energies of H at imperfections in semiconductors are of considerable importance because they govern state selection and thermal stability. Moreover, the latter property is increasingly relevant to technology as H passivation is considered for enhancement of carrier lifetimes and for device isolation. Calculations of these energies have so far been approximate, and the experimental measurements are limited in number and often semiquantitative. It is therefore desirable that a broader

range of accurate binding energies be obtained and that this information be used to refine theoretical treatments of the energetics.

Motion of H on the atomic scale in semiconductors, either as an isolated species in various charge states or within H-impurity complexes, poses experimental and theoretical challenges. An understanding of such motion will be required to determine such technologically important parameters as the diffusion coefficients of H and its electric-field drift mobility. The small mass of H, which results in zero-point energies of several tenths of an eV, will require full quantum-mechanical treatment of H motion in certain circumstances. Indeed, quantum-mechanical tunneling has been demonstrated for several H-impurity complexes in Si and Ge. Moreover, the lighter H analog muonium shows even more pronounced quantum effects. The various modes of motion of H have been extensively discussed for metals, but no such treatment exists for semiconductors.

ACKNOWLEDGMENTS

This panel review was sponsored by the Council on Materials of the U.S. Department of Energy, Office of Basic Energy Sciences, Division of Materials Sciences (DMS-BES). The panel is pleased to acknowledge the support of C. P. Flynn, Director of the Council on Materials, and I. Thomas, DMS-BES Director. K. L. Brower, L. M. Falicov, and C. P. Flynn participated in the discussions and made valuable contributions. J. Smith provided liaison with DMS-BES, and his constructive support enhanced the discussions. H. J. Stein and W. R. Wampler read the manuscript and made valuable suggestions. Support was provided by the University of Illinois at Urbana-Champaign under U.S. Department of Energy Contract DE-AC02-76ER01198.

REFERENCES

Abrefah, J., D. R. Olander, and M. Balooch, 1990, J. Appl. Phys. **67**, 3302.

Akai, H., S. Blügel, R. Zeller, and P. H. Dederichs, 1986, Phys. Rev. Lett. **56**, 2407.

Amore Bonapasta, A., A. Lapiccirella, N. Tomassini, and M. Capizzi, 1987, Phys. Rev. B **36**, 6228.

Amore Bonapasta, A., A. Lapiccirella, N. Tomassini, and M. Capizzi, 1988, Europhys. Lett. **7**, 145.

Amore Bonapasta, A., A. Lapiccirella, N. Tomassini, and M. Capizzi, 1989, Phys. Rev. B **39**, 12630.

Anderson, O. K., 1975, Phys. Rev. B **12**, 3060.

Anderson, R. A., and C. H. Seager, 1990, MRS Proc. **163**, 455.

Andzelm, J., and D. Salahub, 1987, in *Physics and Chemistry of Small Atomic Clusters,* edited by P. Jena, B. K. Rao, and S. N. Khanna (Plenum, New York), p. 867.

Angus, J. C., and C. C. Hayman, 1988, Science **241**, 913.

Antell, G. R., A. T. R. Briggs, B. R. Butler, S. A. Kitching, J. P. Stagg, A. Chen, and D. E. Sykes, 1988, Appl. Phys. Lett. **53**, 758.

Artacho, E., and F. Yndurain, 1989, Solid State Commun. **72**, 393.

Au, J. J., and H. K. Birnbaum, 1978a, Acta Metall. **26**, 1105.

Au, J. J., and H. K. Birnbaum, 1978b, Scr. Metall. **12**, 457.

Bachmann, P. K., and R. Messier, 1989, Chem. Eng. News, May 15, p. 24 (special report).

Bagus, P. S., H. F. Schaefer, and C. W. Bauschlicher, 1983, J. Chem. Phys. **78**, 1390.

Bai, G. R., M. W. Qi, L. M. Xie, and T. S. Shi, 1985, Solid State Commun. **56**, 277.

Baker, C., and H. K. Birnbaum, 1973, Acta Metall. **21**, 865.

Baldereschi, A., and N. O. Lipari, 1976, in *Physics of Semiconductors,* Proceedings of the 13th International Conference, Rome, 1976, edited by F. G. Fumi (North-Holland, Amsterdam/New York/Oxford), p. 595.

Balluffi, R. W., 1978, J. Nucl. Mater. **69-70**, 240.

Baskes, M. I., 1987, Phys. Rev. Lett. **59**, 2666.

Baskes, M. I., S. M. Foiles, and C. F. Melius, 1987, J. Nucl. Mater. **145-147**, 339.

Baskes, M. I., J. S. Nelson, and A. F. Wright, 1989, Phys. Rev. B **40**, 6085.

Beachem, C. D., 1972, Metall. Trans. **3**, 437.

Beaven, P. A., and E. P. Butler, 1980, Acta Metall. **28**, 1349.

Bell, R. J., 1972, *Introductory Fourier Transform Spectroscopy* (Academic, New York).

Benson, R. B., R. K. Dann, and L. W. Roberts, 1968, Trans. Metall. Soc. AIME **242**, 2199.

Bergman, K., M. Stavola, S. J. Pearton, and T. Hayes, 1988, Phys. Rev. B **38**, 9643.

Bergman, K., M. Stavola, S. J. Pearton, and J. Lopata, 1988, Phys. Rev. B **37**, 2770.

Bernstein, I. M., 1974, Scr. Metall. **8**, 343.

Besenbacher, F., H. Bogh, A. A. Pisarev, M. J. Puska, S. Holloway, and J. K. Nørskov, 1984, Nucl. Instrum. Methods B **4**, 374.

Besenbacher, F., S. M. Myers, P. Nordlander, and J. K. Nørskov, 1987, J. Appl. Phys. **61**, 1788.

Besenbacher, F., S. M. Myers, and J. K. Nørskov, 1985, Nucl. Instrum. Methods B **7-8**, 55.

Besenbacher, F., B. Bech Nielsen, and S. M. Myers, 1984, J. Appl. Phys. **56**, 3384.

Besenbacher, F., J. K. Nørskov, M. J. Puska, and S. Holloway, 1985, Phys. Rev. Lett. **55**, 852.

Beshers, D. N., 1958, Acta Metall. **6**, 521.

Birnbaum, H. K., 1979, in *Environment-Sensitive Fracture of Engineering Materials,* edited by Z. A. Foroulis (TMS, New York), p. 326.

Birnbaum, H. K., 1984, J. Less Common Met. **103**, 31.

Birnbaum, H. K., 1990, in *Hydrogen Effects on Material Behavior,* edited by N. R. Moody and A. W. Thompson (TMS AIME, Warrendale, PA), p. 639.

Birnbaum, H. K., M. Grossbeck, and S. Gahr, 1974, in *Hydrogen in Metals,* edited by M. Bernstein and A. Thompson (American Society for Metals, Metals Park, OH), p. 303.

Birnbaum, H. K., I. M. Robertson, G. Bond, and D. Shih, 1986, in *Proceedings of the 11th International Congress on Electron Microscopy,* Kyoto, Japan, edited by T. Imura, S. Marnse, and T. Suzuki (Jpn. Soc. of Electron Microscopy, Tokyo), p. 971.

Blakemore, J. S., 1987, *Semiconductor Statistics* (Dover, New York).

Bock, C. W., and R. L. Redington, 1988, J. Phys. Chem. **92**, 1178, and references therein.

Boland, J. J., 1990, Phys. Rev. Lett. **65**, 3325.

Bonacic-Koutecky, V., P. Fantucci, and J. Koutecky, 1991, Chem. Rev. **91**, 1035.

Bond, G., I. M. Robertson, and H. K. Birnbaum, 1987, Acta Metall. **35**, 2289.
Bond, G., I. M. Robertson, and H. K. Birnbaum, 1988, Acta Metall. **36**, 2193.
Bond, G., I. M. Robertson, and H. K. Birnbaum, 1989, Acta Metall. **37**, 1407.
Boolchand, P., C. T. Ma, M. Marcuso, and P. Jena, 1983, in *Electronic Structure and Properties of Hydrogen in Metals*, edited by P. Jena and C. B. Satterthwaite (Plenum, New York), p. 567.
Borenstein, J. T., D. Tulchinski, and J. W. Corbett, 1990, MRS Proc. **163**, 633.
Bosomworth, D. R., W. Hayes, A. R. L. Spray, and G. D. Watkins, 1970, Proc. R. Soc. London, Ser. A **317**, 133.
Bourret, A., and C. Colliex, 1982, Ultramicroscopy **9**, 183.
Briant, C. L., 1979, Metall. Trans. A **10**, 181.
Briant, C. L., 1981, in *Hydrogen Effects in Metals*, edited by M. Bernstein and A. W. Thompson (TMS AIME, Warrendale, PA), p. 527.
Briddon, P., and R. Jones, 1989, in *Shallow Impurities in Semiconductors 1988*, Proceedings of the Third International Conference held in Linköping, Sweden, 1988, Institute of Physics Conference Series Number 95, edited by B. Monemar (Institute of Physics, Bristol), p. 459.
Briddon, P., R. Jones, and G. M. S. Lister, 1988, J. Phys. C **21**, L1027.
Brower, K. L., 1988, Phys. Rev. B **38**, 9657.
Brower, K. L., 1989, Semicond. Sci. Technol. **4**, 970.
Brower, K. L., 1990, Phys. Rev. B **42**, 3444.
Brower, K. L., and S. M. Myers, 1990, Appl. Phys. Lett. **57**, 162.
Brown, A. R., M. Claybourn, R. Murray, R. S. Nandhra, R. C. Newman, and J. H. Tucker, 1988, Semicond. Sci. Technol. **3**, 591.
Brown, A. R., R. Murray, R. C. Newman, and J. H. Tucker, 1990, MRS Proc. **163**, 555.
Brown, J. A., R. H. Heffner, M. Leon, and M. E. Schillaci, 1979, Phys. Rev. Lett. **43**, 1513.
Bruce, R. H., 1981, J. Appl. Phys. **52**, 7064.
Buda, F., G. L. Chiarotti, R. Car, and M. Parrinello, 1989, Phys. Rev. Lett. **63**, 294.
Bugeat, J. P., A. C. Chami, and E. Ligeon, 1976, Phys. Lett. A **58**, 127.
Capizzi, M., and A. Mittiga, 1987, Appl. Phys. Lett. **50**, 918.
Car, R., and M. Parrinello, 1985, Phys. Rev. Lett. **55**, 2471.
Cardona, M., 1983, Phys. Status Solidi B **118**, 463.
Carslaw, H. S., and J. C. Jaeger, 1959, *Conduction of Heat in Solids* (Clarendon, Oxford).
Chabal, Y. J., 1986, Surf. Sci. **168**, 594.
Chabal, Y. J., G. S. Higashi, and S. B. Christman, 1983, Phys. Rev. B **28**, 4472.
Chakrabarti, U. K., S. J. Pearton, W. S. Hobson, J. Lopata, and V. Swaminathan, 1990, Appl. Phys. Lett. **57**, 887.
Chakraborty, B., R. W. Siegel, and W. E. Pickett, 1981, Phys. Rev. B **24**, 5445.
Chang, H. Y., and C. A. Wert, 1973, Acta Metall. **21**, 1233.
Chang, K. J., and D. J. Chadi, 1988, Phys. Rev. Lett. **60**, 1422.
Chang, K. J., and D. J. Chadi, 1989a, Phys. Rev. Lett. **62**, 937.
Chang, K. J., and D. J. Chadi, 1989b, Phys. Rev. B **40**, 11644.
Chevallier, J., and M. Aucouturier, 1988, Annu. Rev. Mater. Sci. **18**, 219.
Chevallier, J., W. C. Dautremont-Smith, S. J. Pearton, C. W. Tu, and A. Jalil, 1985, in *Proceedings of the 3rd International Symposium on Dry Etching and Plasma Deposition in Microelectronics*, Cathan, France, edited by H. Curien (Soc. Francaise Vide, Paris), p. 161.
Chevallier, J., W. C. Dautremont-Smith, C. W. Tu, and S. J. Pearton, 1985, Appl. Phys. Lett. **47**, 108.
Chevallier, J., A. Jalil, B. Theys, J. C. Pesant, M. Aucouturier, B. Rose, and A. Mircea, 1989, Semicond. Sci. Technol. **4**, 87.
Chevallier, J., B. Pajot, A. Jalil, R. Mostefaoui, R. Rahbi, and M. C. Boisy, 1988, MRS Proc. **104**, 281.
Chu, C. H., and S. K. Estreicher, 1990, Phys. Rev. B **42**, 9486.
Chung, Y., D. W. Langer, R. Becker, and D. C. Look, 1985, IEEE. Trans. Electron Devices **ED-32**, 40.
Clark, E. A., R. Yeske, and H. K. Birnbaum, 1980, Metall. Trans. A **11**, 1903.
Claxton, T. A., A. Evans, and M. C. R. Symons, 1986, J. Chem. Soc. Faraday Trans. **82**, 2031.
Claybourn, M., and R. C. Newman, 1987, Appl. Phys. Lett. **51**, 2197.
Clerjaud, B., D. Cobe, and C. Naud, 1987, Phys. Rev. Lett. **58**, 1755.
Collins, G. S., and R. B. Schuhmann, 1986, Phys. Rev. B **34**, 502.
Corbett, J. W., P. Deák, C. Ortiz, and L. C. Snyder, 1989, J. Nucl. Mater. **169**, 179.
Corbett, J. W., J. L. Lindström, S. J. Pearton, and A. J. Tavendale, 1988, Sol. Cells **24**, 127.
Corbett, J. W., J. L. Lindström, L. C. Snyder, and S. J. Pearton, 1988, MRS Proc. **104**, 229.
Corbett, J. W., R. S. McDonald, and G. D. Watkins, 1964, J. Phys. Chem. Solids **25**, 873.
Corbett, J. W., S. J. Pearton, and M. Stavola, 1990, in *Defect Control in Semiconductors*, edited by K. Sumino (North-Holland, Amsterdam), p. 53.
Corbett, J. W., S. N. Sahu, T. S. Shi, and L. C. Snyder, 1983, Phys. Lett. A **93**, 303.
Cornet, M., and S. Talbot-Besnard, 1980, Jpn. Inst. Metall. Suppl. **21**, 5454.
Cox, D., P. Farget, R. Brickman, M. Y. Hahn, and A. Kaldor, 1990, Catal. Lett. **4**, 271.
Cox, S. F. J., 1987, J. Phys. C **20**, 3187.
Cox, S. F. J., and M. C. R. Symons, 1986, Chem. Phys. Lett. **126**, 516.
Crookes, C. G., D. Lancefield, K. Waterhouse, A. R. Adams, P. D. Greene, and R. W. Glen, 1990, Electron. Lett. **26**, 308.
Cui, Sh.-F., P.-W. Ge, Y.-Q. Zhao, and L. S. Wu, 1979, Acta Phys. Sin. **28**, 791.
Cui, Sh.-F., Zh.-H. Mai, P.-W. Ge, and D.-Y. Sheng, 1982, Kexue Tongbao **27**, 382.
Cui, Sh.-F., Zh.-H. Mai, and L. Ch. Tsien, 1984, Sci. Sin. A **27**, 213.
Danielou, R., J. Fontenille, E. Ligeon, and Y. Fukai, 1984, J. Appl. Phys. **55**, 871.
Dautremont-Smith, W. C., 1988, MRS Proc. **104**, 313.
Dautremont-Smith, W. C., J. Lopata, S. J. Pearton, L. A. Koszi, M. Stavola, and V. Swaminathan, 1989, J. Appl. Phys. **66**, 1993.
Daw, M. S., 1989, Phys. Rev. B **39**, 7441.
Daw, M. S., and M. I. Baskes, 1983, Phys. Rev. Lett. **50**, 1285.
Daw, M. S., and M. I. Baskes, 1984, Phys. Rev. B **29**, 6443.
Daw, M. S., and M. I. Baskes, 1987, in *Chemistry and Physics of Fracture*, edited by R. M. Latanision and R. H. Jones (Martinus Nijhoff, Boston), p. 196.
Daw, M. S., M. I. Baskes, C. L. Bisson, and W. G. Wolfer, 1986, in *Modeling Environmental Effects on Crack Growth Processes*, edited by R. H. Jones and W. W. Gerberich (TMS AIME,

Warrendale, PA), p. 99.
Daw, M. S., and S. M. Foiles, 1987, Phys. Rev. B **35**, 2128.
Deák, P., M. Heinrich, L. C. Snyder, and J. W. Corbett, 1989, Mater. Sci. Eng. B **4**, 57.
Deák, P., L. C. Snyder, and J. W. Corbett, 1988a, in *New Developments in Semiconductor Physics,* edited by G. Ferenczi and T. Beleznay (Springer-Verlag, Berlin), p. 163.
Deák, P., L. C. Snyder, and J. W. Corbett, 1988b, Phys. Rev. B **37**, 6887.
Deák, P., L. C. Synder, J. L. Lindström, J. W. Corbett, S. J. Pearton, and A. J. Tavendale, 1988, Phys. Lett. A **126**, 427.
DeLeo, G. G., M. J. Dorogi, and W. B. Fowler, 1988, Phys. Rev. B **38**, 7520.
DeLeo, G. G., and W. B. Fowler, 1985a, Phys. Rev. B **31**, 6861.
DeLeo, G. G., and W. B. Fowler, 1985b, J. Electron. Mater. A **14**, 745.
DeLeo, G. G., and W. B. Fowler, 1986, Phys. Rev. Lett. **56**, 402.
DeLeo, G. G., and W. B. Fowler, 1988, Phys. Rev. B **38**, 7520.
DeLeo, G. G., and W. B. Fowler, 1989, Bull. Am. Phys. Soc. **34**, 834.
DeLeo, G. G., and W. B. Fowler, 1991, in *Hydrogen in Semiconductors,* edited by J. I. Pankove and N. M. Johnson (Academic, New York), p. 511.
DeLeo, G. G., W. B. Fowler, and T. M. Sudol, 1990, unpublished.
DeLeo, G. G., W. B. Fowler, T. M. Sudol, and K. J. O'Brien, 1990, Phys. Rev. B **41**, 7581.
DeLeo, G. G., W. B. Fowler, and G. D. Watkins, 1984a, Phys. Rev. B **29**, 1819.
DeLeo, G. G., W. B. Fowler, and G. D. Watkins, 1984b, Phys. Rev. B **29**, 3193.
DeLeo, G. G., and T. M. Sudol, 1990, unpublished.
Denteneer, P. J. H., C. G. Van de Walle, and S. T. Pantelides, 1989a, Phys. Rev. Lett. **62**, 1884.
Denteneer, P. J. H., C. G. Van de Walle, and S. T. Pantelides, 1989b, Phys. Rev. B **39**, 10809.
Denteneer, P. J. H., C. G. Van de Walle, and S. T. Pantelides, 1990, Phys. Rev. B **41**, 3885.
Deve, H. E., R. J. Asaro, and N. R. Moody, 1989, Scr. Metall. **23**, 389.
Devonshire, A. F., 1936, Proc. R. Soc. London Ser. A **153**, 601.
Du, Y., Y. Zhang, G. Qin, and X. Meng, 1985, Chin. Phys. **5**, 21.
Dubé, C., and J. I. Hanoka, 1984, Appl. Phys. Lett. **45**, 1135.
Dubé, C., J. I. Hanoka, and D. B. Sanderson, 1984, Appl. Phys. Lett. **44**, 425.
Dutton, R., K. Nuttall, M. P. Puls, and L. A. Simpson, 1977, Metall. Trans. A **8**, 1553.
Eastman, J., F. Heubaum, T. Matsumoto, and H. K. Birnbaum, 1982, Acta Metall. **30**, 1579.
Eastman, J., T. Matsumoto, N. Narita, F. Heubaum, and H. K. Birnbaum, 1981, in *Hydrogen Effects in Metals,* edited by I. M. Bernstein and A. W. Thompson (TMS AIME, Warrendale, PA), p. 397.
Edwards, R. A. H., and W. Eichenauer, 1980, Scr. Metall. **14**, 971.
Eliezer, D., D. Chakrapani, C. Altstetter, and E. N. Pugh, 1979, Metall. Trans. A **10**, 975.
Estle, T. L., S. K. Estreicher, and D. S. Marynick, 1986, Hyperfine Interactions **32**, 637.
Estle, T. L., S. K. Estreicher, and D. S. Marynick, 1987, Phys. Rev. Lett. **58**, 1547.
Estle, T. L., R. F. Kiefl, J. W. Schneider, and C. Schwab, 1990, MRS Proc. **163**, 407.
Estreicher, S. K., 1987, Phys. Rev. B **36**, 9122.
Estreicher, S. K., 1988, Phys. Rev. B **37**, 858.
Estreicher, S. K., 1990, Phys. Rev. B **41**, 9886.
Estreicher, S. K., C. H. Chu, and D. S. Marynick, 1989, Phys. Rev. B **40**, 5739.
Estreicher, S. K., A. K. Ray, J. L. Fry, and D. S. Marynick, 1985, Phys. Rev. Lett. **55**, 1976.
Estreicher, S. K., A. K. Ray, J. L. Fry, and D. S. Marynick, 1986, Phys. Rev. B **34**, 6071.
Estreicher, S. K., L. Throckmorton, and D. S. Marynick, 1989, Phys. Rev. B **39**, 13241.
Eustice, A. L., and O. N. Carlson, 1961, Trans. Am. Soc. Met. **53**, 501.
Fermi, E., 1931, Z. Phys. **71**, 250.
Fiks, V. B., 1959, Fiz. Tverd. Tela (Leningrad) **1**, 16 [Sov. Phys. Solid State **1**, 14 (1959)].
Finnis, M. W., and J. E. Sinclair, 1984, Philos. Mag. A **50**, 45.
Flannagan, T. B., J. F. Lynch, J. D. Clewley, and B. von Turkovich, 1976, J. Less-Common Met. **49**, 13.
Flannagan, T. B., N. B. Mason, and H. K. Birnbaum, 1981, Scr. Metall. **14**, 109.
Foiles, S. M., 1989, Phys. Rev. B **40**, 11502.
Foiles, S. M., M. I. Baskes, and C. F. Melius, 1987, J. Less-Common. Met. **130**, 465.
Frank, R. C., and J. E. Thomas, 1960, J. Phys. Chem. Solids **16**, 144.
Frolov, V. V., and B. N. Mukashev, 1988, Phys. Status Solidi B **148**, K105.
Fukishima, H., and H. K. Birnbaum, 1984, Acta Metall. **32**, 851.
Fuller, C. S., and R. A. Logan, 1957, J. Appl. Phys. **28**, 1427.
Funk, G., and H. Schultz, 1985, Z. Metallkd. **76**, 311.
Gahr, S., and H. K. Birnbaum, 1976, Scr. Metall. **10**, 635.
Gahr, S., and H. K. Birnbaum, 1980, Acta Metall. **28**, 1207.
Gahr, S., M. L. Grossbeck, and H. K. Birnbaum, 1977, Acta Metall. **25**, 135.
Gelatt, C. D., Jr., H. Ehrenreich, and J. A. Weiss, 1978, Phys. Rev. B **17**, 1940.
Gerasimenko, N. N., M. Rollé, L. J. Cheng, Y. H. Lee, J. C. Corelli, and J. W. Corbett, 1979, Phys. Status Solidi B **90**, 689.
Gillan, M. J., 1988, Philos. Mag. A **58**, 257.
Gillan, M. J., 1989, J. Chem. **85**, 521.
Gorelkinskii, Yu. V., and N. N. Nevinnyi, 1983, Nucl. Instrum. Methods **209-210**, 677.
Gorelkinskii, Yu. V., and N. N. Nevinnyi, 1987, Sov. Tech. Phys. Lett. **13**, 45 [Pis'ma Zh. Tekh. Fiz. **13**, 105 (1987)].
Gorelkinskii, Yu. V., V. O. Sigle, and Z. S. Takiyev, 1974, Phys. Status Solidi A **22**, K55.
Gray, P. V., and D. M. Brown, 1966, Appl. Phys. Lett. **8**, 31.
Grekhov, A. M., V. M. Gun'ko, G. M. Klapchenko, and Y. P. Tsyashchenko, 1983, Sov. Phys. Semicond. **17**, 1186.
Grossbeck, M. L., M. Amano, and H. K. Birnbaum, 1976, J. Less-Common Met. **49**, 357.
Grossbeck, M. L., and H. K. Birnbaum, 1977, Acta Metall. **25**, 125.
Gupta, M., 1989, Z. Phys. **163**, 517.
Gupta, M., and A. J. Freeman, 1978, Phys. Rev. B **17**, 3029.
Gupta, P., V. L. Colvin, and S. M. George, 1988, Phys. Rev. B **37**, 8234.
Gutsev, G. L., G. S. Myakenkaya, V. V. Frolov, and V. B. Glazman, 1989, Phys. Status Solidi B **153**, 659.
Haegel, N. M., 1985, M. S. and Ph.D. theses (University of California), Lawrence Berkeley Laboratory Reports Nos. LBL-

16694 and LBL-20627.
Haegel, N. M., and E. E. Haller, 1986, SPIE Proc. **659**, 188.
Häkkinen, H., S. Mäkinen, and M. Manninen, 1990, Phys. Rev. B **41**, 12441.
Hall, R. N., 1974, IEEE Trans. Nucl. Sci. **NS-21**, No. 1, 260.
Hall, R. N., 1975, Inst. Phys. Conf. Ser. **23**, 190.
Hall, R. N., and J. H. Racette, 1964, J. Appl. Phys. **35**, 379.
Haller, E. E., 1978, Phys. Rev. Lett. **40**, 584.
Haller, E. E., 1986, Adv. Solid State Phys. **26**, 203.
Haller, E. E., 1989, in *Shallow Impurities in Semiconductors, 1988,* edited by B. Monemar, Institute of Physics Conference Series No. **95** (Institute of Physics, Bristol/Philadelphia), p. 425.
Haller, E. E., and L. M. Falicov, 1978, Phys. Rev. Lett. **41**, 1192.
Haller, E. E., and L. M. Falicov, 1979, Inst. Phys. Conf. Ser. **43**, 1039.
Haller, E. E., and W. L. Hansen, 1974a, Solid State Commun. **15**, 687.
Haller, E. E., and W. L. Hansen, 1974b, IEEE Trans. Nucl. Sci. **NS-21**, 279.
Haller, E. E., W. L. Hansen, and F. S. Goulding, 1981, Adv. Phys. **30**, 93.
Haller, E. E., W. L. Hansen, P. N. Luke, R. E. McMurray, Jr., and B. Jarrett, 1982, IEEE Trans. Nucl. Sci. **NS-29**, 745.
Haller, E. E., G. S. Hubbard, and W. L. Hansen, 1977, IEEE Trans. Nucl. Sci. **NS-24**, 48.
Haller, E. E., G. S. Hubbard, W. L. Hansen, and A. Seeger, 1977, Inst. Phys. Conf. Ser. **31**, 309.
Haller, E. E., B. Joós, and L. M. Falicov, 1980, Phys. Rev. B **21**, 4729.
Hanninen, H., and T. Hakarainen, 1980, Corrosion **36**, 47.
Hanoka, J. I., C. H. Seager, D. J. Sharp, and J. K. G. Panitz, 1983, Appl. Phys. Lett. **42**, 618.
Hansen, W. L., E. E. Haller, and P. N. Luke, 1982, IEEE Trans. Nucl. Sci. **NS-29**, No. 1, 738.
Hardie, D., and P. McIntyre, 1973, Metall. Trans. **4**, 1247.
Hautojärvi, P., H. Huomo, M. Pulka, and A. Vehanen, 1985, Phys. Rev. B **32**, 4326.
Hehre, W. J., L. Radom, P. V. R. Schleyer, and J. A. Pople, 1986, *Ab-Initio Molecular Orbital Theory* (Wiley, New York).
Higashi, G. S., Y. J. Chabal, G. W. Trucks, and K. Raghavachari, 1990, Appl. Phys. Lett. **56**, 656.
Hirth, J. P., 1980, Philos. Trans. R. Soc. London, Ser. A **295**, 139.
Hirth, J. P., and J. Lothe, 1968, *Dislocations in Solids* (McGraw-Hill, New York).
Hirth, J. P., and J. R. Rice, 1980, Metall. Trans. A **11**, 1501.
Hohenberg, H., and W. Kohn, 1964, Phys. Rev. B **136**, 864.
Hong, G. W., and J. Y. Lee, 1983, J. Mater. Sci. **18**, 271.
Hoshino, T., T. Asada, and A. Terakura, 1989, Phys. Rev. B **39**, 5468.
Hrostowski, H. J., and B. J. Alder, 1960, J. Chem. Phys. **33**, 980.
Huang, X. Y., W. Mader, J. A. Eastman, and R. Kirchheim, 1988, Scr. Metall. **22**, 1109.
Huang, X. Y., W. Mader, and R. Kirchheim, 1991, Acta Metall. **39**, 893.
Hubbard, G. S., and E. E. Haller, 1980, J. Electron. Mater. **9**, No. 1, 51.
Hull, D., 1975, *Introduction to Dislocations* (Pergamon, New York).
Hwang, C., and I. M. Bernstein, 1982, Scr. Metall. **16**, 341.
Hwang, C., and I. M. Bernstein, 1986, Acta Metall. **34**, 1011.
Irmscher, K., H. Klose, and K. Maas, 1984, J. Phys. C **17**, 6317.
Jacobsen, K. W., J. K. Nørskov, and M. J. Puska, 1987, Phys. Rev. B **35**, 7423.
Jalil, A., J. Chevallier, R. Azouay, and A. Mircea, 1986, J. Appl. Phys. **59**, 3774.
Jansson, U., and K. J. Uram, 1989, J. Chem. Phys. **91**, 7978.
Jaros, M., and S. Brand, 1979, J. Phys. C **12**, 525.
Jena, P., F. Y. Fradin, and D. E. Ellis, 1979, Phys. Rev. B **20**, 3543.
Jena, P., R. M. Nieminen, M. J. Puska, and M. Manninen, 1985, Phys. Rev. B **31**, 7612.
Jena, P., M. J. Ponnambalam, and M. Manninen, 1981, Phys. Rev. B **24**, 2884.
Jena, P., B. K. Rao, and J. N. Khanna, 1987, Eds., *Physics and Chemistry of Small Atomic Clusters* (Plenum, New York).
Jena, P., and K. S. Singwi, 1978, Phys. Rev. B **17**, 3518.
Jeng, S.-J., G. S. Oehrlein, and G. J. Scilla, 1988, Appl. Phys. Lett. **53**, 1755.
Jepsen, O., R. M. Nieminen, and J. Madsen, 1980, Solid State Commun. **34**, 575.
Johnson, N. M., 1985a, Appl. Phys. Lett. **47**, 874.
Johnson, N. M., 1985b, Phys. Rev. B **31**, 5525.
Johnson, N. M., R. D. Burnham, R. A. Street, and R. C. Thornton, 1986, Phys. Rev. B **33**, 1102.
Johnson, N. M., and S. K. Hahn, 1986, Appl. Phys. Lett. **48**, 709.
Johnson, N. M., and C. Herring, 1988, Phys. Rev. B **38**, 1581.
Johnson, N. M., and C. Herring, 1989a, in *Shallow Impurities in Semiconductors 1988,* Institute of Physics Conference Series No. 95, edited by B. Monemar (Institute of Physics, Bristol), p. 415.
Johnson, N. M., and C. Herring, 1989b, in *Defects in Semiconductors 15,* edited by G. Ferenczi, Mater. Sci. Forum **38-41**, 961.
Johnson, N. M., C. Herring, and D. J. Chadi, 1986a, Phys. Rev. Lett. **56**, 769.
Johnson, N. M., C. Herring, and D. J. Chadi, 1986b, Phys. Rev. Lett. **56**, 2224.
Johnson, N. M., C. Herring, and D. J. Chadi, 1987, Phys. Rev. Lett. **59**, 2116.
Johnson, N. M., C. Herring, C. Doland, J. Walker, G. Anderson, and F. Ponce, 1992, Mater. Sci. Forum **83-87**, 33.
Johnson, N. M., F. A. Ponce, R. A. Street, and R. J. Nemanich, 1987, Phys. Rev. B **35**, 4166.
Joós, B., E. E. Haller, and L. M. Falicov, 1980, Phys. Rev. B **22**, 832.
Kahn, J. M., 1986, Ph.D. thesis (University of California), Lawrence Berkeley Laboratory Report No. LBL-22652.
Kahn, J. M., L. M. Falicov, and E. E. Haller, 1986, Phys. Rev. Lett. **57**, 2077.
Kahn, J. M., R. E. McMurray, Jr., E. E. Haller, and L. M. Falicov, 1987, Phys. Rev. B **36**, 8001.
Kahn, L. M., F. Perrot, and M. Rasolt, 1980, Phys. Rev. B **21**, 5594.
Kaiser, W., P. H. Keck, and C. F. Lange, 1956, Phys. Rev. **101**, 1264.
Kalejs, J. P., and S. Rajendra, 1989, Appl. Phys. Lett. **55**, 2763.
Kazmerski, L. L., 1985, J. Vac. Sci. Technol. A **3**, 1287.
Kiefl, R. F., M. Celio, T. L. Estle, S. R. Kreitzman, G. M. Luke, T. M. Riseman, and E. J. Ansaldo, 1988, Phys. Rev. Lett. **60**, 224.
Kiefl, R. F., and T. L. Estle, 1991, in *Hydrogen in Semiconductors,* edited by J. I. Pankove and N. M. Johnson (Academic, New York), p. 547.

Kimerling, L. C., and J. M. Poate, 1974, in *Lattice Defects in Semiconductors, 1974,* edited by F. A. Huntley (Institute of Physics, London), p. 126.
Kimura, A., and H. K. Birnbaum, 1987a, Scr. Metall. **21**, 53.
Kimura, A., and H. K. Birnbaum, 1987b, Acta Metall. **35**, 1077.
Kimura, A., and H. K. Birnbaum, 1990, Acta Metall. **38**, 1343.
Kirchheim, R., 1981, Acta Metall. **29**, 845.
Kirchheim, R., 1982, Acta Metall. **30**, 1069.
Kirchheim, R., 1988, Prog. Mater. Sci. **32**, 261.
Kirchheim, R., E. Fromm, and E. Wicke, 1989, Eds., *Proceedings of the International Symposium on Metal-Hydrogen Systems: Fundamentals and Applications,* Z. Phys. Chem. [NF] **163-164**.
Kirchheim, R., and J. P. Hirth, 1987, Acta Metall. **35**, 2899.
Kirchheim, R., X. Y. Huang, H.-D. Carstanjen, and J. J. Rush, 1987, in *Chemistry and Physics of Fracture,* edited by R. M. Latanision and R. H. Jones (Martinus-Nijhoff, Boston), p. 580.
Kisielowski-Kemmerich, C., W. Beyer, and H. Alexander, 1990, unpublished.
Koehler, B. G., C. H. Mak, D. A. Arthur, P. A. Coon, and S. M. George, 1988, J. Chem. Phys. **89**, 1709.
Kogan, Sh. M., and T. M. Lifshits, 1977, Phys. Status Solidi A **39**, 11.
Kohn, W., and L. J. Sham, 1965, Phys. Rev. **140**, A1133.
Korpas, L., J. W. Corbett, and S. K. Estreicher, 1991, Superlatt. Microstruct. **10**, 121.
Korpas, L., J. W. Corbett, and S. K. Estreicher, 1992, Mater. Sci. Forum **83-87**, 27.
Kozuch, D. M., M. Stavola, S. J. Pearton, C. R. Abernathy, and J. Lopata, 1990, MRS Proc. **163**, 477.
Kumnick, A. J., and H. H. Johnson, 1980, Acta Metall. **28**, 33.
Kuntz, P. J., 1976, in *Dynamics of Molecular Collisions,* Part B, edited by W. M. Miller (Plenum, New York).
Ladna, B., C. Loxton, and H. K. Birnbaum, 1986, Acta Metall. **34**, 988.
Lasser, R., and B. Lengeler, 1978, Phys. Rev. B **18**, 637.
Lassila, D., and H. K. Birnbaum, 1987, Acta Metall. **35**, 1815.
Lee, J. K., 1981, *Interatomic Potentials and Crystalline Defects* (AIME, Warrendale, PA).
Lee, S. R., S. M. Myers, and R. G. Spulak, 1989, J. Appl. Phys. **66**, 1137.
Lee, T. C., I. M. Robertson, and H. K. Birnbaum, 1989, Acta Metall. **37**, 407.
Lengeler, B., S. Mantl, and W. Triftshäuser, 1978, J. Phys. F **8**, 1691.
Lewis, M. B., 1984, J. Nucl. Mater. **125**, 152.
Li, J. C. M., R. Oriani, and L. S. Darken, 1966, Z. Phys. Chem. N. F. **49**, 271.
Lifshits, T. M., and F. Ya. Nad', 1965, Sov. Phys. Dokl. **10**, 532.
Ligeon, E., J. P. Bugeat, R. Danielou, J. Fontenille, and A. Guivarch, 1980, J. Radioanal. Chem. **55**, 367.
Ligeon, E., R. Danielou, J. Fontenille, and R. Eymery, 1986, J. Appl. Phys. **59**, 108.
Linderoth, S., H. Rajainmäki, B. Nielsen, H. E. Hansen, R. M. Nieminen, and K. Petersen, 1987, Mater. Sci. Forum **15-18**, 751.
Linderoth, S., H. Rajainmäki, and R. M. Niemeinen, 1987, Phys. Rev. B **35**, 5524.
Lindgren, B., and D. E. Ellis, 1982, Phys. Rev. B **26**, 636.
Lindström, J. L., G. S. Oehrlein, G. J. Scilla, A. S. Yapsir, and J. W. Corbett, 1989, J. Appl. Phys. **65**, 3297.
Liu, F., M. Challa, S. N. Khanna, and P. Jena, 1989, Phys. Rev. Lett. **63**, 1396.
Liu, F., B. K. Rao, S. N. Khanna, and P. Jena, 1989, Solid State Commun. **72**, 891.
Liu, R., N. Narita, C. J. Altstetter, H. K. Birnbaum, and E. N. Pugh, 1980, Metall. Trans. A **11**, 1563.
Lopata, J., W. C. Dautremont-Smith, S. J. Pearton, J. W. Lee, and N. T. Ha, 1990, MRS Proc. **163**, 501.
Lösch, K., 1987, Ph.D. thesis (University of Stuttgart).
Louat, N., 1956, Proc. Phys. Soc. London Sect. B **69**, 459.
Louthan, M. R., Jr., J. A. Donovan, and D. E. Rawl, Jr., 1973, Corrosion **29**, 108.
Lucovsky, G., 1979, Solid State Commun. **29**, 571.
Luke, P. N., and E. E. Haller, 1986, J. Appl. Phys. **59**, 2724.
Lynch, S. P., 1986, J. Mater. Sci. **21**, 692.
Lynch, S. P., 1988, Acta Metall. **36**, 2639.
Ma, Ah.-H., Sh.-F. Cui, P.-W. Ge, and L.-Ch. Tsien, 1981, Acta Crystallogr. Sect. A **31**, Suppl. c-254.
Magerl, A., B. Berre, and G. Alefeld, 1975, Phys. Status Solidi A **28**, 591.
Mainwood, A., and A. M. Stoneham, 1980, J. Phys. C **17**, 2513.
Mainwood, A., and A. M. Stoneham, 1983, Physica B **116**, 101.
Makenas, B., and H. K. Birnbaum, 1980, Acta Metall. **28**, 979.
Manninen, M., 1986, Phys. Rev. B **34**, 8486.
Manninen, M., and R. M. Nieminen, 1979, J. Phys. F **9**, 1333.
Manninen, M., M. J. Puska, R. M. Nieminen, and P. Jena, 1984, Phys. Rev. B **30**, 1065.
Maric, Dj. M., P. F. Meier, and S. K. Estreicher, 1990, unpublished.
Maric, Dj. M., S. Vogel, P. F. Meier, and S. K. Estreicher, 1989, Phys. Rev. B **40**, 8545.
Marwick, A. D., G. S. Oehrlein, and N. M. Johnson, 1987, Phys. Rev. B **36**, 4539.
Mathiot, D., 1989, Phys. Rev. B **40**, 5867.
Matsui, H., H. Kimura, and A. Kimura, 1979, Mater. Sci. Eng. **40**, 227.
Matsui, H., H. Kimura, and S. Moriya, 1979, Mater. Sci. Eng. **40**, 207.
Matsumoto, T., 1977, J. Phys. Soc. Jpn. **42**, 1583.
Matsumoto, T., and H. K. Birnbaum, 1980, Trans. Jpn. Inst. Met. **21**, 493.
Matsumoto, T., J. Eastman, and H. K. Birnbaum, 1981, Scr. Metall. **15**, 1033.
Maulik, P., and J. Burke, 1975, Scr. Metall. **9**, 17.
Mazzolai, F. M., and H. K. Birnbaum, 1985a, J. Phys. F **15**, 507.
Mazzolai, F. M., and H. K. Birnbaum, 1985b, J. Phys. F **15**, 525.
McCormick, P. G., 1988, Acta Metall. **36**, 3061.
McKergow, M. W., D. K. Ross, J. E. Bonnet, I. S. Anderson, and O. Shaerpf, 1987, J. Phys. C **20**, 2909.
McMahon, C. J., Jr., and V. Vitek, 1979, Acta Metall. **27**, 507.
McMullen, T., M. J. Stott, and E. Zaremba, 1987, Phys. Rev. B **35**, 1076.
McMurray, R. E., Jr., N. M. Haegel, J. M. Kahn, and E. E. Haller, 1987, Solid State Commun. **61**, 27.
McNabb, A., and P. Foster, 1963, Metall. Trans. **245**, 618.
Messmer, R. P., and C. L. Briant, 1982, Acta Metall. **30**, 457.
Moehrle, M., 1990, Appl. Phys. Lett. **56**, 542.
Moody, N. R., S. L. Robinson, S. M. Myers, and F. A. Greulich, 1989, Acta Metall. **37**, 281.
Moody, N. R., and A. W. Thompson, 1990, Eds., *Hydrogen Effects on Material Behavior* (TMS AIME, Warrendale, PA).
Moriya, S., H. Matsui, and H. Kimura, 1979, Mater. Sci. Eng. **40**, 217.
Mortensen, K., D. M. Chen, P. J. Bedrossian, J. A. Golovchenko, and F. Besenbacher, 1991, Phys. Rev. B **43**, 1816.

Moruzzi, V. L., J. Janak, and A. R. Williams, 1978, *Calculated Electronic Properties of Metals* (Pergamon, New York).
Mueller, W. M., J. P. Blackledge, and G. G. Libowitz, 1968, *Metal Hydrides* (Academic, New York).
Mukashev, B. N., K. H. Nussupov, and M. F. Tamendarov, 1979a, Phys. Status Solidi B **96**, K17.
Mukashev, B. N., K. N. Nussupov, and M. F. Tamendarov, 1979b, Phys. Lett. A **72**, 381.
Mukashev, B. N., M. F. Tamendarov, and S. K. Tokmoldin, 1989, in *Defects in Semiconductors 15,* edited by G. Ferenczi, Mater. Sci. Forum **38-41**, 1039.
Muro, K., and A. J. Sievers, 1986, Phys. Rev. Lett. **57**, 897.
Mütschele, T., and R. Kirchheim, 1987, Scr. Metall. **21**, 135.
Myers, S. M., 1988, MRS Proc. **107**, 105.
Myers, S. M., and F. Besenbacher, 1986, **60**, 3499.
Myers, S. M., F. Besenbacher, and J. K. Nørskov, 1985, J. Appl. Phys. **58**, 1841.
Myers, S. M., and D. M. Follstaedt, 1988, J. Appl. Phys. **63**, 1942.
Myers, S. M., D. M. Follstaedt, H. J. Stein, and W. R. Wampler, 1992, Mater. Sci. Forum **83-87**, 81.
Myers, S. M., P. Nordlander, F. Besenbacher, and J. K. Nørskov, 1986, Phys. Rev. B **33**, 854.
Myers, S. M., S. T. Picraux, and R. E. Stoltz, 1979, J. Appl. Phys. **50**, 5710.
Myers, S. M., P. M. Richards, W. R. Wampler, and F. Besenbacher, 1989, J. Nucl. Mater. **165**, 9.
Myers, S. M., W. R. Wampler, F. Besenbacher, S. L. Robinson, and N. R. Moody, 1985, Mater. Sci. Eng. **69**, 397.
Narita, N., C. Altstetter, and H. K. Birnbaum, 1982, Metall. Trans. A **13**, 135.
Narita, N., and H. K. Birnbaum, 1980, Scr. Metall. **14**, 1355.
Navarro, H., J. Griffin, E. E. Haller, and R. E. McMurray, Jr., 1986, Solid State Commun. **64**, 1297.
Nelson, H. G., D. P. Williams, and J. E. Stein, 1972, Metall. Trans. **3**, 469.
Newman, R. C., and J. Woodhead, 1980, Radiat. Eff. **53**, 41.
Nielsen, B. Bech, 1988, Phys. Rev. B **37**, 6353.
Nielsen, B. Bech, J. U. Andersen, and S. J. Pearton, 1988, Phys. Rev. Lett. **60**, 321.
Nielsen, B. Bech, J. Olajos, and H. G. Grimmeiss, 1989a, Phys. Rev. B **39**, 3330.
Nielsen, B. Bech, J. Olajos, and H. G. Grimmeiss, 1989b, in *Defects in Semiconductors 15,* edited by G. Ferenczi, Mater. Sci. Forum **38-41**, 1003.
Nordlander, P., J. K. Nørskov, and F. Besenbacher, 1986, J. Phys. F **16**, 1161.
Northrup, D. O., 1979, in *Environment-Sensitive Fracture of Engineering Materials,* edited by Z. A. Foroulis (TMS, New York), p. 451.
Nørskov, J. K., 1982, Phys. Rev. B **26**, 2875.
Nørskov, J. K., and F. Besenbacher, 1987, J. Less-Common Met. **130**, 475.
Nørskov, J. K., F. Besenbacher, J. Bøttiger, B. B. Nielsen, and A. A. Pisarev, 1982, Phys. Rev. Lett. **49**, 1420.
Nørskov, J. K., and N. D. Lang, 1980, Phys. Rev. B **21**, 2131.
Nuttall, K., 1976, in *Effects of Hydrogen on the Behavior of Materials,* edited by A. W. Thompson and I. M. Bernstein (TMS AIME, Warrendale, PA), p. 441.
Oates, A. S., M. J. Binns, R. C. Newman, J. H. Tucker, J. G. Wilkes, and A. Wilkinson, 1984, J. Phys. C **17**, 5695.
Obodrikov, V. I., L. N. Safronov, and L. S. Smirnov, 1976, Sov. Phys. Semicond. **10**, 814.
Ohmura, Y., Y. Zohta, and M. Kanagawa, 1972, Solid State Commun. **21**, 263.
Ohmura, Y., Y. Zohta, and M. Kanagawa, 1973, Phys. Status Solidi A **15**, 93.
Omeljanovsky, E. M., A. V. Pakhomov, and A. Y. Polyakov, 1989, in *Defects in Semicontuctors 15,* Proceedings of the 15th International Conference on Defects in Semiconductors ICD5-15, August 1988, Budapest, Hungary, edited by G. Ferenczi (Mater. Sci. Forum **38-41**, 1063).
Omeljanovsky, E. M., A. V. Pakhomov, A. J. Polyakov, and A. N. Govorkov, 1988, in *Proceedings of the Fifth Conference on Semi-Insulating III-V Materials,* Malmo, Sweden, edited by G. Grossmann and L. Ledebo (Adam Hilger, Bristol), p. 75.
Onyewuenyi, O. A., and J. P. Hirth, 1983, Metall. Trans. A **14**, 259.
Oriani, R. A., 1970, Acta Metall. **18**, 147.
Oriani, R. A., and P. H. Josephic, 1974, Acta Metall. **22**, 1065.
Oriani, R. A., and P. H. Josephic, 1977, Acta Metall. **25**, 979.
Ortiz, C., P. Deák, L. C. Snyder, and J. W. Corbett, 1990, unpublished.
Osip'yan, Y. A., A. M. Rtishchev, É. A. Shteinman, E. B. Yakimov, and N. A. Yarykin, 1982, Sov. Phys. JETP **55**, 294.
Owen, C. V., and T. E. Scott, 1972, Metall. Trans. **3**, 1715.
Paesler, M., S. C. Agarwal, and R. Zallen, 1989, Eds., *Proceedings of the 13th International Conference on Amorphous and Liquid Semiconductors,* J. Non-Cryst. Solids **114**.
Pajot, B., 1989, in *Proceedings of the 3rd International Conference on Shallow Impurities in Semiconductors 1988,* Institute of Physics Conference Series No. 95, edited by B. Monemar (Institute of Physics, Bristol, U.K.), p. 437.
Pajot, B., 1990, MRS Proc. **163**, 465.
Pajot, B., A. Chari, M. Aucouturier, M. Astier, and A. Chantre, 1988, Solid State Commun. **67**, 855.
Pajot, B., J. Chevallier, A. Chaumont, and R. Azoulay, 1988, MRS Proc. **104**, 345.
Pajot, B., J. Chevallier, A. Jalil, and B. Rose, 1989, Semicond. Sci. Technol.. **4**, 91.
Pajot, B., R. C. Newman, R. Murray, A. Jalil, J. Chevallier, and R. Azouay, 1988, Phys. Rev. B **37**, 4188.
Pakulis, E. J., 1983, J. Magn. Reson. **51**, 490.
Pakulis, E. J., and C. D. Jeffries, 1981, Phys. Rev. Lett. **47**, 1859.
Pan, N., S. S. Bose, M. H. Kein, G. E. Stillman, F. Chambers, G. Devane, C. R. Ito, and M. Feng, 1987, Appl. Phys. Lett. **51**, 596.
Pankove, J. I., D. E. Carlson, J. E. Berkeyheiser, and R. O. Wance, 1983, Phys. Rev. Lett. **51**, 2224.
Pankove, J. I., and N. M. Johnson, 1991, Eds., *Hydrogen in Semiconductors* (Academic, New York).
Pankove, J. I., R. O. Wance, and J. E. Berkeyheiser, 1984, Appl. Phys. Lett. **45**, 1100.
Pankove, J. I., P. J. Zanzucchi, C. W. Magee, and G. Lucovsky, 1985, Appl. Phys. Lett. **46**, 421.
Pantelides, S. T., 1987, Appl. Phys. Lett. **50**, 995.
Park, C. N., T. B. Flanagan, and H. J. Lee, 1987, J. Korean Inst. Met. **25**, 41.
Parks, E., K. Liu, S. C. Richtsmeir, L. G. Pobo, and S. J. Riley, 1985, J. Chem. Phys. **82**, 5470.
Paton, N. E., and J. C. Williams, 1974, in *Hydrogen in Metals,* edited by M. Bernstein and A. Thompson (American Society for Metals, Metals Park, OH), p. 409.
Patterson, B. D., 1988, Rev. Mod. Phys. **60**, 69.
Pearton, S. J., U. K. Chakrabarti, A. P. Kinsella, D. Johson, and C. Constantine, 1990, Appl. Phys. Lett. **56**, 1424.
Pearton, S. J., A. M. Chantre, L. C. Kimerling, K. D. Cum-

mings, and W. C. Dautremont-Smith, 1986, MRS Proc. **59**, 475.
Pearton, S. J., J. W. Corbett, and T.-S. Shi, 1987, Appl. Phys. A **43**, 153.
Pearton, S. J., W. C. Dautremont-Smith, J. Chevallier, C. W. Tu, and K. D. Cummings, 1986, J. Appl. Phys. **59**, 2821.
Pearton, S. J., W. C. Dautremont-Smith, J. Lopata, C. W. Tu, and C. R. Abernathy, 1987, Phys. Rev. B **36**, 4260.
Pearton, S. J., W. C. Dautremeont-Smith, C. W. Tu, J. C. Nabity, V. Swaminathan, M. Stavola, and J. Chevallier, 1987, in *GaAs and Related Compounds 1986,* Institute of Physics Conference Series No. 83, edited by W. T. Lindley (Institute of Physics, Bristol, U.K.), p. 289.
Pearton, S. J., and J. M. Kahn, 1983, Phys. Status Solidi A **78**, K65.
Pearton, S. J., M. Stavola, and J. W. Corbett, 1989, in *Defects in Semiconductors 15,* Proceedings of the 15th International Conference on Defects in Semiconductors, August 1988, Budapest, Hungary, edited by G. Ferenczi, Mater. Sci. Forum **38-41**, 25.
Pearton, S. J., and A. J. Tavendale, 1982, Electron. Lett. **18**, 715.
Pearton, S. J., C. S. Wu, M. Stavola, F. Ren, J. Lopata, and W. C. Dautremont-Smith, 1987, Appl. Phys. Lett. **51**, 496.
Peierls, R. E., 1965, *Quantum Theory of Solids* (Clarendon, Oxford).
Peisl, H., 1978, in *Hydrogen in Metals,* Vol. I, edited by G. Alefeld and J. Völkl (Springer-Verlag, Berlin), p. 53.
Petzinger, K., and R. Munjal, 1977, Phys. Rev. B **3**, 1560.
Pfeiffer, G., and H. Wipf, 1976, J. Phys. F **6**, 167.
Pflueger, R. J., J. C. Corelli, and J. W. Corbett, 1985, Phys. Status Solidi A **1**, K49.
Pickett, W. E., 1981, Phys. Rev. B **23**, 6603.
Picraux, S. T., 1976, in *Ion Beam Surface Layer Analysis,* edited by O. Meyer, G. Linker, and F. Käppeler (Plenum, New York), Vol. 2, p. 527.
Picraux, S. T., 1981, Nucl. Instrum. Methods **182–183**, 413.
Picraux, S. T. and F. L. Vook, 1974, Phys. Rev. Lett. **33**, 1216.
Picraux, S. T., and F. L. Vook, 1978, Phys. Rev. B **18**, 2066.
Pine, D. J., and R. M. Cotts, 1983, Phys. Rev. B **28**, 641.
Podloucky, R., R. Zeller, and P. H. Dederichs, 1980, Phys. Rev. B **22**, 5777.
Pohoryles, B., 1981, Phys. Status Solidi A **67**, K75.
Poindexter, E. H., 1989, Ed., *Metal-Oxide-Semiconductor Structures,* Semicond. Sci. Technol. **4**, 970.
Popovic, Z. D., M. J. Stott, J. P. Carbotte, and G. R. Piercy, 1976, Phys. Rev. B **13**, 590.
Pressouyre, G. M., and I. M. Bernstein, 1978, Metall. Trans. A **9**, 1571.
Puska, M. J., and R. M. Nieminen, 1984, Phys. Rev. B **29**, 5382.
Puska, M. J., R. M. Nieminen, and M. Manninen, 1981, Phys. Rev. B **24**, 3037.
Qi, M. W., G. R. Bai, T. S. Shi, and L. M. Xie, 1985, Mater. Lett. **3**, 467.
Raisanen, J., J. Keinonen, V. Kartunen, and I. Koponen, 1988, J. Appl. Phys. **64**, 2334.
Rajainmäki, H., S. Linderoth, H. E. Hansen, and R. M. Nieminen, 1988, J. Phys. F **18**, 1109.
Rajainmäki, H., S. Linderoth, R. M. Nieminen, and H. E. Hansen, 1987, Mater. Sci. Forum **15-18**, 611.
Rao, B. K., and P. Jena, 1985, Phys. Rev. B **32**, 2058.
Rao, B. K., S. N. Khanna, and P. Jena, 1991, Phys. Rev. B **43**, 1416.
Reider, G. A., U. Höfer, and T. F. Heinz, 1991, J. Chem. Phys. **94**, 4080.
Richter, D., J. J. Rush, and J. M. Rowe, 1983, Phys. Rev. B **27**, 6227.
Richter, D., J. Töpler, and T. Springer, 1976, J. Phys. F **6**, L93.
Riecke, E., B. Johnen, and H. J. Grabke, 1985, Werkst. Korros. **36**, 435.
Robertson, I. M., and H. K. Birnbaum, 1986, Acta Metall. **34**, 353.
Robertson, I. M., H. Hanninen, and H. K. Birnbaum, 1990, unpublished.
Robertson, I. M., T. Tabata, W. Wei, F. Heubaum, and H. K. Birnbaum, 1984, Scr. Metall. **18**, 841.
Rodrigues, J. A., and R. Kirchheim, 1983, Scr. Metall. **17**, 159.
Rosan, K., and H. Wipf, 1976, Phys. Status Solidi A **38**, 611.
Rossnagel, S. M., J. J. Cuomo, and W. D. Westwood, 1990, Eds., *Handbook of Plasma Processing Technology* (Noyes, Park Ridge, NJ).
Rozenak, P., I. M. Robertson, and H. K. Birnbaum, 1990, Acta Metall. **38**, 2031.
Sah, C.-T., J. Y.-C. Sun, and J. J.-T. Tzou, 1983, Appl. Phys. Lett. **43**, 204.
Sahu, S. N., S. K. Mishra, K. C. Mishra, A. Coker, T. P. Das, C. K. Mitra, L. C. Snyder, and A. Glodeanu, 1983, Phys. Rev. Lett. **50**, 913.
Sahu, S. N., T. S. Shi, P. W. Ge, A. Hiraki, T. Imura, M. Tashiro, V. A. Singh, and J. W. Corbett, 1982, J. Chem. Phys. **77**, 4330.
Schiller, P., 1976, Nuovo Cimento B **33**, 226.
Schöber, T., and H. Wenzl, 1978, in *Hydrogen in Metals, Vol. II,* edited by G. Alefeld and J. Völkl (Springer-Verlag, Berlin), p. 11.
Schröder, S., and W. Thiel, 1985, J. Am. Chem. Soc. **107**, 4422.
Schuegraf, K. K., 1988, Ed., *Handbook of Thin-Film Deposition Processes and Techniques* (Noyes, Park Ridge, NJ).
Schulze, G., and M. Henzler, 1983, Surf. Sci. **124**, 336.
Schwuttke, G. H., 1971, in *Ion Implantation,* edited by F. H. Eisen and L. T. Chadderton (Gordon & Breach, New York), p. 139.
Seager, C. H., and R. A. Anderson, 1988, Appl. Phys. Lett. **53**, 1181.
Seager, C. H., and R. A. Anderson, 1990a, MRS Proc. **163**, 431.
Seager, C. H., and R. A. Anderson, 1990b, Solid State Commun. **76**, 285.
Seager, C. H., R. A. Anderson, and D. K. Brice, 1990, J. Appl. Phys. **68**, 3268.
Seager, C. H., R. A. Anderson, and J. K. G. Panitz, 1987, J. Mater. Res. **2**, 96.
Seager, C. H., and D. S. Ginley, 1979, Appl. Phys. Lett. **34**, 337.
Seccombe, S. D., and D. M. Korn, 1972, Solid State Commun. **11**, 1539.
Sherman, D. H., C. V. Owen, and T. E. Scott, 1968, Trans. Metall. Soc. AIME **242**, 1775.
Shi, T. S., S. N. Sahu, J. W. Corbett, and L. C. Snyder, 1984, Sci. Sin. **27**, 98.
Shi, T. S., S. N. Sahu, G. S. Oehrlein, A. Hiraki, and J. W. Corbett, 1982, Phys. Status Solidi B **74**, 329.
Shi, T. S., L. M. Xie, G. R. Bai, and M. W. Qi, 1985, Phys. Status Solidi B **131**, 511.
Shih, D., and H. K. Birnbaum, 1986, in *Modeling Environmental Effects on Crack Growth Processes,* edited by R. H. Jones and W. Gerberich (TMS AIME, Warrendale, PA), p. 355.
Shih, D., I. M. Robertson, and H. K. Birnbaum, 1988, Acta Metall. **36**, 111.
Shirley, A. I., and C. K. Hall, 1983, Scr. Metall. **17**, 1003.

Shirley, A. I., and C. K. Hall, 1984, Acta Metall. **32**, 49.
Shirley, A. I., C. K. Hall, and N. J. Prince, 1983, Acta Metall. **31**, 985.
Simpson, L. A., and M. P. Puls, 1979, Metall. Trans. A **10**, 1093.
Singh, M., and J. Weber, 1989, Appl. Phys. Lett. **54**, 424.
Singh, V. A., J. W. Corbett, C. Weigel, and L. M. Roth, 1978, Phys. Lett. A **65**, 261.
Singh, V. A., C. Weigel, J. W. Corbett, and L. M. Roth, 1977, Phys. Status Solidi B **81**, 637.
Sinniah, K., M. G. Sherman, L. B. Lewis, W. H. Weinberg, J. T. Yates, and K. C. Janda, 1990, J. Chem. Phys. **92**, 5700.
Sirois, E., P. Sofronis, and H. K. Birnbaum, 1992, *Parkins Symposium* (TMS AIME, Warrendale, PA), in press.
Springer, T., 1978, in *Hydrogen in Metals,* Vol. I, edited by G. Alefeld and J. Völkl (Springer-Verlag, Berlin), p. 75.
Stavola, M., K. Bergman, S. J. Pearton, and J. Lopata, 1988, Phys. Rev. Lett. **61**, 2786.
Stavola, M., J. R. Patel, L. C. Kimerling, and R. E. Freeland, 1983, Appl. Phys. Lett. **42**, 73.
Stavola, M., and S. J. Pearton, 1991, in *Hydrogen in Semiconductors,* edited by J. I. Pankove and N. M. Johnson (Academic, New York), p. 139.
Stavola, M., S. J. Pearton, J. Lopata, C. R. Abernathy, and K. Bergman, 1989, Phys. Rev. B **39**, 8051.
Stavola, M., S. J. Pearton, J. Lopata, and W. C. Dautremont-Smith, 1987, Appl. Phys. Lett. **50**, 1086.
Stavola, M., S. J. Pearton, J. Lopata, and W. C. Dautremont-Smith, 1988, Phys. Rev. B **37**, 8313.
Steigerwald, E. A., F. W. Schaller, and A. R. Troiano, 1960, Trans. Metall. Soc. AIME **218**, 832.
Stein, H. J., 1975, J. Electron. Mater. **4**, 159.
Stein, H. J., 1989, in *Silicon Nitride and Silicon Dioxide Thin Insulating Films,* ECS Proceedings No. 89-7, edited by S. B. Bibyk, V. J. Kapoor, and N. S. Alvi (Electrochemical Society, Pennington, NJ), p. 3.
Stein, H. J., 1990, Appl. Phys. Lett. **57**, 792.
Stein, H. J., 1991, Nucl. Instrum. Methods B **59-60**, 1106.
Stein, H. J., and S. K. Hahn, 1990, Appl. Phys. Lett. **56**, 63.
Stein, H. J., S. K. Hahn, and S. C. Shatas, 1986, J. Appl. Phys. **59**, 3495.
Stoloff, N. S., 1990, in *Hydrogen Effects on Material Behavior,* edited by N. R. Moody and A. W. Thompson (TMS, Warrendale, PA), p. 483.
Stoneham, A. M., 1989, Phys. Rev. Lett. **63**, 1027.
Stott, M. J., and E. Zaremba, 1980, Phys. Rev. B **22**, 1564.
Sun, Z., and D. Tomanek, 1989, Phys. Rev. Lett. **63**, 59.
Svensson, B. G., A. Hallén, and B. U. R. Sundqvist, 1990, unpublished.
Switendick, A. C., 1989, Z. Phys. **163**, 527.
Symons, M. C. R., 1984, Hyperfine Interactions **17-19**, 771.
Szeles, C., and A. Vértes, 1987, J. Phys. F **17**, 2031.
Tabata, T., and H. K. Birnbaum, 1983, Scr. Metall. **17**, 947.
Tabata, T., and H. K. Birnbaum, 1984, Scr. Metall. **18**, 231.
Tabata, T., and H. K. Birnbaum, 1985, Trans. Jpn. Inst. Met. **24**, 485.
Takano, S., and T. Suzuki, 1974, Acta Metall. **22**, 265.
Tanaka, S., and H. Kimura, 1979, Trans. Jpn. Inst. Met. **20**, 647.
Tatarkiewicz, J., and M. Stutzman, 1988, in Phys. Stat. Sol. B **149**, K95.
Tavendale, A. J., D. Alexiev, and A. A. Williams, 1985, Appl. Phys. Lett. **47**, 316.
Tavendale, A. J., S. J. Pearton, and A. A. Williams, 1990, Appl. Phys. Lett. **56**, 949.
Tavendale, A. J., S. J. Pearton, A. A. Williams, and D. Alexiev, 1990, Appl. Phys. Lett. **56**, 1457.
Thomas, G. J., 1981, in *Hydrogen Effects in Metals,* edited by I. M. Bernstein and A. W. Thompson (TMS-AIME, Warrendale, PA), p. 77.
Tomanek, D., and M. A. Schluter, 1987, Phys. Rev. B **36**, 1208.
Tsuru, T., and R. M. Latanision, 1982, Scr. Metall. **16**, 575.
Upton, T. H., 1986, Phys. Rev. Lett. **56**, 2168.
Van der Pauw, L. J., 1958, Philips Res. Rep. **13**, 1.
Van de Walle, C. G., 1990, Phys. Rev. Lett. **64**, 669.
Van de Walle, C. G., 1991, in *Hydrogen in Semiconductors,* edited by J. I. Pankove and N. M. Johnson (Academic, New York), p. 585.
Van de Walle, C. G., Y. Bar-Yam, and S. T. Pantelides, 1988, Phys. Rev. Lett. **60**, 2761.
Van de Walle, C. G., P. J. H. Denteneer, Y. Bar-Yam, and S. T. Pantelides, 1989, Phys. Rev. B **39**, 10791.
Van Wieringen, A., and N. Warmoltz, 1956, Physica **22**, 849.
Veal, B. W., D. J. Lam, and D. G. Westlake, 1979, Phys. Rev. B **19**, 2856.
Vehoff, H., C. Laird, and D. J. Duquette, 1987, Acta Metall. **35**, 2877.
Vehoff, H., and W. Rothe, 1983, Acta Metall. **31**, 1781.
Verbruggen, A. H., R. Griessen, and J. H. Rector, 1984, Phys. Rev. Lett. **52**, 1625.
Viccaro, P. J., G. K. Shenoy, B. D. Dunlap, D. G. Westlake, S. K. Malik, and W. E. Wallace, 1979, J. Phys. (Paris) **40**, C2-157.
Vitek, V., and G. J. Wang, 1982, J. Phys. (Paris) Colloq. **43**, C6.
Vogel, S., M. Celio, Dj. M. Maric, and P. F. Meier, 1989, J. Phys.: Condens. Matter **1**, 4729.
Wang, L. P., L. Z. Zhang, W. X. Zhu, X. T. Lu, and G. G. Qin, 1990, Physica B **158**, 113.
Watkins, G. D., 1989, Mater. Sci. Forum **38-41**, 39.
Watkins, G. D., W. B. Fowler, M. Stavola, G. G. DeLeo, D. M. Kozuch, S. J. Pearton, and J. Lopata, 1990, Phys. Rev. Lett. **64**, 467.
Weber, J., F. Bantien, S. J. Pearton, and W. C. Dautremont-Smith, 1986, in *Proceedings of the 14th International Conference on Defects in Semiconductors,* edited by H. J. von Bardeleben, Mater. Sci. Forum **10-12**, 579.
Weber, J., S. J. Pearton, and W. C. Dautremont-Smith, 1986, Appl. Phys. Lett. **49**, 1181.
Weber, J., and M. Singh, 1988, MRS Proc. **104**, 325.
Westlake, D. G., 1969, Trans. Am. Soc. Met. **62**, 1000.
Whetten, R. L., D. M. Cox, D. J. Trevor, and A. Kaldor, 1985, Phys. Rev. Lett. **54**, 1494.
Whiteman, M. B., and A. R. Troiano, 1965, Corrosion **21**, 53.
Williams, A. R., P. J. Feibelman, and N. D. Lang, 1982, Phys. Rev. B **26**, 5433.
Winter, J., V. Philipps, U. Samm, and B. Schweer, 1989, Eds., *Proceedings of the 8th International Conference on Plasma-Surface Interactions in Controlled Fusion Devices,* J. Nucl. Mater. **162-164**.
Wise, M. L., B. G. Koehler, P. Gupta, P. A. Coon, and S. M. George, 1991, Surf. Sci. **258**, 166.
Wolfer, W. G., and M. I. Baskes, 1985, Acta Metall. **33**, 2005.
Wood, T. W., and R. D. Daniels, 1965, Trans. Am. Inst. Mech. Eng. **233**, 898.
Yapsir, A. S., P. Deák, R. K. Singh, L. C. Snyder, J. W. Corbett, and T.-M. Lu, 1988, Phys. Rev. B **38**, 9936.
Young, F. W., Jr., 1978, J. Nucl. Mater. **69-70**, 310.
Zavada, J. M., H. A. Jenkinson, R. G. Sarkis, and R. G. Wilson, 1985, J. Appl. Phys. **58**, 3731.

Zeides, F., 1986, Ph.D. thesis (University of Illinois).
Zeides, F., and H. K. Birnbaum, 1990, unpublished.
Zeller, R., 1987, in *Current Trends in the Physics of Materials,* edited by M. Yussouff (World Scientific, Singapore), p. 332.
Zhang S. B., and D. J. Chadi, 1990, Phys. Rev. B **41**, 3882.
Zhang, S. B., and W. B. Jackson, 1991, Phys. Rev. B **43**, 12142.
Zhang, T.-Y., W. Y. Chu, and C. M. Hsiao, 1984, Scr. Metall. **18**, 1421.
Zhang, T.-Y., and P. Haasen, 1989, Philos. Mag. A **60**, 15.
Zhang, Zh.-N., and Zh.-J. Xu, 1982, Acta Phys. Sin. **31**, 994.
Zhu, J., N. M. Johnson, and C. Herring, 1990, Phys. Rev. B **41**, 12354.